An investigation into the interaction partners of the scaffold protein human CNK1 in the NF-κB pathway

Holisha Moodley

Thesis submitted in fulfilment of the requirements for the degree of Master of Science (Microbiology)

January 2019

ABSTRACT

The protein connector enhancer of KSR1 (CNK1) plays a role in a number of signalling pathways including those involved in cell proliferation, cell growth and differentiation. De-regulation of these pathways has been linked to the promotion of oncogenic signalling. The involvement of CNK1 in all of these diverse pathways indicates a need to better understand the role of this protein within the cell and within key signalling networks. The research provides a platform to understand the intricate relationships that occur between these key signalling networks with the potential to identify new drug targets.

CNK1 is multifunctional scaffolding protein that has binding domains that mediate and co-ordinate signalling within the MAPK, Hippo, PI3K/AKT, JNK and NF-κB pathways as well as downstream of the AT_2 receptor. The activity of CNK1 is regulated through its interactions with a range of different binding partners within these pathways. Of particular interest to this research is the role of CNK1 in NF-κB signalling. The deregulation of the NF-κB pathway is implicated in chronic inflammation, tissue damage and induction of cervical and breast cancer. CNK1 has been reported to regulate the non-canonical branch of the NF-κB pathway, upstream of the IKK complex however new findings lead to uncertainty about these conclusions. In addition, the interacting partner of CNK1 in the NF-κB pathway has not been elucidated.

In this thesis, we aim to identify the binding partners of CNK1 in the NF-κB pathway. First, we validate an epitope-tagged CNK1-expression construct to express elevated levels of CNK1 in cervical cancer cells. We report that the expression of myc-CNK1 is comparable to endogenous CNK1. Cells expressing elevated CNK1 levels were used in traditional co-immunoprecipitation reactions to identify potential CNK1-interacting proteins. We present data that indicates a potential role for NIK in the CNK1 signalling complex. We discuss the weaknesses of the traditional co-immunoprecipitation reactions and design an alternative co-immunoprecipitation technique with which to study CNK1-interacting partners. In this system, a promiscuous biotin ligase fused to the protein sequence for CNK1 (BirA-CNK1) is used to label proteins proximal to CNK1 with biotin. Using this BirA- CNK1-expressing construct in cervical cancer cells, we demonstrate that CNK1 interacts with IKKα-IKKβ in the NF-κB pathway.

ACKNOWLEDGEMENTS

To my Parents: All my accomplishments are in your honour. I will always dedicate my successes to the both of you as a testament of all the strength and support you've unconditionally given me. Thank you for letting me create my own path and being there for me every step of the way.

Dr Meesbah Jiwaji: It has truly been a learning curve. In the midst of self-doubt, you gave me the space and courage to push through, for that I'm incredibly grateful. Thank you for being not only a supervisor, but someone that challenged and inspired me in all aspects of life. Sincerely, THANK YOU for everything.

Prof Rosemary Dorrington: Thank you for everything you've contributed to enriching my work. I'm very grateful to have had not one, but two incredible supervisors to help me through my projects. I've learned a lot from you, and I'll carry that with me always.

Janet Awino Awando: words cannot describe how much value you've brought into my life in such a short space of time. Thank you for the laughs, the support and guidance. Like Prv, I'll always be there for you.

Mart-Mari De Bruyn: Thank you for keeping my spirits high with your mastery of puns and for always being willing to help me by sharing your insights, I appreciate it.

Lab 417: Thank you for letting me be a part of Team Awesome, it truly was awesome.

TABLE OF CONTENTS

ACKNOWLEDGEMENTS 3

LIST OF FIGURES 9

LIST OF TABLES 11

CHAPTER 1: LITERATURE REVIEW 14

CHAPTER 2: METHODS AND MATERIALS 23

CHAPTER 3: THE EXPRESSION AND VALIDATION OF EPITOPE-TAGGED HUMAN CNK1 29

CHAPTER 4: IDENTIFICATION OF THE INTERACTING PARTNERS OF CNK1 IN THE NF-κB PATHWAY 49

CHAPTER 5: DEVELOPMENT OF AN IN VIVO PROXIMITY LABELLING SYSTEM TO IDENTIFY THE INTERACTING PARTNERS OF CNK1 IN THE NF-κB PATHWAY 68

CHAPTER 6: FINAL DISCUSSION AND CONCLUSIONS 87

APPENDICES 89

REFERENCES 96

CHAPTER 1: LITERATURE REVIEW **14**

1.1 Signal Transduction 14

1.1.1 Regulation 14

1.2 Cervical Cancer 15

1.2.1 Introduction 15

1.2.2 Human papillomavirus genome and oncoproteins 16

1.2.3 Cervical Cancer and NF-κB 17

1.3 NF-κB Signalling 17

1.3.1 Introduction 17

1.3.2 NF-κB transcription factors 19

1.3.3 IκB proteins 19

1.3.4 Canonical signalling upon activation 20

1.3.5 Non-canonical signalling upon activation 21

1.3.6 Regulators of NF-κB signalling 22

1.3.7 Aims of Thesis 22

CHAPTER 2: METHODS AND MATERIALS 23

2.1 HeLa cell culture 23

2.2 Generation of plasmids 23

2.3 Plasmid DNA extractions: BioRad Quantum Prep™ Plasmid Midiprep Kit 23

2.4 Transfections: Xfect™ (Clontech, CLO-631318) 23

Protocol (Adapted from Xfect™ manual) 23

2.5 HeLa Cell Treatments 24

2.6 Cell lysis: CelLytic® 24

2.7 Primary Antibodies 25

2.8 Secondary Antibodies 25

2.9 Confocal Immunofluorescence Microscopy 25

Cell harvesting and mounting 25

Image J Analysis 26

Statistical analysis using Statistica™ 26

2.10 Immunoprecipitation: Pierce™ Protein A/G Magnetic Beads 26

Protocol (Adapted from Pierce™ Protein A/G Magnetic Beads): 26

2.11 Immunoprecipitation: Streptavidin beads 27

2.12 SDS-PAGE 27

2.13 Western Blot Analysis 28

CHAPTER 3: THE EXPRESSION AND VALIDATION OF EPITOPE-TAGGED HUMAN CNK1 29

3.1 INTRODUCTION 29

3.1.1 Connector enhancer of CNK1 29

3.1.2 Epitope Tags Overview 29

3.1.3 cMyc tag 30

3.1.4 FLAG™ tag 30

3.1.5 Problem Statement 30

3.2 RESULTS AND DISCUSSION 31

3.2.1 The expression of endogenous CNK1 in HeLa cells 31

3.2.2 The development and expression of Myc-CNK1. 33

3.2.3 Detection of FLAG-CNK1 using confocal immunofluorescence microscopy 35

3.2.4 Antibody specificity 37

3.2.5 Development of EGFP-N1 epitope-tagged constructs 37

3.2.6 Development of EGFP-C1 epitope-tagged constructs 40

3.2.7 Development of Myc-NuLS encoding EGFP constructs 44

3.3 CONCLUSIONS 48

CHAPTER 4: IDENTIFICATION OF THE INTERACTING PARTNERS OF CNK1 IN THE NF-κB PATHWAY 49

4.1 INTRODUCTION 49

4.1.1 CNK1 interacting partners 49

4.1.2 CNK1 in the NF-κB pathway 51

4.1.3 Problem Statement 51

4.2 RESULTS AND DISCUSSION 53

4.2.1. The fluorescence levels of endogenous CNK1 in HeLa cells activated with TNFα 53

4.2.2. Analysis of Myc-CNK1-interacting partners in HeLa cells 53

4.2.3. Investigating the effect of stabilizing the immunoprecipitation complexes on the identification of the binding partners of CNK1 57

4.2.4 Relative densitometric analysis of immunoprecipitated proteins 61

4.2.5. Co-localisation studies of CNK1 with p-NIK and NIK using confocal immunofluorescence microscopy 63

4.3 CONCLUSIONS 67

CHAPTER 5: DEVELOPMENT OF AN IN VIVO PROXIMITY LABELLING SYSTEM TO IDENTIFY THE INTERACTING PARTNERS OF CNK1 IN THE NF-κB PATHWAY 68

5.1 INTRODUCTION 68

5.1.1 Overview 68

5.1.2 BirA: a promiscuous humanised biotin ligase 68

5.1.3 Problem Statement 70

5.2 RESULTS & DISCUSSION 70

5.2.1 The development of a humanised BirA-CNK1 expression construct 70

5.2.2 Analysis of HeLa cells transfected with the Myc-BirA expressing construct 71

5.2.3 Western blot analysis BirA-transfected HeLa cells 73

5.2.4 Analysis of BirA-CNK1 expression in HeLa cells 74

5.2.5 Immunoprecipitation of BirA-CNK1 and its interacting partners after induction with TNFα 77

5.2.6 Mass spectrometric analysis of proteins immunoprecipitated with BirA-CNK1....80

5.2.7 Do IKKα or IKKβ interact with CNK1 in the NF-κB pathway?....80

5.3 CONCLUSIONS....85

CHAPTER 6: FINAL DISCUSSION AND CONCLUSIONS....87

APPENDICES....89

A. The specificity of anti-FLAG, anti-MYC and anti-CNK1 antibodies....89

A1.1 Untransfected HeLa cells....89

A1.2 Myc-CNK1 transfected HeLa cells 90

A1.3 FLAG-CNK1 transfected HeLa cells 91

B. The quantification of the level of fluorescence of endogenous CNK1, Myc-CNK1 and FLAG-CNK1 in the nucleus and the nucleolus. 92

C. The quantification of the level of fluorescence of endogenous CNK1, Myc-CNK1 and FLAG-CNK1 in the nucleus and the nucleolus. 93

REFERENCES....96

LIST OF FIGURES

Figure 1.1: The effect of scaffold protein on the signal output of a pathway at different concentrations.. 15

Figure 1.2: The genome map of Human Papillomavirus strain 16 and 18 observed in cervical cancer.. 17

Figure 1.3: The Canonical and Non-Canonical activation pathways of NF-κB Signalling.....18

Figure 1.4: NF-κB signalling proteins. 20

Figure 3.1: Levels of endogenous CNK1 in HeLa cells detected using confocal immunofluorescence microscopy.. 32

Figure 3.2: Localisation studies of Myc-CNK1 in HeLa cells using confocal immunofluorescence microscopy.. 34

Figure 3.3: Localisation studies of FLAG-CNK1 in HeLa cells using confocal immunofluorescence microscopy.. 36

Figure 3.4: Plasmid map of EGFP-N1 and DNA sequence analysis of epitope-encoding EGFP-N1.....38

Figure 3.5: Localisation studies of epitope-tagged EGFP-N1 in HeLa cells using confocal immunofluorescence microscopy.. 39

Figure 3.6: Plasmid map and sequencing of EGFP-C1.. 41

Figure 3.7: Localisation studies of tagged EGFP-C1 in HeLa cells using confocal immunofluorescence microscopy.. 42

Figure 3.8: Analysis of the Myc and FLAG epitope tag sequence. 43

Figure 3.9: Cloning the Myc: NuLS into EGFP-N1 and EGFP-C1. 44

Figure 3.10: Localisation studies of altered Myc tag (Myc: NuLS) fused to EGFP-N1 and EGFP-C1 in HeLa cells using confocal immunofluorescence microscopy......45

Figure 3.11: The expression of EGFP-CNK1 observed using confocal immunofluorescence microscopy......47

Figure 4.1: CNK1 protein sequence and interacting regions. 52

Figure 4.2: Endogenous CNK1 in TNFα-treated HeLa cells. 54

Figure 4.3: Western blot analysis of CNK1 from HeLa cells, immunoprecipitated with anti-Myc antibodies. 55

Figure 4.4: Western blot analysis of stabilized immunoprecipitation complexes of CNK1 and its interacting partners. 58

Figure 4.5: Analysis of the binding sites of the anti-CNK1 and anti-Myc epitope tag antibodies. 59

Figure 4.6: Relative densitometric analysis of proteins of interest in the immunoprecipitation reactions.. 62

Figure 4.7: Co-localisation of CNK1 with RAF-1 in HeLa cells using confocal immunofluorescence microscopy. 65

Figure 4.8: Co-localisation of CNK1 with NIK & p-NIK in HeLa cells using confocal immunofluorescence microscopy. 66

Figure 5.1: Schematic of the reaction that would occur between the promiscuous BirA-fused CNK1 and its proximal partners.. 69

Figure 5.2: Plasmid map of the BirA-expressing plasmid Myc-BirA-Gtx-EGFP DNA and sequence analysis of BirA-CNK1.. 71

Figure 5.3: Detection of Myc-BirA expression using confocal immunofluorescence microscopy in HeLa cells transfected with the BirA-expressing construct. 72

Figure 5.4: Western blot analysis of the expression of BirA in HeLa cells. 73

Figure 5.5: Evaluation of BirA-CNK1 expression in HeLa cells using confocal immunofluorescence microscopy.. 75

Figure 5.6: Western blot analysis of protein lysates from HeLa cells transfected with BirA-CNK1 and treated with TNFα and biotin. 76

Figure 5.7: Efficiency of Bir-CNK1 immunoprecipitation reactions. 78

Figure 5.8: Co-localization studies of IKKα/β and CNK1 using confocal immunofluorescence microscopy. 81

Figure 5.9: IKKα/β interacts with CNK1 83

Figure 6.1: CNK1-interacting proteins in the NF-κB pathway.....88

Figure A1: Antibody specificity in untransfected HeLa cells.. 89

Figure A2: Antibody specificity of Myc-CNK1 transfected HeLa cells. 90

Figure A3: Antibody specificity of FLAG-CNK1 transfected HeLa cells. 91

Figure B1: ImageJ analysis of CNK1 fluorescence in HeLa cells.....92

Figure C1: ImageJ analysis of Myc- and FLAG-tagged EGFP fluorescence in HeLa cells.. .93

LIST OF TABLES

Table 5.1: Mass Spectrometry analysis of potential interacting partners of CNK1 in the NF-κB signalling. 80

Appendix D. Sequence of the primers used in this study. 94

LIST OF ABBREVIATIONS, SYMBOLS AND UNITS

AF = alexa fluor

AKT = protein kinase B

ARD = ankyrin repeat domains

AT_2 = angiotensin type II

BAFF-R = B-cell activating factor receptor

BAT = biotin acceptor tag

BCR = B-cell receptors

bioAMP = biotinoyl-5'AMP

BirA = biotin protein ligase

CC = coiled-coil domain

CNK1 = connector enhancer of KSR1

CRIC = conserved region in cnk

CTCF = corrected total cell fluorescence

CTD = C-terminal domain

DAPI = 4',6-diamidino-2-phenylindole

DFC = dense fibrillar components

DMEM = Dulbecco's modified Eagle medium

EGF = epidermal growth factor

EGFP = enhanced green fluorescent protein

Epp = eppendorf / microcentrifuge tube

FC = fibrillar center

GC = granular component

HC = heavy chain

HPV = human papillomavirus

HRP = horseradish peroxidase

IF = immunofluorescence microscopy

IKK = IκB kinase

IL-1R = interleukin-1 receptor

IκB = inhibitory kappa B

IP = immunoprecipitations

IRES = Internal ribosomal entry site

JNK = c-Jun N-terminal kinase

LC = light chain

LTβ = lymphotoxin β receptor

LYS = Lysate

MAP kinase = mitogen activated protein kinase

MS = mass spectrometry

NEMO = NF-κB essential modulator

NF-κB = nuclear factor kappa-B

NIK = NF-κB-inducing kinase

NLS = nuclear localisation signals

NK cells = natural killer cells

NTD = N-terminal domain

NuLS = nucleolus localisation signal

PBS = phosphate buffer saline

PDZ = PSD-96/Dlg-A/ZO-1

PH = pleckstrin homology

pI = isoelectric point

PI3K = phosphoinositide-3-kinase

PID = processing-inhibitory domain

RAF = rapidly accelerated fibrosarcoma

RHD = rel homology domain

RT = room temperature

SAM = sterile α-motif

SRD = signal response domain

TAD = transactivation domains

TLR = toll-like receptor

TNF = tumour necrosis factor

TNFR = tumour necrosis factor receptor

°C = degree Celsius

µg = microgram

µL = microlitre

µm = micrometre

µM = micromolar

kDa = kilodaltons

mM = millimolar

ng = nanogram

nm = nanometre

CHAPTER 1: LITERATURE REVIEW

1.1 Signal Transduction

An organism's ability to develop, differentiate and adapt is achieved through cellular communication, regulated by signalling pathways (Berridge, 2008). Signalling pathways are activated by the stimulation of cell surface receptors with extracellular substances. The induction of signal transduction with effector molecules initiates a cascade of intracellular interactions comprising proteins, amino acids, lipids and secondary messengers (Chen, et al., 2014). Two regulation mechanisms that are key for this research report are phosphorylation and the action of scaffold proteins.

1.1.1 Regulation

Phosphorylation: In cellular signalling, the protein cascade is directed by phosphorylation events mediated by protein kinases and phosphatases. These in turn induce key cellular processes including gene transcription, translation, differentiation, proliferation and intracellular communication (Tanabe, 2017).

There are two main groups of kinases: Serine/Threonine kinases and Tyrosine kinases, and the Serine/Threonine kinases are responsible for the majority of phosphorylation events (Day, et al., 2016). Protein kinases regulate signalling by transferring the terminal phosphate group from ATP to amino acid residues. These events result in the transduction of the signal to other proteins that recognise the phosphorylated residues (Vihinen, 2003). Signal transduction is a strong protein dependent event that result in changes in gene expression; these changes in the levels of gene expression and subsequent protein synthesis play a vital role in the regulation of protein levels within the cells (Lee & Yaffe, 2016).

Scaffold Proteins: Scaffold proteins are important components of intracellular signalling. They are responsible for mediating the recruitment and formation of signalling complexes that facilitate interactions which in turn regulate new responses and output behaviours in signal transduction (Pan, et al., 2012).

Scaffold proteins regulate signal transduction by catalysing modifications of proteins or by recruiting specific regulators of the protein complexes (Pan, et al., 2012). Scaffold proteins alter the localisation, amplitude and duration of signalling events. The presence of a scaffold protein in a pathway at concentrations relative to the concentration of its interactors promotes an increase in the signal throughput of the pathway (Ferrell, 2000). However, an overabundance of the scaffold protein results in the sequestration of activating kinases from

substrates, diluting the pathway components and so signal transduction (Figure 1.1) (Burack & Shaw, 2000).

Scaffold proteins are composed of multiple domains or motifs that allow them to interact with multiple partners, promote cross talk between signalling networks, and to control regulatory components to diversify signalling behaviours and mediate new responses (Good et al, 2011; Pan et al, 2012).

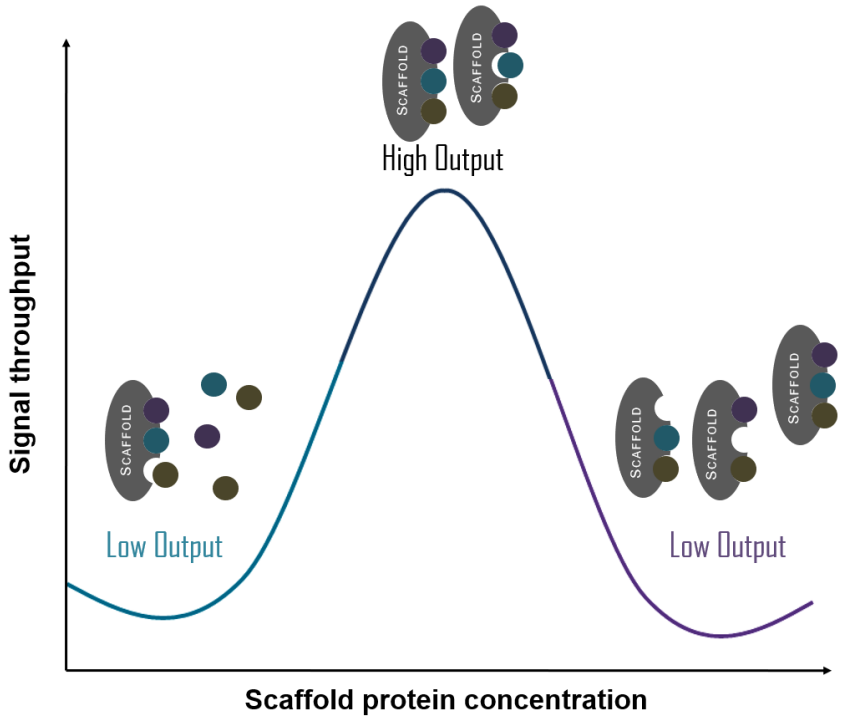

Figure 1.1: The effect of scaffold proteins on the signal output of a pathway at different concentrations. (Adapted from: Pansare, 2013).

1.2 Cervical Cancer

1.2.1 Introduction

Cancers are described as the miscommunication of cell signalling which in turn promote the deregulation of intracellular pathways involved in key cellular processes (Milella, et al., 2010). In cervical carcinomas, the Human Papillomavirus (HPV) is identified as the main risk factor in tumorigenesis. A total of 75% of observed cervical malignancies are caused by HPV16 and HPV18 (Ghim, et al., 2002). The high-risk HPV type, 16 and 18 have been observed to be fundamentally linked with the aetiology of cervical cancer (Schwarz, et al., 1985). In a cervical cancer biopsy study, it is indicated that over 95% contained high risk HPV genomes integrated into the host genome (zur Hausen, 2009). A phenomenon enhanced by the expression of the high-risk HPV oncoproteins E6 and E7 (zur Hausen, 2009). HPV induced carcinomas can develop from the infection of immature metaplastic cells of the transformation zone in the

cervix by HPV, resulting in a range of epithelial lesions, which serve as precursors for carcinogenesis (Ghim, et al., 2002). HPV-induced cervical carcinomas can develop within two years of infection, in which time only a minor portion of individuals progress to cervical intraepithelial neoplasia or invasive cancer. These progression events are known to occur over a span of 10-30 years (Ma, et al., 2000). The slow development of an HPV infection to cervical cancer is suggestive of other cellular events that are required for carcinogenesis (Ma, et al., 2000).

1.2.2 Human papillomavirus genome and oncoproteins

Papillomaviruses are non-enveloped viral particles that contain double stranded circular DNA encapsulated within an icosahedral capsid (Doorbar, 2006). The viral genome (Figure 1.2) of HPV differs between strains, however the majority are ~8000 bp in size and encodes three main regions: an E region encoding the early proteins (E1-E7), an L region encoding the late structural proteins (L1-L2) and a non-coding region responsible for the replication and transcription of HPV (Venuti, et al., 2011).

The high-risk oncoproteins in cervical cancer are E5-E7, which have been observed to interact in cellular signalling pathways and to promote tumour progression and immune invasion (Venuti, et al., 2011). E6 is responsible for the degradation of the tumour suppressor p53, preventing normal repair of chance mutations in the cellular genome (Doorbar, 2006). E7 is observed to interact with retinoblastoma (Rb) protein resulting in Rb inactivation and promotion of intraepithelial neoplastic progression (Venuti, et al., 2011). The oncoprotein E5 plays a role in the phosphorylation cascades initiated by tyrosine kinase growth factor receptors that are responsible for the activation of *ras* at the plasma membrane, thus evoking the recruitment of RAF activation of the MAPK-ERK pathway (Branca, et al., 2004).

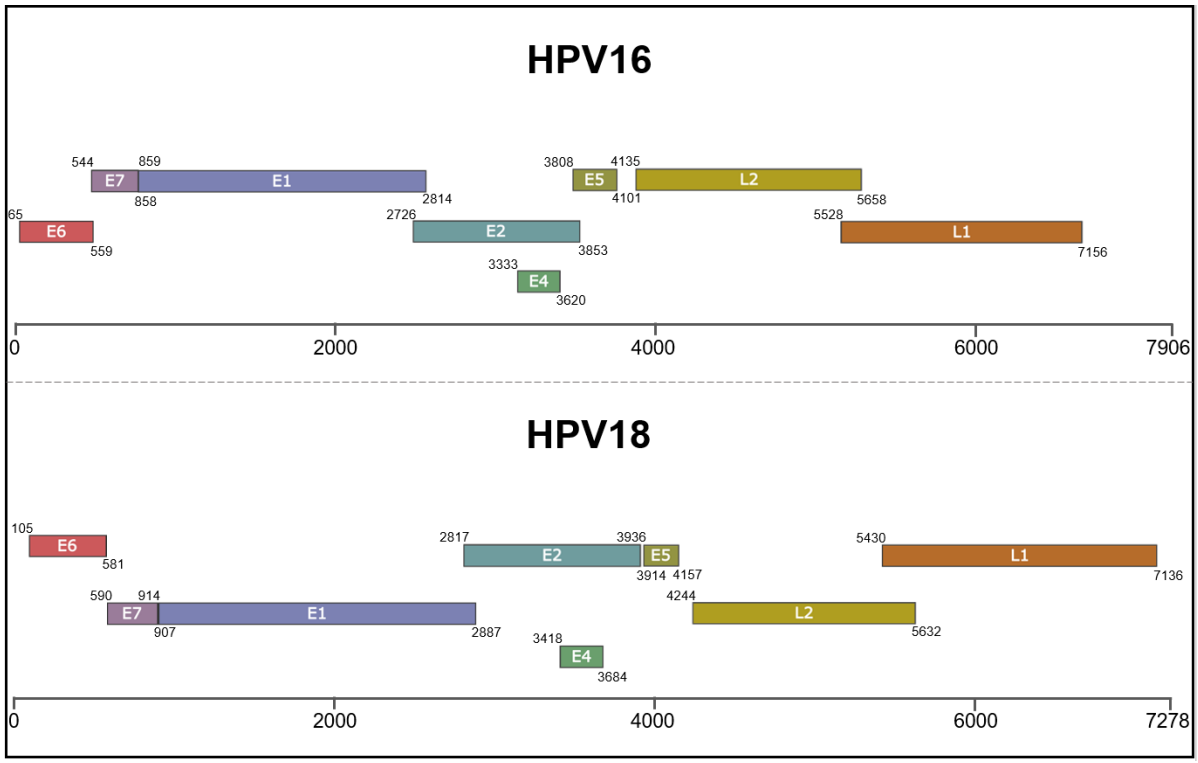

Figure 1.2: The genome map of Human Papillomavirus strain 16 and 18 observed in cervical cancer. (Adapted from Baker & Calef, 1996; Wang et al, 2011).

1.2.3 Cervical Cancer and NF-κB

The NF-κB pathway is involved in the innate and adaptive immune responses initiated by a HPV infection and result in chronic inflammation, which in turn has been linked to the promotion of early carcinogenesis (Tilborghs, et al., 2017). NF-κB is constitutively activated during the progression of HPV infection leading to cervical intraepithelial neoplasia and cervical carcinomas; a linear relationship has been observed between the expression of cytoplasmic NF-κB factors and an increase in the severity of carcinogenesis (Tilborghs, et al., 2017).

The persistence of HPV infections and collective mutations within the HPV genome promote a reduction in the effectiveness of NF-κB inhibitory signals. This exacerbates the impact of the HPV infection on HPV-induced carcinogenesis (Tilborghs, et al., 2017).

1.3 NF-κB Signalling

1.3.1 Introduction

NF-κB signalling mediates the transcription of genes responsible for key cellular processes including cell survival, cell proliferation, innate and adaptive immunity, inflammatory responses and cell development (Courtois & Gilmore, 2006). The constitutive activation of

NF-κB signalling is observed to mediate inflammatory diseases such as rheumatoid arthritis, inflammatory bowel disease, multiple sclerosis and chronic inflammation (Verma, 2004).
The deregulation of NF-κB signalling is observed as a key mediator in oncogenic signalling promoting cervical and breast cancer (Fritz & Radziwell, 2010). The NF-κB signalling pathway comprises of two activation pathways: Canonical/Classical (Figure 1.3 I) and Non-canonical/Alternative pathways (Figure 1.3 II).

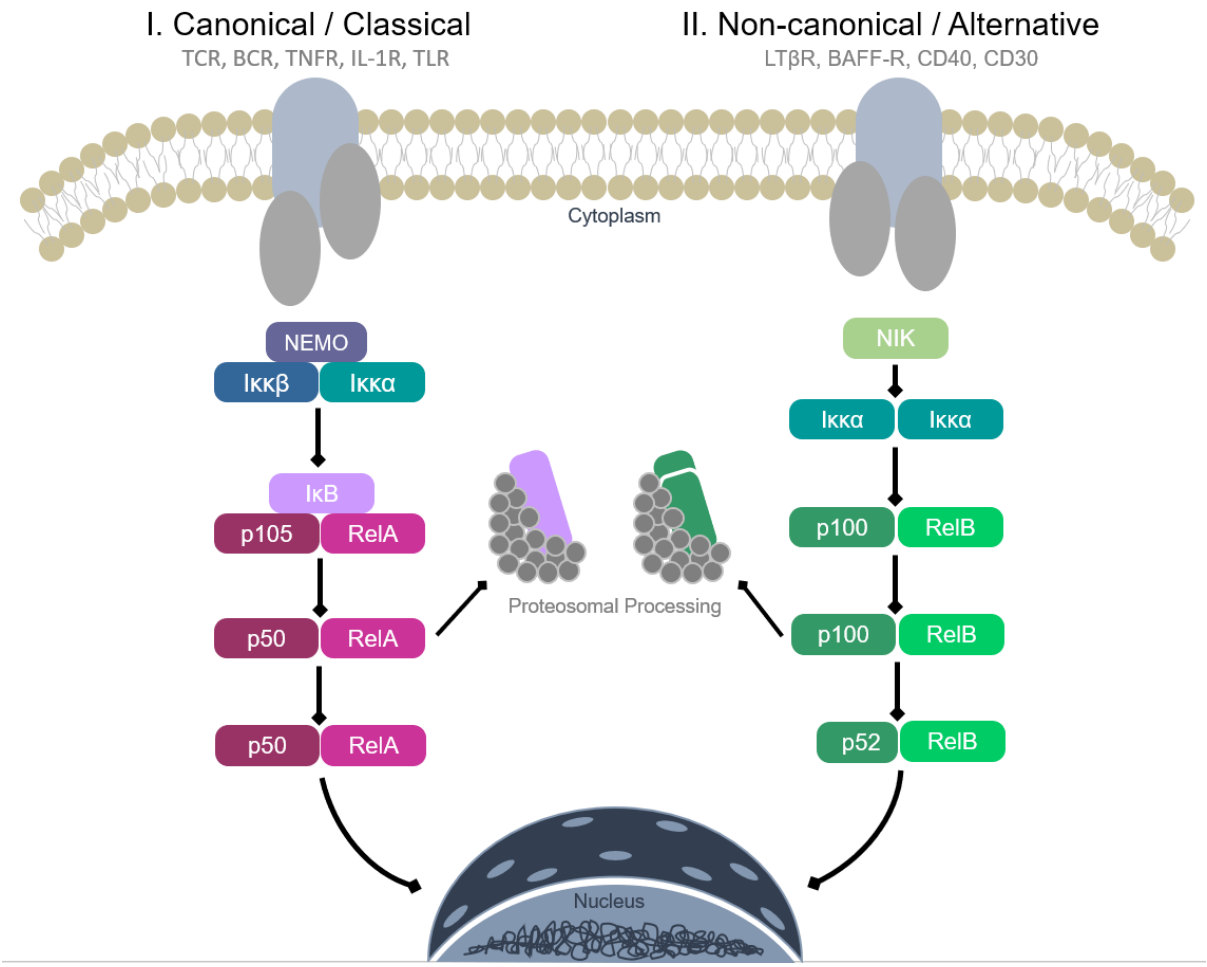

Figure 1.3: The Canonical and Non-Canonical activation pathways of NF-κB Signalling. I): NF-κB signalling of the canonical/classical pathway via the TCR:T-cell receptors , BCR: B-cell receptors, TNFR: tumour necrosis factor receptor, TLR: Toll-like receptor and IL-1R: interleukin-1 receptor; II): NF-κB signalling of the non- canonical/alternative pathway via the LTβ: lymphotoxin β receptor, BAFF-R: B-cell activating factor , CD40 and CD30 receptors. (Adapted from Pansare, 2012; Napetsching and Wu, 2013; Nishikori, 2005)

1.3.2 NF-κB transcription factors

The NF-κB protein family is composed of 5 key members (Figure 1.4) consisting of RelA (p65), RelB, c-Rel, NF-κB1 (p105/p50) and NF-κB2 (p100/p52) encoded by genes *rela, relc, crel, nfkb1 and nfkb2* respectively (O'Dea & Hoffmann, 2009).

The family of NF-κB protein share a common a Rel homology domain (RHD) at the N-terminal (Figure 1.4) which is responsible for mediating nuclear translocation, dimerization and DNA binding through the formation of homodimers and heterodimers (Moynagh, 2005). The dimers of the NF-κB proteins possess different functionalities; some are transcriptional activators whereas other requires the recruitment of co-activator proteins for activation (O'Dea & Hoffmann, 2009).

The RHD of NF-κB proteins further comprise of two main domains, the N-terminal domain (NTD) and the C-terminal domain (CTD). Both these regions are responsible for encircling target DNA (Napetschnig & Wu, 2013) but separately. The NTD is responsible primarily for recognising and interacting with target DNA sequences at defined DNA bases. In contrast, the CTD is responsible for the dimerization and mediation of a phosphate interaction with DNA or nonspecific interactions with the DNA sugar-phosphate backbone (Napetschnig & Wu, 2013).

The transcriptionally active members of the NF-κB family are the RelA, RelB and c-Rel proteins which possess transactivation domains (TAD) at their C-terminal, whereas NF-κB1(p50) and NF-κB1(p52) lack the region and therefore act as DNA-binding agents (Schmitz, et al., 1995).

1.3.3 IκB proteins

In unstimulated cells, the NF-κB transcription factors are associated with inhibitory kappa B (IκB) proteins (Hoesel & Schmid, 2013). The IκB protein family is comprised of 3 main members (Figure 1.4) consisting of IκBα, IκBβ and IκBε encoded by genes *nfkbia, nfkbib* and *nfkbie* respectively (O'Dea & Hoffmann, 2009).

The IκB family of proteins all possess an ankyrin repeat domain (ARD) which associates with NF-κB dimers (Figure 1.4). The binding of IκB to NF-κB dimers are responsible for masking the nuclear localisation signal (NLS) encoded within NF-κB transcription factors preventing their nuclear translocation (Moynagh, 2005).

The activation of NF-κB transcription factors is dependent on the degradation of the associated IκB protein, which is achieved with cleavage by the 26S proteasome. The proteosomal cleavage of IκB is induced by the phosphorylation with IκB kinases (such as IKKα, IKKβ and IKKγ) and by the ubiquitination of the signal responsive domain (SRD) of IκB proteins (Figure

1.4) (Moynagh, 2005). The NF-κB transcription factors p105 and p100 both encode SRD, and these proteins are cleaved into p50 and p52 respectively upon activation. The cleaved products permit the nuclear translocation of the transcription factors (Hoesel & Schmid, 2013).

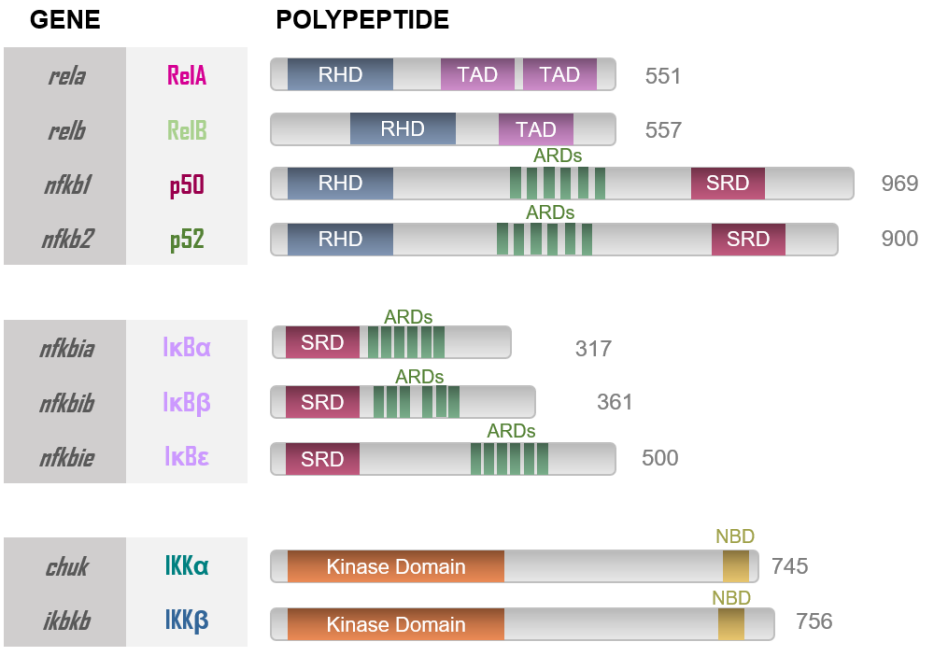

Figure 1.4: NF-κB signalling proteins. RHD: Rel Homology Domain mediates dimerization and DNA binding, TAD: Transcriptional Activation Domain mediates activation of transcription, SRD: Signal Responsive Domain which are sites for phosphorylation and ubiquitination, ARD: Ankyrin Repeat Domain mediates interaction with NF-κB dimers, CC: coiled coil domain, NBD: NEMO Binding Domain. (Adapted from O'Dea and Hoffman, 2009; Hoesel and Schimd, 2013).

1.3.4 Canonical signalling upon activation

The canonical pathway of NF-κB signalling (Figure 1.3) is activated by the interactions of external ligands to the T-cell receptors (TCR), B-cell receptors (BCR), tumour necrosis factor receptors (TNFR1/2) or Toll-like receptors (TLR) such as interleukin-1 receptor (IL-1R) superfamily (Nishikori, 2005).

Ligands responsible for the activation of the canonical pathway include proinflammatory cytokines such as TNFα and IL-1β, as well as pathogen derived substances such as lipopolysaccharides (LPS) or CpG (Lawrence, 2009).The stimulation of the canonical pathway mediates a protein cascade promoting the expression of genes required for cell survival responses, inflammatory responses, adhesion molecules, cytokines and chemokines (Nishikori, 2005).

In inactivated cells, the NF-κB dimer RelA-p50, is associated with the inhibitory protein IκBα which is responsible for preventing the nuclear translocation of the RelA-p50 complex and inhibiting any gene transcription (Hoesel & Schmid, 2013).

The activation of the canonical pathway (Figure 1.3 I) promotes the recruitment of the adapter protein TRAF-6 which associates with and activates TAK1, promoting the stimulation of the canonical IKK complex (Moynagh, 2005). The IKK complex comprises of two catalytic subunits IKKα, IKKβ and a regulatory subunit IKKγ (also referred to as NF-κB essential modulator: NEMO). IKKγ and IKKβ are exclusively involved in NF-κB signalling through the canonical pathway whereas IKKα is associated with both the canonical and non-canonical pathways (Napetschnig & Wu, 2013).

The activation of the IKK complex mediates the phosphorylation of the serine residues in the SRD of the inhibitory protein IκBα, promoting the ubiquitination and degradation of the inhibitory region by the 26S proteasome (Napetschnig & Wu, 2013). The release of the inhibitory effect of IκBα on the RelA-p50 complex permits its translocation to the nucleus and the transcription of genes susceptible to the canonical NF-κB pathway (Hoesel & Schmid, 2013).

1.3.5 Non-canonical signalling upon activation

The non-canonical pathway is activated by the binding of ligands to certain members of the TNFR family such as the lymphotoxin β receptor (LTβR), B-cell activating factor (BAFF-R), CD40 and CD30. Ligands stimulating the activation of the non-canonical pathway include cytokines from the TNF-family such as lymphotoxin β (TNFSF3), CD40 ligand (CD40L) ,B-cell activator factor (BAFF and TNFSF13B) as well as receptor activator of NF-κB ligand (RANKL and TNFSF11) (Lawrence, 2009; O'Dea & Hoffmann, 2009).

The activation of the non-canonical NF-κB pathway regulates the development of the adaptive immune system as well as the development of lymphoid organs (Nishikori, 2005). In inactivated cells, the processing-inhibitory domain (PID) located on the C-terminal of p100 is responsible for preventing the nuclear translocation of the NF-κB dimer: RelB-p100, and so inhibiting gene transcription (Xiao, et al., 2001). The activation of the non-canonical pathway (Figure 1.3 II) leads to the stimulation of the NF-κB inducing kinase (NIK) which phosphorylates and activates the IKK complex, the IKK complex is comprised of an IKKα dimer (Hoesel & Schmid, 2013).

Both the IKK complex and NIK mediate the phosphorylation of the serine residues 866 and 870 in the SRD region of p100 (in the p100-RelB complex), promoting ubiquitination by an E3 ubiquitin ligase which results in its partial degradation by the 26S proteasome (Napetschnig

& Wu, 2013; Hoesel & Schmid, 2013). The proteasomal degradation of the PID of p100 to p52 allows the exposure of a nuclear localisation signal and promotes the nuclear translocation of the mature RelB-p52 complex for the transcription of genes activated by the non-canonical NF-κB pathway (Hoesel & Schmid, 2013).

1.3.6 Regulators of NF-κB signalling

There are two key regulators of the NF-κB pathway that are relevant to this study.

TNFα: Tumour Necrosis Factor (TNFα) is a prototypic member of the TNF superfamily of ligands which interacts with CD40, TNFR1 and TNFR2 (Horuichi *et al*, 2010). These receptors are involved in the activation of a number of signalling pathways including JNK, ERK, MAPK and both branches of NF-κB signalling. The multifunctional cytokine is produced and expressed by a variety of immune cells such as T-cells, B-cells, NK cells and macrophages. TNFα is known to induce immune responses as well playing a role in human inflammatory diseases (Horuichi *et al*, 2010).

CNK1: This protein has been shown to play a role as a mediator of oncogenic signalling in the NF-κB pathway (Fritz and Radziwill, 2010), however the interacting partners of CNK1 in the NF-κB pathway have not been established in current literature.

1.3.7 Aims of Thesis

Determining the interacting partners of CNK1 in the NF-κB pathway provides an opportunity for a deeper understanding of the intricate relationships and irregularities that occur within oncogenic signalling pathways. This gives us the opportunity to develop a better understanding of the factors that promote cervical cancer as well as to identify new potential targets for drug therapy.

In this thesis, we will investigate the interacting partners of CNK1 in NF-κB signalling. We intend to use techniques that have been traditionally used to identify protein-protein interactions and will use CNK1 as the bait protein. These include immunoprecipitation and western analysis using antibodies targeted towards proteins of interest. We will also develop a proximity-based labelling system, using CNK1 as the label-instigator, to identify interacting protein in an unbiased manner. In addition to identifying the proteins that interact with CNK1 in the NF-κB pathway, we will develop a deeper understanding of signalling in cervical cancer, which leads towards the development of potent therapeutics to new drug targets.

CHAPTER 2: METHODS AND MATERIALS

2.1 HeLa cell culture

Human cervical cancer HeLa cells (Cellonex, Separations, South Africa) were cultured in Dulbecco's Modified Eagle Medium (Invitrogen; 41966-029) supplemented with 4 mM L-glutamine and 10% heat inactivated foetal bovine serum (BioChrom; BC/S0615-HI) at 37°C in an atmosphere that contained 5% CO_2.

2.2 Generation of plasmids

The *CNK1* cDNA sequence identical to the *Homo sapiens* CNKSR1 sequence (Genbank accession number AAH12797.1) was cloned into the plasmid vector pRK5 containing a Myc-tag at the N-terminal (pRK5Myc-CNK1, a generous gift from Roby Urcia, University of Aberdeen). Oligonucleotides encoding the sequences for the FLAG tag, the Myc tag or the modified Myc tag (NuLS) were synthesized by Eurofins MWG Operon (Europe) or Inqaba Biotec (South Africa). These oligonucleotides were annealed and cloned into the plasmid pRK5 + CNK1 or the CLONTECH plasmids pEGFP-C1 or pEGFP-N1.

2.3 Plasmid DNA extractions: BioRad Quantum Prep™ Plasmid Midiprep Kit

All plasmids were purified from bacterial cultures using the BioRad Quantum Prep™ kit. The Plasmid Midiprep Protocol was followed as per the instruction manual (http://www.bio-rad.com/webroot/web/pdf/lsr /literature /4100111.pdf). The concentration of purified plasmid DNA was measured using a Nanodrop 2000 (Fermentas).

2.4 Transfections: Xfect™ (Clontech, CLO-631318)

Protocol (Adapted from Xfect™ manual)

Day 1: In a microcentrifuge tube, DNA was diluted in Xfect reaction buffer and mixed by vortexing. Xfect polymer was added to the mixture and samples were left to stand for 10 mins. The medium was aspirated from the HeLa cells and the transfection mixture was added dropwise to cells. The samples were topped with DMEM supplemented with 4 mM L-glutamine; 10 % foetal calf serum and incubated overnight.

Samples were set up in microcentrifuge tubes as follows:

Samples	DNA	Xfect buffer (final dilution volume)	Xfect Polymer	DMEM
24 well	500 ng	25 µl	0.3 µl	250 µl
T75	40 ug	500 µl	12 µl	10 ml

Day 2: The transfection mix was aspirated from cells and replaced with DMEM supplemented with 4 mM L-glutamine; 10 % foetal calf serum. Transfected cells were placed in an incubator at 37°C with 5% CO_2 and proteins were expressed for 24-48 hours. Any induction times are included within this time period.

2.5 HeLa Cell Treatments

TNFα: The spent medium was aspirated from HeLa cells and cells were treated with 100ng/ml TNFα in DMEM supplemented with 4 mM L-glutamine; 10 % foetal calf serum for 15 minutes at 37°C with 5% CO_2.

Biotin: The medium was aspirated from HeLa cells and treated with 50 µM of biotin in 15ml DMEM supplemented with 4 mM L-glutamine; 10 % foetal calf serum for 24 hours at 37°C with 5% CO_2.

Fixative: The medium in T75 flasks of HeLa cells were aspirated after expression and washed with PBS. The cells were then treated with 5 ml 4% paraformaldehyde for 15 mins at room temperature.

2.6 Cell lysis: CelLytic®

HeLa cells were rinsed with phosphate buffered saline (PBS). CelLytic® reagent (Sigma-Aldrich; C2978) was added to each sample (24 well: 150 µl, T75: 1 ml) and incubated on a shaker for 15 minutes at room temperature. Cell were scraped at 5-minute intervals during the incubation. The cell lysates were placed in centrifuge tube were centrifuged at 12 000 x g for 10 minutes. The pellet was discarded, and the supernatant was stored at -80 °C.

2.7 Primary Antibodies

ANTIBODY	SPECIES	CATALOG NO.
Anti-human CNK1	Mouse	BD Transduction Labs: 611734
Anti-Myc tag (Clone 4A6)	Mouse	Millipore: 5-724-25UG
Anti-FLAG® (Clone 2EL-1B11)	Mouse	Millipore: 2392244
RAF-1 (C-20)	Rabbit	Santa Cruz: sc-227
Fibrillarin	Rabbit	Cell Signalling: 2639
p-NIK	Goat	Santa Cruz sc-12957
NIK	Rabbit	Santa Cruz sc-7211
IKKα/β	Rabbit	Biocom/Biotech AB194528

2.8 Secondary Antibodies

ANTIBODY	CATALOG NO.
Donkey α-rabbit Alexa Fluor 488	Invitrogen: A21206
Goat α-mouse Alexa Fluor 546	Invitrogen: A11003
Goat α-rabbit Alexa Fluor 633	Invitrogen: A21070
Goat α-mouse IgG (H+L) HRP-conjugate	Advansta: R-05071-500
Goat α-rabbit IgG (H+L) HRP-conjugate	Advansta: R-05072-500

2.9 Confocal Immunofluorescence Microscopy

Cell harvesting and mounting

1 x 10^5 HeLa cells were plated on a glass coverslip in a 24-well plate and cultured overnight. Cells were washed with PBS (8 g NaCl, 0.2 g KCl, 1.44 g Na_2HPO_4, 0.24 g KH_2PO_4 per litre, pH 7.0) then fixed with 4% paraformaldehyde for 15 minutes at room temperature. The coverslips were re-washed with PBS before permeabilisation with permeabilisation buffer (5% goat serum, 10% sucrose, 1% Triton X-100 in PBS) for 15 minutes at room temperature.

A total volume of 250 µl of primary antibody in permeabilisation buffer (1:500) was added to the cells and incubated for 90 minutes at room temperature. 250 µl of the secondary antibody in permeabilisation buffer (1:500) was added to the cells and incubated for 30 minutes at room temperature. The cells were washed with PBS 3 times for a period of 10 minutes each, DAPI (Sigma; 072M4015V) in PBS (1:2500) was added to the cells during the 2nd wash. The coverslips were mounted onto slides using DAKO (S3023) mounting medium and left to dry in a light proof container for 2 days. The slides were visualised on the Zeiss LSM 780 laser scanning confocal microscope using the x63 objective. All images were acquired using the same exposure and detector settings for each spectral channel. The Zen 2011 Blue/Black

software was used to acquire images from the Zeiss LSM780 microscope and to perform image overlays.

Image J Analysis

The corrected total cell fluorescence (CTCF) of the confocal immunofluorescence images were measured and analysed using Image J. CTCF = Integrated density – (Area of the cell x Mean of Background).

Statistical analysis using Statistica™

Datasets were tested for normalisation of distribution (Shapiro-Wilks Test) and homogeneity of variance (Levene's Test) for independent samples (parametric assumptions). If parametric assumptions were met, a Student's T-test was performed for a dataset with multiple means and two groups. Where there were more than two groups, a One-Way ANOVA was performed for a dataset with multiple means. If parametric assumptions were not met, a Mann-Whitney U test was performed for a dataset with multiple means and two groups. Where there were more than two groups, a Kruskal-Wallis test was performed for a dataset with multiple means.

2.10 Immunoprecipitation: Pierce™ Protein A/G Magnetic Beads

Protocol (Adapted from Pierce™ Protein A/G Magnetic Beads):

Day 1: HeLa lysates from T75 flasks were combined with 10 µg of primary antibody. Samples were incubated rotating overnight at 4°C.

Day 2: 0.5 mg of Pierce Protein A/G Magnetic Beads (Cat: 88802) were placed into a microcentrifuge tube. The beads were washed with 200 µl of wash buffer (Tris-buffered saline containing 0.05% Tween-20) and gently vortexed to mix. Samples were placed onto a magnetic stand to collect the beads against the side of the tube for 2 minutes. The supernatant was discarded, and beads were rewashed with 1 mL of wash buffer. Microcentrifuge tubes were inverted several times to mix then placed on the magnet stand for 2 minutes. The supernatant was discarded, and bead collected for immunoprecipitations. The antibody-lysate mixture was added to the beads and incubated rotating at room temperature for 2 hours. Beads were collected using a magnetic stand and supernatant was removed. The beads were washed with 500 µl of Wash Buffer and gently mixed by vortexing. The beads were collected, and the supernatant was discarded.

500 µl of purified water was added to the tube and the sample was gently mixed. The beads were collected on a magnetic stand and the supernatant was discarded. The beads were resuspended in 500 µl CelLytic. Samples were stored at -80°C until further use.

2.11 Immunoprecipitation: Streptavidin beads

Day 1: HeLa lysates from T75 were combined with 0.5 mg streptavidin magnetic beads in a microcentrifuge tube and incubated rotating overnight at 4°C.

Day 2: The lysate-bead mixture was placed onto a magnetic stand for 2 minutes to collect the magnetic streptavidin beads against the side of the tube. The lysate was removed, and the beads were stored in protease inhibitor (Roche, 04693159001) at -80°C until further use.

2.12 SDS-PAGE

15 µl of the cell lysate was added to 5 µl of a 4 x SDS loading buffer (1M Tris-HCl pH 6.8, 0.8 g SDS, 4 ml 100% glycerol, β-mercaptoethanol, 0.1 % bromophenol blue). The samples were boiled at 100 °C for 5 minutes, followed by incubation on ice for 10 minutes. 20 µl of the sample and 10 µl of an Unstained Protein Molecular Weight Marker (Thermo scientific, 26610) were loaded onto a 10% or 12% SDS gel, prepared as follows:

	Resolving			**Stacking**
	10 %	**12%**		**4%**
30% Bis-Acrylamide	3.3 mL	4 mL	**30%Bis-Acrylamide**	0.66 mL
dddH$_2$0	2.8 mL	2.1 mL	**dddH$_2$0**	3.58 mL
1M Tris pH 8	3.75 mL	3.75 mL	**1M Tris pH 6.8**	0.625 mL
10% SDS	100 µL	100 µL	**10% SDS**	100 µL
10% APS	37.5 µL	37.5 µL	**10% APS**	71.25 µL
TEMED	8.25 µL	8.25 µL	**TEMED**	6.8 µL
Total	**10 mL**	**10 mL**	**Total**	**5 mL**

The gels were run with 1% SDS running buffer (10X SDS-PAGE, 30g/L Tris, 144 g glycine, 10 g SDS) at 150 Volts (BioRad Power Pac 300V) until the dye front was at the bottom of the gel.

2.13 Western Blot Analysis

The proteins were transferred onto a polyvinylidene fluoride (PVDF) membrane (Immobilon-P, Merck Millipore; IPVH00010) with transfer buffer (14.28 g Glycine, 3.03g Tris, 200 mL methanol, made up to 1L with $dddH_20$) using a Mini Trans-Blot® Electrophoretic Transfer Cell (Bio-Rad; 170-3930) at 350 mAmps for 1 hour. The success of the transfer was determined by Ponceau staining. The PVDF membranes were blocked overnight with Blotto (5% non-fat milk powder in TBST (pH 7.5, 6.05 g Tris, 8.76 g NaCl, 1 mL Tween-20 made up to 1L with $dddH_20$)) at room temperature. The PVDF membranes were incubated with the primary antibodies (1:500) diluted in blocking solution (1% BSA in TBST) at room temperature for 24 hours overnight. The PVDF membrane was washed with TBST (3 washes, 10 minutes each). The PVDF membranes were incubated with the secondary antibodies diluted (1:20000) in blocking solution (1% BSA in TBST) at room temperature for 30 minutes with constant agitation. Antibody binding was detected using WesternBright™ ECL Chemiluminescent HRP Substrate (Advansta; K-1204-D20) in a Bio-Rad Molecular Imager® ChemiDoc™ XRS and analysed using Image Lab™ Software.

CHAPTER 3: THE EXPRESSION AND VALIDATION OF EPITOPE-TAGGED HUMAN CNK1

3.1 INTRODUCTION

3.1.1 Connector enhancer of CNK1

Connector enhancer of KSR1 (CNK1) is encoded by the *cnk* gene. The protein contains no catalytic domains but possesses multiple regions that are involved in the interaction with signalling molecules, highlighting its role as a signalling mediator (Therrien, et al., 1998).

In mammals, 5 homologs of CNK are expressed: CNK1 (Figure 3.1A), CNK2A, CNK2B, CNK3A and CNK3B (Jaffe, et al., 2004). All members of CNK contain a sterile-α-motif (SAM), conserved region in CNK (CRIC), conserved coiled region (CC) and a PSD-95/DLG/ZO-1 (PDZ) domain (Kolch, 2000). All homologs except for CNK3 contain a Pleckstrin homology (PH) domain (Kolch, 2000).

The SAM domain of CNK1 promotes protein-protein interactions via homo-heterodimerisation and has been indicated to bind to the Angiotensin II type 2 (AT_2) receptor (Fritz & Radziwell, 2011). The CRIC domain also interacts with AT_2 receptors and folds into amphipathic helices (Fritz & Radziwell, 2011). The CC domain interacts with cytohesin, a guanine nucleotide exchange factor for Arf-GTPases. The PDZ domain interacts with internal ligands, dimerises with other PDZ domains or binds to lipid and C-terminal motifs (Fritz & Radziwell, 2011).

CNK1 has been observed to promote oncogenic signalling in pathways involved in cell proliferation, cell growth and differentiation such as the RAF-MEK-ERK pathway, the RalGDS pathway and the AKT pathway (Fritz, et al., 2010).

3.1.2 Epitope Tags Overview

Epitope tagging is a method for the detection, characterisation and purification of proteins *in vivo* (Jarvik & Telmer, 1998). Epitope tags are small peptide sequences consisting of 6-30 amino acids (Jarvik & Telmer, 1998) which are attached to the N-terminal or C-terminal of a recombinant protein, producing an immunoreactive product that is detected using (often commercially) available antibodies (Brizzard, 2008). There are a number of validated antibodies available for epitope tags, providing multiple opportunities to detect recombinant proteins and these can be tailored to meet the needs of the experiments. Overall, epitope tagging provides a sensitive method to detect specific tags, to distinguish proteins of interest from related but untagged proteins *in vivo* and *in vitro* (Jarvik & Telmer, 1998). Importantly, the small size of the epitope tag reduces the possibility of structural or biological interference

between the tag and the recombinant protein (Jarvik & Telmer, 1998) and so permits interrogation of the biological properties of the protein of interest.

3.1.3 cMyc tag

The cMyc tag is a ten amino acids peptide consisting of residues EQKLISEEDL derived from the c-Myc gene product (Zhao, et al., 2013). The cMyc epitope tag can be attached at either the N or C terminus of a protein and has a high affinity of detection with the 9E10 antibody (Zhao, et al., 2013).

3.1.4 FLAG™ tag

The FLAG™ tag is a short hydrophilic tag, eight amino acids in length and consisting of the DYKDDDDK residues (Einhauer & Jungbauer, 2001). The FLAG tag can be attached at either the N or C terminus of a protein and is detectable with monoclonal M1, M2 and M5 antibodies (Zhao, et al., 2013). The FLAG tag also encodes an internal enterokinase cleavage site represented by the C-terminal residues DDDDK (Einhauer & Jungbauer, 2001) permitting the separation of the FLAG tag from the expressed protein.

3.1.5 Problem Statement

To study the interacting partners of CNK1, we need sufficient protein within the cell such that it can be detected using analytical techniques including confocal immunofluorescence microscopy and western blot analysis.

In this chapter, we will evaluate the endogenous levels of CNK1. If the levels of endogenous CNK1 are not sufficient, we will increase the levels of the protein of interest using epitope-tagged CNK1-expression constructs.

3.2 RESULTS AND DISCUSSION

3.2.1 The expression of endogenous CNK1 in HeLa cells

The expression of endogenous CNK1 was evaluated in HeLa cells using confocal immunofluorescence microscopy (Figure 3.1B). The cells were probed with a primary antibody targeted against CNK1. Endogenous CNK1 is expressed at low levels in the HeLa cells. CNK1 was detected in both the cytoplasm as well as in the nucleus, however the levels in the nucleus were lower than those in the cytoplasm (Figure 3.1B). The largest and most prominent organelle is the nucleus of the cell and housed within it are internal compartments referred to as nucleoli (Shaw, 2005). Mammalian nucleoli have three main structural regions consisting of a fibrillar center (FC), dense fibrillar components (DFC) both fixed within a granular component (GC) (Hernandez-Verdun, 2004). To evaluate the nuclear distribution of CNK1, we probed the HeLa cells with an antibody specific for fibrillarin, which is a marker for the nucleolus of the nucleus. The intensity of fluorescence was measured across a cell (indicted by the arrow on MERGE) and represented graphically (Figure 3.1C). There were no significant differences in the levels of CNK1 between the nucleolus and the nucleus (Figure 3.1C) however with the low levels of CNK1 it was not possible to draw definitive conclusions.

Our observations indicated that we would need to develop a CNK1 expression construct to generate elevated levels of CNK1 in the HeLa cells.

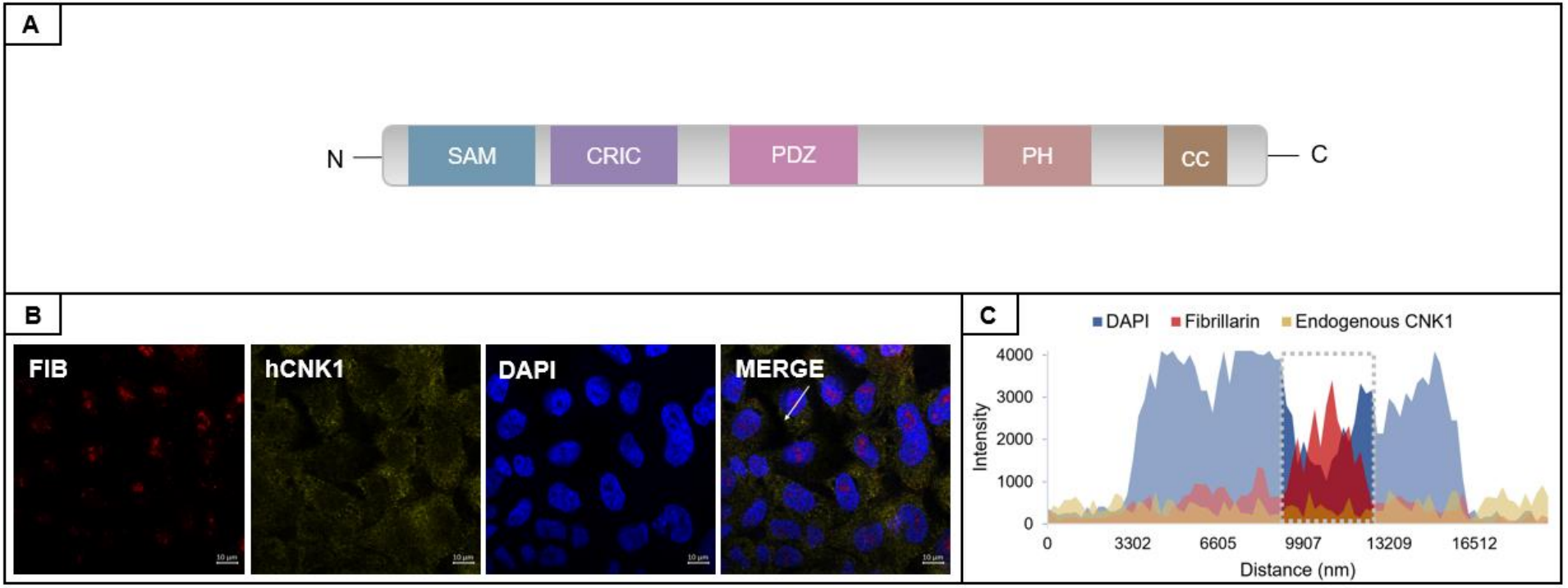

Figure 3.1: Levels of endogenous CNK1 in HeLa cells detected using confocal immunofluorescence microscopy. 1: A – Schematic of human CNK1 gene. CNK1 contains a sterile-α-motif (SAM), conserved region in CNK (CRIC), a PSD-95/DLG/ZO-1 (PDZ) domain, a Pleckstrin homology (PH) domain and a coiled region (CC). B - Immunofluorescence microscopy images of endogenous CNK1 and Fibrillarin in HeLa cells. C – Profile of immunofluorescence levels of endogenous CNK1 and fibrillarin through a single HeLa cell. Quantification of the immunofluorescence is present in Appendix B, Figure B1. Scale bars represent 10 μm.

3.2.2 The development and expression of Myc-CNK1.

We acquired a recombinant plasmid, pRK5-Myc-CNK1 (6832 bp) that encodes the cDNA sequence for CNK1 downstream of a high expression CMV promoter (Figure 3.2A). In this construct, CNK1 is tagged at the N terminal to a Myc epitope tag (Figure 3.2B) which permits the detection of the myc-CNK1 protein, ~90 kDa, with two specific antibodies; an anti-Myc and an anti-CNK1 antibody. We will refer to this plasmid as Myc-CNK1. The identity of the Myc-CNK1 was evaluated using restriction enzyme analysis with the enzymes *Bam* HI, *Cla* I and *Eco* RI (data not shown) and confirmed using Sanger sequencing. The sequence for the Myc-epitope tag fused to CNK1 is shown in Figure 3.2B.

HeLa cells were transfected with Myc-CNK1 and the expression of the protein of interest was detected using confocal immunofluorescence microscopy. The cells were probed with primary antibodies targeted to the Myc epitope tag and fibrillarin.

Cells transfected with Myc-CNK1 demonstrated elevated levels of CNK1 (Figure 3.2C vs. Figure 3.1B). Quantification of the level of fluorescence indicated an approximately 3-6 fold increase in the level of fluorescence (Figure 3.2D) for Myc-CNK1 compared to endogenous CNK1 (Figure 3.1B). This fluorescence was present in the cytoplasm and in the nucleus, there were elevated levels of cytoplasmic fluorescence and a noticeable increase in nuclear fluorescence. There was also a clear lack of Myc-CNK1 fluorescence in the nucleolar region of the Myc-CNK1-transfected cells (Figure 3.2C). The nucleolus is marked as the region that has a reduced level of DAPI fluorescence as well as an increased level of fibrillarin protein, a main structural component of the nucleolus (Scheer & Weisenberger, 1994) (Figure 3.2C).

The intensity of fluorescence was measured across a cell (indicted by the arrow on MERGE, Figure 3.2C) and graphically represented (Figure 3.2D). This graph indicates the reduced level of Myc-CNK1 in the area where DAPI fluorescence decreases and the fibrillarin increases indicating the validity of this observation. If this distribution of CNK1 occurred for both endogenous CNK1 as well as Myc-CNK1, it could be indicative of the cellular localization of CNK1. Alternatively, if this observation was only valid for Myc-CNK1, but not for endogenous CNK1, then this would be a consequence of the epitope tag.

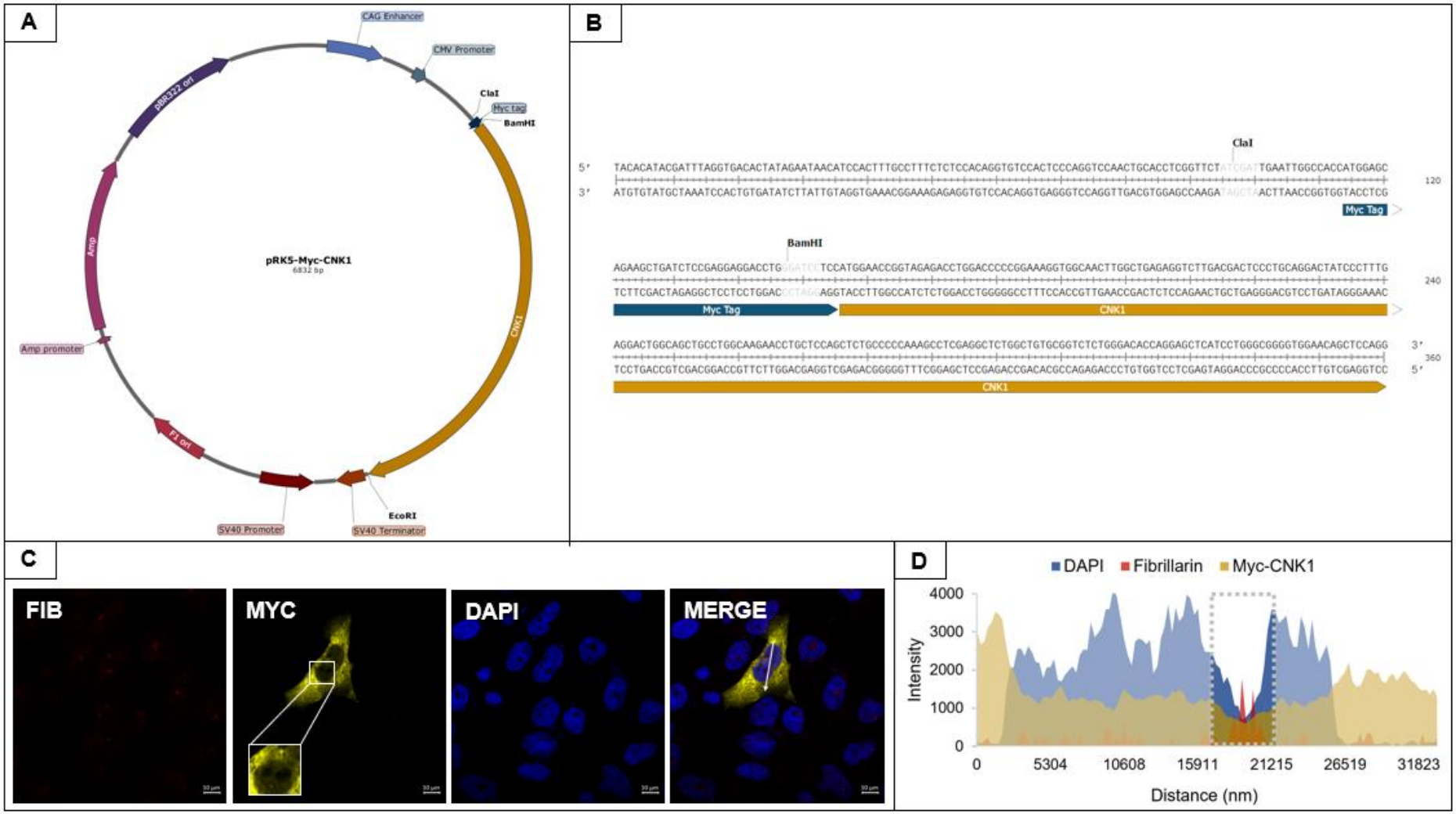

Figure 3.2: Localisation studies of Myc-CNK1 in HeLa cells using confocal immunofluorescence microscopy. A – Plasmid map of Myc-CNK1; B – Sequence showing the Myc-tag at the N-terminal of CNK1; C - Immunofluorescence microscopy images of HeLa cells transfected with Myc-CNK1 and probed for endogenous fibrillarin, D – Profile of immunofluorescence levels of transfected Myc-CNK1 and endogenous fibrillarin through a single HeLa cell. Quantification of the immunofluorescence is present in Appendix B, Figure B1. Scale bars represent 10 μm.

3.2.3 Detection of FLAG-CNK1 using confocal immunofluorescence microscopy

To better understand the protein localization observed for endogenous CNK1 and Myc-CNK1 using confocal immunofluorescence microscopy, we decided to test a second epitope tag upstream of CNK1.

The plasmid, pRK5-FLAG-CNK1 (6826 bp) encodes CNK1 tagged with at the N terminal of the protein with a FLAG tag (Figure 3.3A). This fusion protein should be detectable by both the anti-FLAG and anti-CNK1 antibodies. We will refer to the ~90 kDa protein generated by this construct as FLAG-CNK1. The plasmid DNA was analysed using restriction analysis with *Cla* I and *Bam* HI (data not shown) and confirmed using Sanger sequencing. The DNA sequence (confirmed by Sanger sequencing) for the FLAG epitope tag and CNK1 is shown in Figure 3.3B.

The plasmid expressing FLAG-CNK1 was transfected into HeLa cells and the fixed cells were probed with antibodies targeted against the FLAG epitope tag and fibrillarin (Figure 3.3C). Cells transfected with FLAG-CNK1 expressing DNA showed higher levels of immunofluorescence with anti-FLAG antibodies. The fluorescence levels of FLAG-CNK1 are approximately 4-fold higher than those obtained for endogenous CNK1 (Figure 3.3D vs. Figure 3.1C). The immunofluorescence was present in the cytoplasm and the nucleus; however, again we observed voids in the FLAG-CNK1 fluorescence within the nucleus of the transfected cells. The intensity of fluorescence was measured across a cell (indicted by the arrow on MERGE, Figure 3.3C) and graphically represented (Figure 3.3D). As we observed for Myc-CNK1, the levels of FLAG-CNK1 are lower in the nucleolus than they are in the nucleus and in the cytoplasm of the HeLa cell.

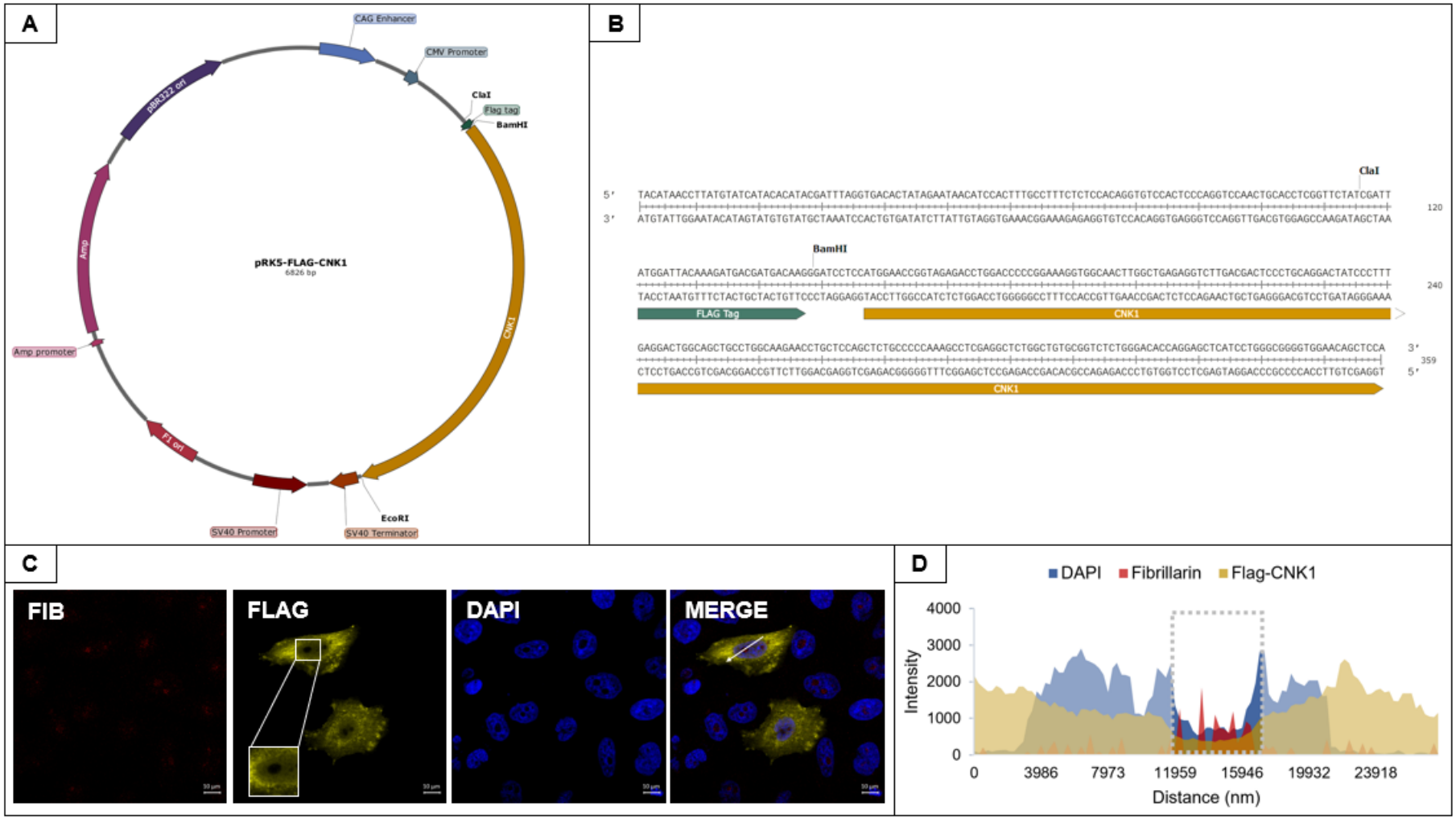

Figure 3.3: Localisation studies of FLAG-CNK1 in HeLa cells using confocal immunofluorescence microscopy. A – Plasmid map of FLAG-CNK1; B – Sequence data showing the FLAG-tag at the N-terminal of CNK1; C - Immunofluorescence microscopy images of HeLa cells transfected with FLAG-CNK1 and probed for endogenous fibrillarin, C – Profile of immunofluorescence levels of transfected FLAG-CNK1 and endogenous fibrillarin through a single HeLa cell. Quantification of the immunofluorescence is present in Appendix B, Figure B1. Scale bars represent 10 μm.

The observation that Myc-CNK1 and FLAG-CNK1 were present in the cytoplasm and the nucleus but were excluded from the nucleolus led us to query the effect of the Myc and FLAG epitope tags on the cellular distribution of CNK1. To address these queries, we decided to insert the Myc and FLAG epitope tags at the N terminal and C terminal of a commonly used fluorescent reporter protein, EGFP. EGFP is a 29 kDa protein (Akbar & Kim, 2005) that is distributed throughout the cell, the cytoplasm and the nucleus, by passive diffusion (Lange, et al., 2007). The intention was to determine the effect of the Myc and FLAG epitope tags on the localisation of EGFP in the HeLa cell.

3.2.4 Antibody specificity

Untransfected (Appendix A1.1), Myc-CNK1 transfected (Appendix A1.2) and FLAG-CNK1-transfected (Appendix A1.3) cells were probed with antibodies directed against endogenous CNK1, the Myc epitope tag and the FLAG epitope tag (Appendix A). These samples were used to optimize the parameters for confocal immunofluorescence microscopy. These data show that the antibodies for CNK1, Myc tag and FLAG tag specifically detect the targets of interest.

3.2.5 Development of EGFP-N1 epitope-tagged constructs

EGFP-N1 encodes EGFP with a multiple cloning site at the N-terminal of the sequence encoding the reporter protein (Figure 3.4A). Oligonucleotides encoding the Myc or FLAG tag were inserted at the N terminal using the restriction enzymes *Hind* III and *Kpn* I. Sanger sequencing was used to validate Myc and FLAG epitope tag encoding plasmids (Figure 3.4B and Figure 3.4C respectively).

HeLa cells were transfected with EGFP-N1, Myc-EGFP-N1 or FLAG-EGFP-N1 and analysed using confocal immunofluorescence microscopy (Figure 3.5). EGFP was distributed throughout the cell; in the cytoplasm and the nucleus (Figure 3.5, 1A). A profile of the immunofluorescence indicated no reduction in the nucleous of the nucleus (Figure 3.5, 1B). The EGFP was not detected by anti-Myc or anti-FLAG primary antibodies (data not shown).

In contrast to EGFP, Myc-EGFP and FLAG-EGFP (detected using anti-Myc and anti-FLAG antibodies respectively) was detected in the cytoplasm and the nucleus, but the epitope-tagged EGFP was excluded from the nucleoli of the nucleus (Figure 3.5, 2A and 3A). This reduction was also observed in the profile of the immunofluorescence taken across a single HeLa cell (indicated by the arrow in Figure 3.5, 1A, 1B and 1C, in the image labelled MERGE).

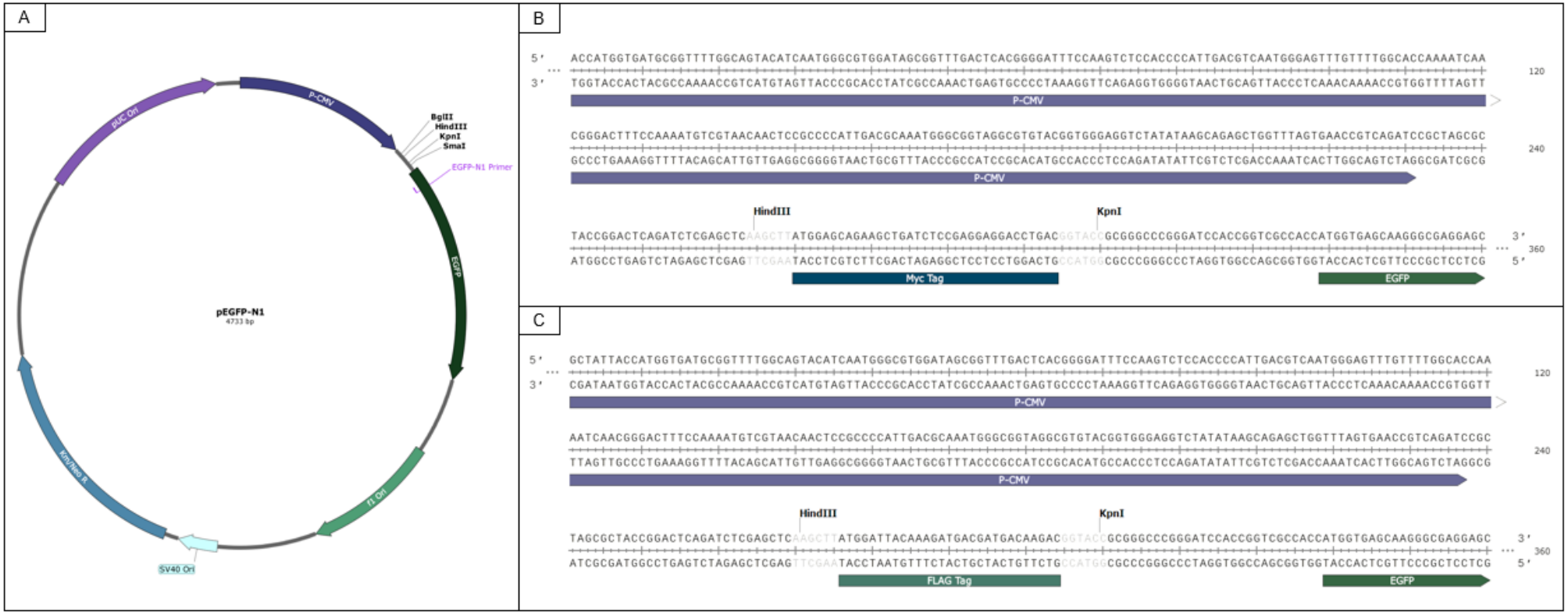

Figure 3.4: Plasmid map of EGFP-N1 and DNA sequence analysis of epitope-encoding EGFP-N1. A - Plasmid map of EGFP-N1; DNA sequence showing the Myc (B) and FLAG (C) tags in EGFP-N1.

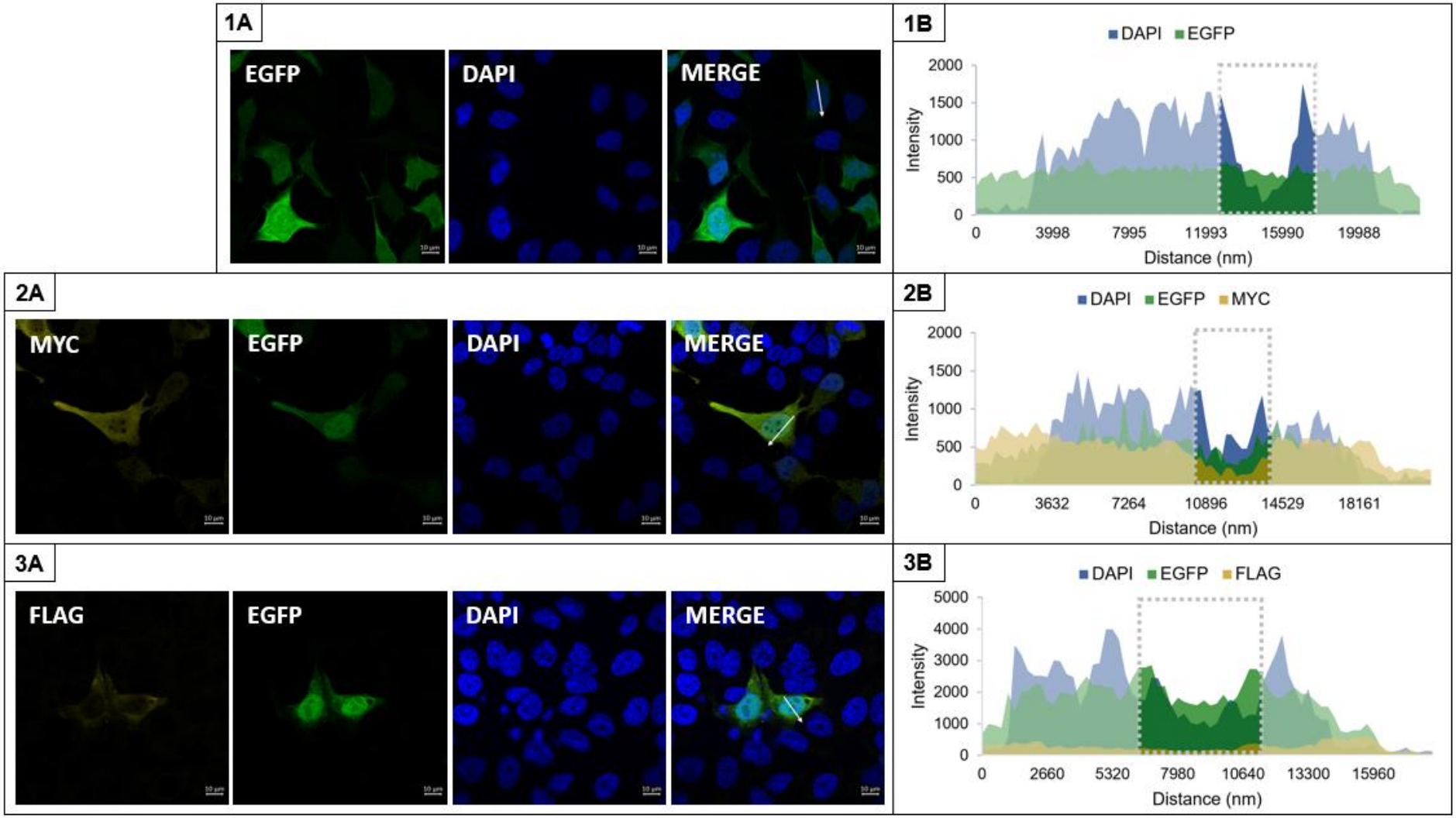

Figure 3.5: Localisation studies of epitope-tagged EGFP-N1 in HeLa cells using confocal immunofluorescence microscopy. 1A - Immunofluorescence microscopy images of EGFP expressed in HeLa cells transfected with EGFP-N1, 1B – Profile of immunofluorescence levels through a single HeLa cell. 2A - Immunofluorescence microscopy images of HeLa cells transfected with Myc-tagged EGFP, 2B – Profile of immunofluorescence levels in a single cell transfected with Myc-EGFP. 3A - Immunofluorescence microscopy images of HeLa cells transfected with Flag-tagged EGFP, 3B – Profile of immunofluorescence levels in a single cell transfected with FLAG-EGFP-N1. Quantification of the immunofluorescence is present in Appendix C, Figure C1. Scale bars represent 10 μm.

3.2.6 Development of EGFP-C1 epitope-tagged constructs

EGFP-C1 encodes for EGFP with a multiple cloning site at the C-terminal of the fluorescent reporter protein (Figure 3.6A). Oligonucleotides encoding the Myc and FLAG epitope tags were inserted into the *Hind* III and *Kpn* I restriction enzyme sites and the integrity of the constructs was confirmed using Sanger sequencing (Figure 3.6B and 3.6C, respectively).

Constructs expressing EGFP-C1, Myc-EGFP-C1 and FLAG-EGFP-C1 were transfected into HeLa cells and the immunofluorescence detected using confocal immunofluorescence microscopy. The EGFP protein was detected throughout the cell, in the cytoplasm, the nucleus and also the nucleolus (Figure 3.7, 1A). The profile of the fluorescence indicates no noticeable reduction in the level of fluorescence in any specific part of the cell (Figure 3.7, 1B). In contrast, the Myc-EGFP-C1 and FLAG-EGFP-C1 immunofluorescence (detected using anti-Myc and anti-FLAG antibodies respectively) was present in the cytoplasm and the nucleus but was excluded from the nucleolus of the nucleus (Figure 3.7, 2A and 3A). A profile of the immunofluorescence across a single cell also appears to support this observation (Figure 3.7), but to a lesser degree than was observed for the Myc- and FLAG-tagged EGFP constructs above (Figure 3.5).

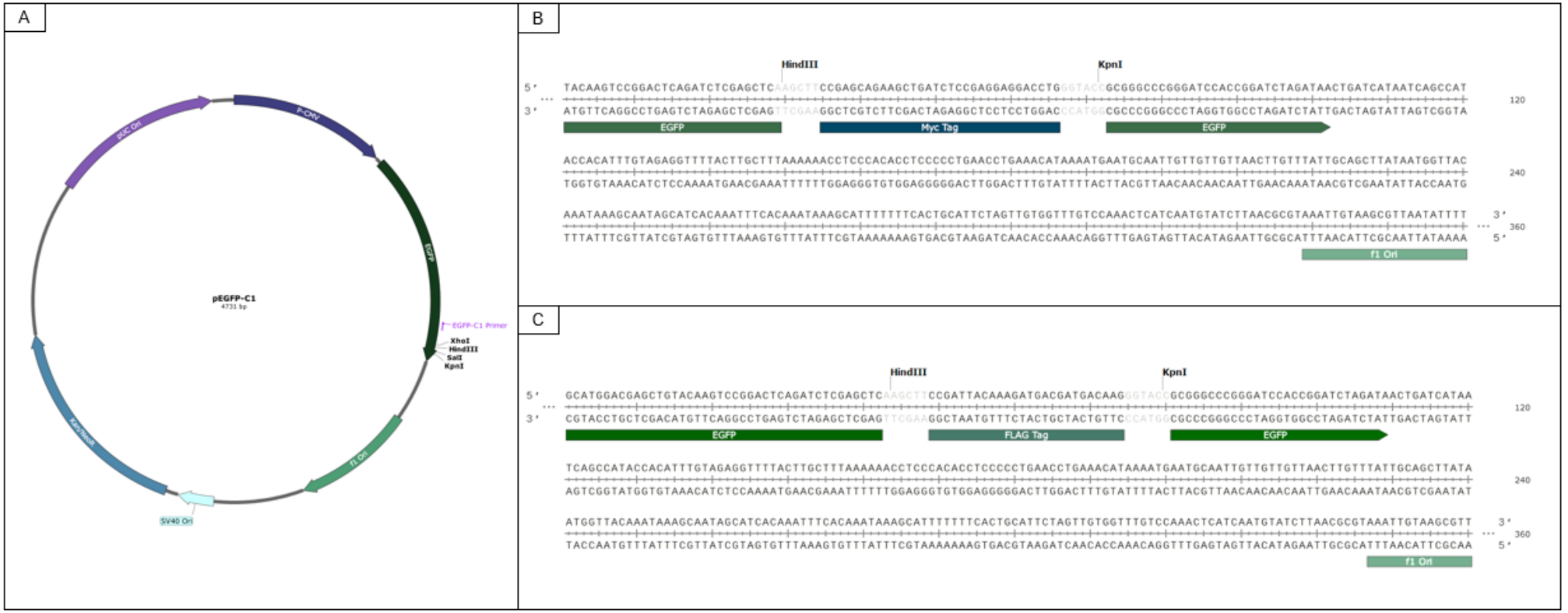

Figure 3.6: Plasmid map and sequencing of EGFP-C1. A - Plasmid map of EGFP-C1; DNA sequence showing the Myc (B) and FLAG (C) tag in EGFP-C1.

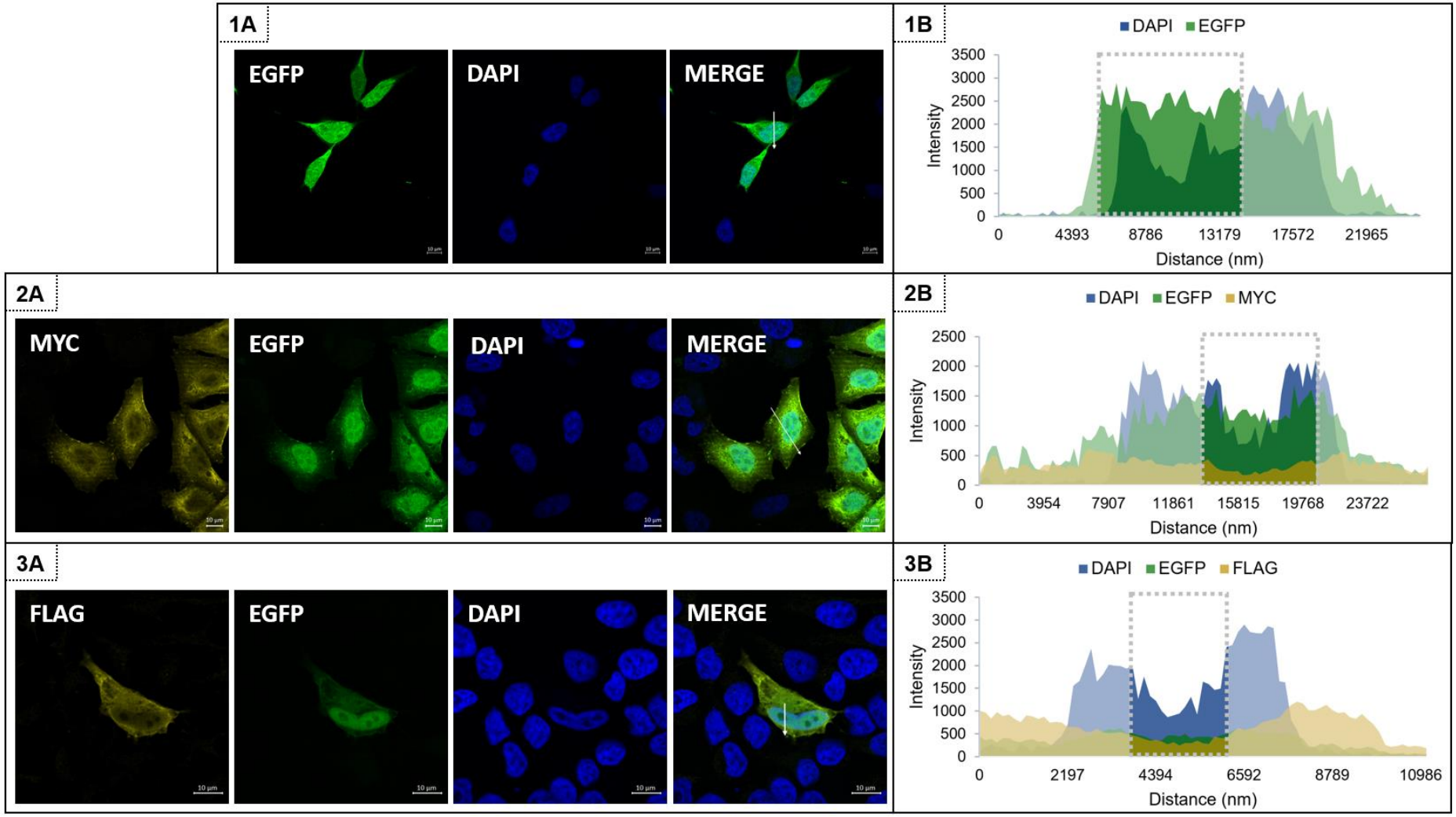

Figure 3.7: Localisation studies of tagged EGFP-C1 in HeLa cells using confocal immunofluorescence microscopy. 1A - Immunofluorescence microscopy images of HeLa cells transfected with EGFP-C1, 1B – Profile of immunofluorescence levels of a single EGFP-C1-expressing cell. 2A - Immunofluorescence microscopy images of HeLa cells transfected with Myc-EGFP-C1, 2B – Profile of immunofluorescence levels of a cell transfected with Myc-EGFP-C1. 3A - Immunofluorescence microscopy images of cells of FLAG-EGFP-C1 transfected HeLa cells, 3B – Profile of immunofluorescence levels through a single cell expressing FLAG-EGFP-C1. Quantification of the immunofluorescence is present in Appendix C, Figure C1. Scale bars represent 10 μm.

The detection of the reduction in nucleolar fluorescence for HeLa cells transfected with epitope-tagged constructs was visually apparent (Figures 3.2C, 3.3C, 3.5 and 3.7). The quantification of the fluorescence in the microscopy images using ImageJ was a challenge. We highlighted areas of interest manually and quantified fluorescence therein. Any slight movement outside the desired regions resulted in changes in the levels of fluorescence. The quantification of fluorescence data does support our observations and we provide this data in Appendices B and C but we are not belabouring the data.

The linkage of the Myc and FLAG epitope tags to EGFP resulted in a change in the localization of the EGFP protein. There was a noticeable reduction in the level of EGFP in the nucleolus of epitope-tagged EGFP expressing constructs than those expressing untagged EGFP. This effect was observed when the epitope tag was placed at both the N and the C terminal of EGFP.

In an attempt to understand why we observed this change in fluorescence, we studied the sequence of the Myc and FLAG epitope tags (Figure 3.8).

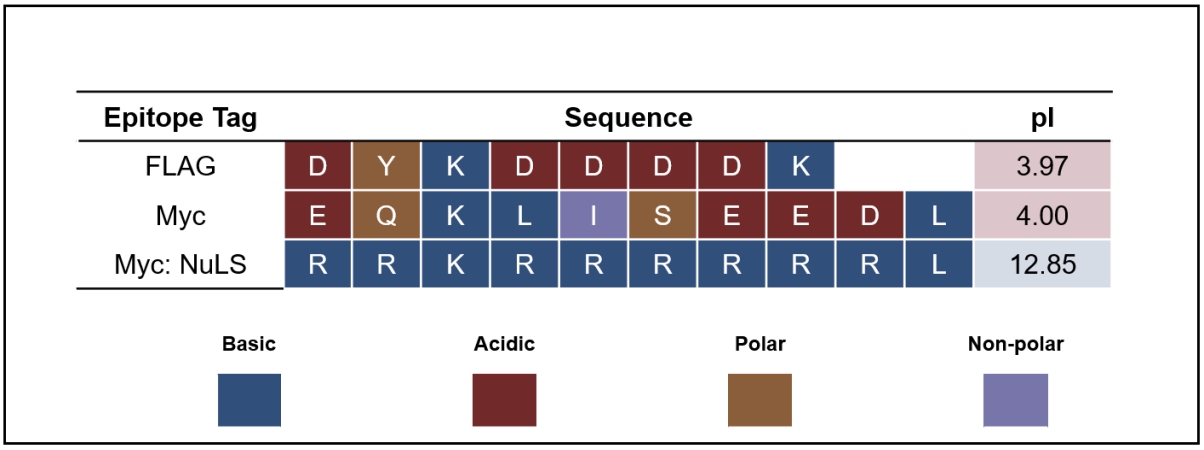

Figure 3.8: Analysis of the Myc and FLAG epitope tag sequence.

The Myc tag is encoded by residues EQKLISEEDL in which E and D are acidic residues, Q and E are polar residues and K and L are basic residues, contributing to an overall pI of 3.97. The FLAG tag is encoded by DYKDDDDK, in which D is an acidic residue, Y is polar residue and K is a basic residue, contributing to an overall pI of 4.00. Both the Myc and the FLAG tag are therefore acidic sequences. In a search of the literature, we found that Martin *et al.*, had performed a study on the localization of sequences with varying pI values and found that sequences with an acidic pI were excluded from the nucleolus and those with an elevated pI (12.6 and higher) were localized to the nucleolus (Martin, et al., 2015). The elevated pI of over 12.6 was achieved by the inclusion of 4 to 6 arginine residues within a sequence of 15 amino acids. As the nucleolar compartment is acidic in comparison the surrounding nucleoplasm, it

provides a suitable electrochemical environment to bind poly-arginine containing proteins resulting in their localization (Martin, et al., 2015).

The findings of Martin *et al.* led us to hypothesize that the low pI of the Myc and FLAG tags may be the primary reason for the exclusion of the epitope-tagged EGFP from the nucleolus of the nucleus in HeLa cells. To determine if this was the case, oligonucleotides encoding a modified Myc sequence (Myc: NuLS, Figure 3.8) was designed where the acidic, polar and non-polar residues were replaced with arginine residues, to provide an epitope tag with an overall pI of 12.85.

3.2.7 Development of Myc-NuLS encoding EGFP constructs

Oligonucleotides encoding Myc: NuLS were inserted into the *Bgl* II and *Sma* I restriction sites of EGFP-N1 and into the *Xho* I and *Sal* I restriction sites of EGFP-C1. The integrity of the DNA sequence in the constructs was validated using Sanger sequencing (Figure 3.9A and 3.9B).

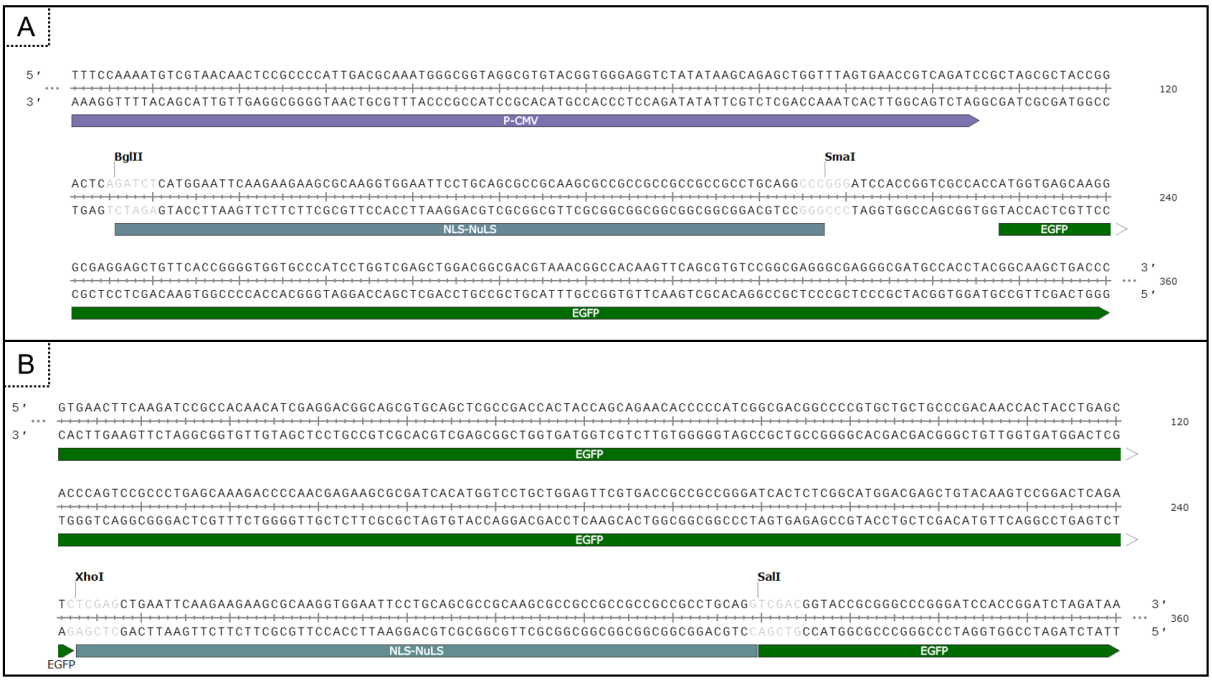

Figure 3.9: Cloning the Myc: NuLS into EGFP-N1 and EGFP-C1. A – DNA sequence analysis of the Myc-NuLS at the N terminal of EGFP, B- DNA sequence analysis of the Myc: NuLS at the C terminal of EGFP.

Constructs expressing the Myc: NuLS sequence were transfected into HeLa cells and the fixed cells were analysed by confocal immunofluorescence microscopy (Figure 3.10).

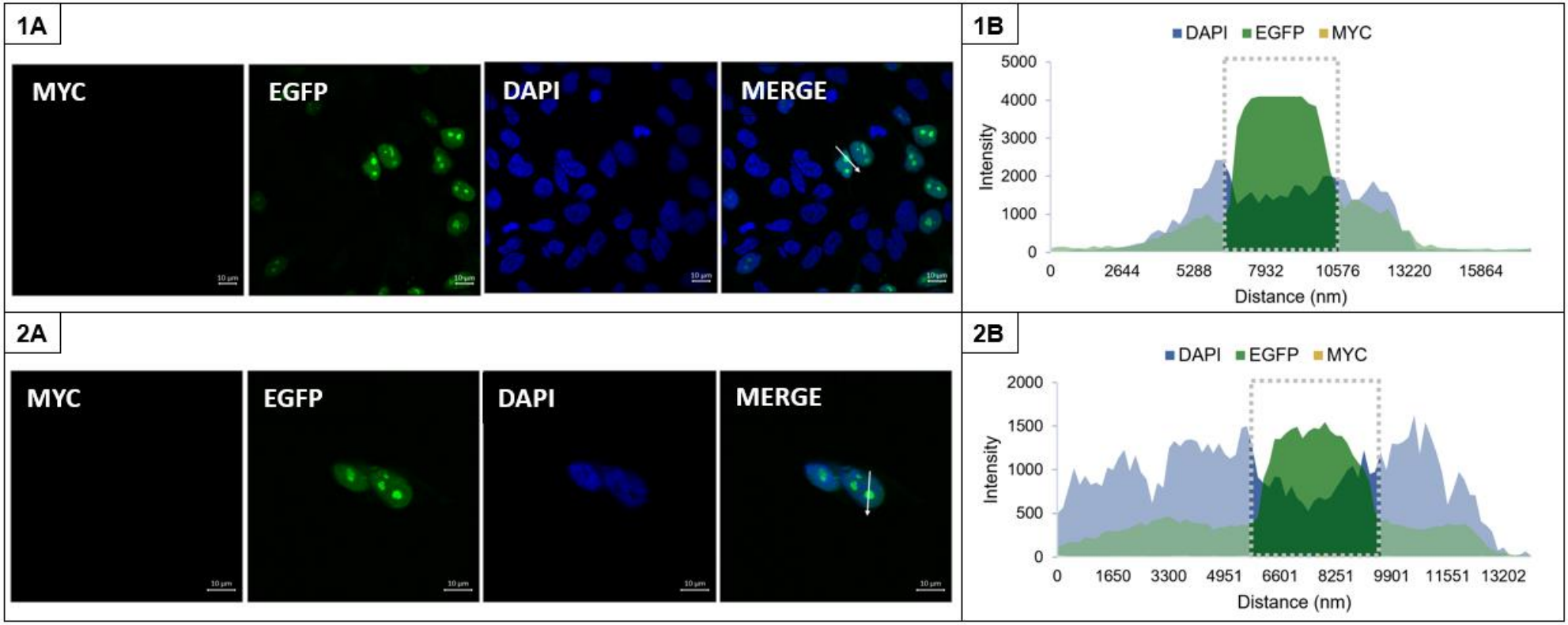

Figure 3.10: Localisation studies of altered Myc tag (Myc: NuLS) fused to EGFP-N1 and EGFP-C1 in HeLa cells using confocal immunofluorescence microscopy. 1A - Immunofluorescence microscopy images of HeLa cells transfected with NLS-NuLS tagged EGFP-N1, 1B – Profile of immunofluorescence levels of a single HeLa cell transfected with Myc: NuLS tagged EGFP-N1. 2A - Immunofluorescence microscopy images of HeLa cells transfected with Myc: NuLS EGFP-C1, 2B – Profile of immunofluorescence levels of a single cell transfected with Myc: NuLS tagged EGFP-C1. Quantification of the immunofluorescence is present in Appendix C, Figure C1. Scale bars represent 10 μm.

HeLa cells transfected with Myc: NuLS EGFP-N1 and Myc: NuLS EGFP-C1 both showed nuclear, and particularly nucleolar, localization of EGFP (Figure 3.10). The intensity of fluorescence was measured across a cell (indicted by the arrow in MERGE, Figure 3.10 1A and 1B) and graphically represented. The immunofluorescence data corroborates the visual observation that the Myc: NuLS EGFP-N1 and Myc: NuLS EGFP-C1 were localised to the nucleoli of the nuclei of the cells.

We therefore conclude that the modification of the Myc tag to remove the acidic residues and to include the basic residues results in a change in the localization of EGFP within the cell. These data support the observations previously reported by Martin *et al* (2015).

We have observed that the Myc and FLAG tags result in the exclusion of the CNK1 and EGFP from the nucleolus of the HeLa cell nucleus. The question that remains- what is the nuclear localization of endogenous CNK1 in the HeLa cell? The use of epitope tags that alter the localization of a protein of interest, in this case CNK1 is not appropriate in a study that examines the interacting partners of that protein. To address this question, we decided to generate a CNK1-EGFP fusion construct and to visualise the localization of elevated levels of CNK1-EGFP in the HeLa cell.

CNK1 was excised from Myc-CNK1 using *Bam* HI and *Eco* RI and cloned into the *Bgl* II and *Eco* RI sites of EGFP-C1. The junctions of the construct were validated using Sanger sequencing (data not shown). This CNK1-EGFP construct was transfected into HeLa cells and the cells examined by confocal immunofluorescence microscopy (Figure 3.11).

CNK1-EGFP based EGFP fluorescence was present primarily in the cytoplasm of HeLa cells but fluorescence was also detected in the nucleus. The levels of fluorescence were 6-8 fold higher in CNK1-EGFP expressing HeLa cells (Figure 3.11A) than the fluorescence of endogenous CNK1 in HeLa cells (Figure 3.1C).

Interestingly, visually, we detect lower levels of fluorescence in the nucleolar regions of the nuclei of CNK1-EGFP transfected HeLa cells (Figure 3.11A). This reduction in fluorescence can be attributed to the presence of CNK1 in the CNK1-EGFP fusion. We do observe a small reduction in the profile of the immunofluorescence data however these data are not clear (Figure 3.11B). Based on our visual observation of the confocal immunofluorescence data, we conclude that the CNK1-EGFP is also excluded from the nucleolus of the HeLa cells.

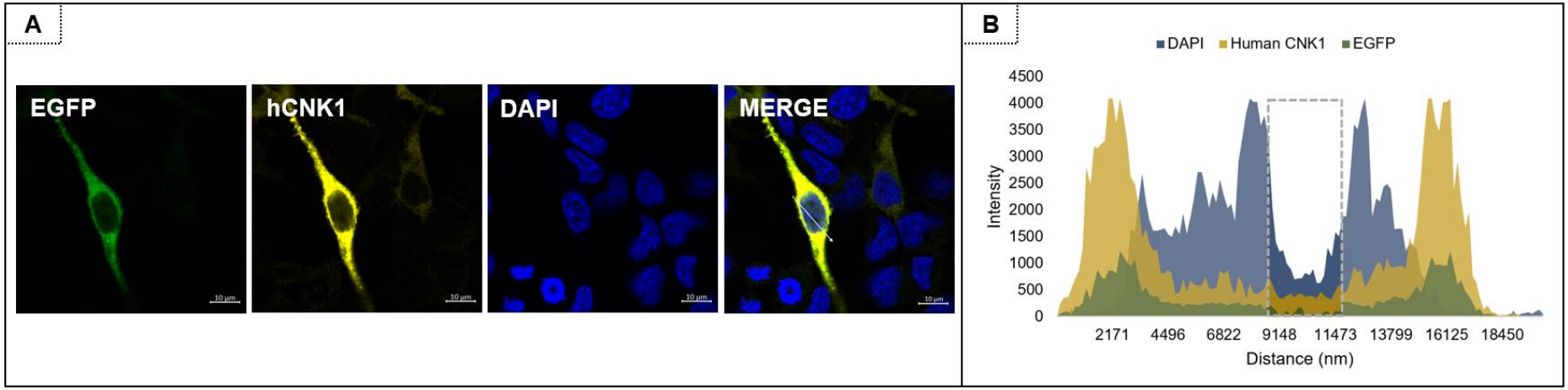

Figure 3.11: The expression of EGFP-CNK1 observed using confocal immunofluorescence microscopy. A - Immunofluorescence microscopy images of HeLa cells transfected with CNK1-EGFP, B – Profile of immunofluorescence levels of a single HeLa cell transfected with CNK1-EGFP. Scale bars represent 10 μm.

3.3 CONCLUSIONS

We wish to study the interaction partners of CNK1 in HeLa cells. To ensure that our interaction data are meaningful, we need to validate our ability to detect our protein of interest, CNK1. In addition, we need to ensure that the epitope-tagged constructs that we use to overexpress our protein of interest generate a protein that is comparable to the endogenous CNK1. As we are interested in identifying the interacting partners of CNK1, we used confocal immunofluorescence microscopy to test the specificity of the antibodies used in this study, to demonstrate the expression of CNK1 and to study the localization of CNK1 in the cell.

In this chapter, we highlighted that the levels of endogenous CNK1 are low. This has implications in the use of the endogenous proteins in the identification of binding partners. In an attempt to address this, we enhanced the levels of expression by using a CNK1 expression plasmid, which produced a Myc-tagged protein. Using this construct, we successfully elevated the levels of detectable CNK1 in the cell.

We noticed during the course of our experiments that Myc-CNK1 and FLAG-CNK1 were excluded from the nucleolus of the nuclei in the HeLa cell. This is an interesting observation, and not one that has been reported previously for either the Myc or the FLAG tag. This data highlights the potential consequences of the addition of epitope tags on protein structure, function and localization. The number and size of nucleoli in mammalian cells differ, they are dependent on rDNA synthesis and ribosomal assembly (Banski, et al., 2010). The nucleolus also hosts critical proteins such as chaperones, co-chaperones and multitasking proteins (Banski, et al., 2010). The nucleolus composition varies dependent on cellular processes such as cell cycle progression, signalling responses to stress, tumour development and viral infections (Raska, et al., 2006). The nucleolus is dynamic, it is not bound by a lipid membrane and many proteins harboured within it or translocating between the nucleus and the nucleolus do not possess a distinctive nucleolus localisation signal (O'Day & Catalana, 2013).

We performed experiments to explain why the Myc and FLAG epitope tags resulted in the nucleolar exclusion of CNK1. In addition, we used CNK1-EGFP to show that the CNK1 protein itself is excluded from the nucleolus, an observation not well established in current literature. In this chapter we validated the use of the Myc and FLAG epitope tags in the design of CNK1 overexpression constructs for further interaction studies. In the next chapter, we shall perform co-immunoprecipitation experiments to identify the binding partners of CNK1 in the NF-κB pathway.

CHAPTER 4: IDENTIFICATION OF THE INTERACTING PARTNERS OF CNK1 IN THE NF-κB PATHWAY

4.1 INTRODUCTION

4.1.1 CNK1 interacting partners

CNK1 is involved in a number of key mammalian cellular pathways. The role of CNK1 in the MAPK pathway, which is involved in cell proliferation (Anselmo et al, 2002; Ziogas et al, 2005) has been well defined. In this pathway, CNK1 acts as a scaffold protein aligning RAS, Raf, MEK and KSR to facilitate the stimulation of the signal cascade (Claperon and Therrien, 2007; Therrien et al, 1998; Pan et al, 2012). CNK1 also interacts with the angiotensin II receptor suggesting that it may mediate signalling downstream of the AT_2 receptor resulting in antiproliferative responses (Fritz and Radziwill 2005). The interaction of CNK1 with RASSF1A and the RASSF1A-MST protein complex results in CNK1-induced apoptosis (Rabizadeh et al. 2004). The RASSF1 proteins have a role in the Hippo pathway that determines the size and the shape of the organ development (Fausti et al. 2012). Binding of CNK1 to cytohesin at the cell membrane mediates a signal cascade through the PI3K/AKT pathway (Fritz and Radziwill 2011), key to insulin signalling (Lim et al. 2010), raising the possibility that CNK1 may play a role in diabetes. Data have shown CNK1 binding to Rho-specific guanine exchange factors results in the specificity of signalling downstream of Rho in the JNK pathway (Cho et al, 2014; Jaffe et al, 2005). The JNK pathway has been identified as having a role in cancer, neurological disorders and inflammation (Sabapathy, 2012). In addition, CNK1 is a tumour promoter protein that is functional in breast cancer cells and plays a role in the NF-κB pathway (Fritz and Radziwill, 2010). This is particularly interesting considering the role of NF-κB in inflammation and the increasing body of evidence linking inflammation with cancer, and particularly breast cancer (Lu et al, 2006; Karin et al, 2002). The diversity of pathways in which CNK1 functions underscores the importance of CNK1 in mammalian cells.

To better understand the role of CNK1 in these pathways, we investigate the interactions between CNK1 and its partner proteins.

i. Cytohesin

Cytohesin, belonging to a family of guanine nucleotide exchange factor (GEFs), has been described as an interacting partner of CNK1 in insulin signalling mediating AKT activation (Lim , et al., 2010). Cytohesin possesses a coiled coil domain, which interacts with the C-

terminal (Figure 4.1.A) of CNK1 (Lim , et al., 2010). Insulin stimulation promotes the accumulation of CNK1 and recruitment of cytohesin to the plasma membrane. The assembly of this complex facilitates the activation of PI3K/AKT signalling (Lim , et al., 2010).

ii. AKT

CNK1 is a regulator of AKT-dependent cell proliferation. Here, CNK1 binds directly to AKT to induce positive feedback (Fischer, et al., 2015). In growth stimulated cells, the Ser22 (Figure 4.1.B) of the SAM domain of CNK1 is responsible for AKT phosphorylation. AKT phosphorylation induces oligomerization of CNK1, resulting in an increased affinity for active AKT (Fischer, et al., 2017). In proliferating cells, the presence of EGF results in the phosphorylation of Thr8 (Figure 4.1.C) within the SAM domain of CNK1 causing inhibition of AKT-CNK interaction and abrogation of CNK1-mediated AKT signalling (Fischer, et al., 2017).

iii. RAF

RAF-1 is a regulator of proliferation, differentiation and apoptosis, all of which are critical cellular pathways (Ziogas, et al., 2005).

We mentioned above that CNK1 mediates EGF-dependent AKT signalling. AKT also interacts with RAF and AKT-RAF cross talk results in RAF- dependent ERK activation in differentiated cells. At low doses of EGF, CNK1 binds RAF causing activation of ERK (Fischer , et al., 2016). At high doses of EGF, CNK1 binds to active AKT causing the inhibition of RAF and supressing activation of ERK (Fischer , et al., 2016). The inhibition of ERK activation by AKT-CNK1 complex is not observed in proliferating cells, only in differentiating cells (Fischer , et al., 2016). RAF-1 is also activated by CNK1 in an SRC-dependent tyrosine phosphorylation manner (Ziogas, et al., 2005). The key regulatory sites for this activation are located at Tyr26, Tyr519 and Tyr665 of CNK1 (Figure 4.1.D-F). Induction with platelet-derived growth factor (PDGF) facilitates the dimerization of CNK1 by phosphorylation at Tyr26 (Figure 4.1.D) enabling binding of CNK1 to SRC (Fischer, et al., 2015). The binding of SRC results in the phosphorylation of the regulatory tyrosine sites of CNK1 allowing the CNK1-SRC complex to form a trimeric structure with pre-activated RAF-1 (Fischer, et al., 2015). The phosphorylation of CNK1 at Tyr519 (Figure 4.1.E) promotes the nuclear localisation of CNK1 (Fischer, et al., 2015).

iv. Rho & Ras

The Rho GTPase family is responsible for a variety of cellular responses such as cytoskeletal rearrangements, changes in gene expression and cellular transformations (Jaffe, et al., 2004). Rho is in its active state when bound to GTP, which permits interactions between Rho and effector molecules such as CNK1. Rho has been indicated to bind to the PH domain (Figure 3.1.G) in a GTP-dependent manner (Jaffe, et al., 2004). CNK1 interacts with Rhophilin (Rho effector) and RalGDS (RAS effector) mediating cross talk between the two (Rho and Ras) signalling pathways (Jaffe, et al., 2004). Mutation of the SAM domain or CRIC domain inhibits the ability of CNK1 to interact with activated RAS (Jaffe, et al., 2004) highlighting these interactions as key in activation of the Ras pathway.

4.1.2 CNK1 in the NF-κB pathway

We have discussed the canonical and non-canonical NF-κB pathways in the literature review. In 2010, Fritz and Radziwill reported that CNK1 played a role in the NF-κB pathway. The authors showed that there was a link between the level of CNK1 and the level of NF-κB2 (p52), indicating that CNK1 was involved in the non-canonical pathway. Fritz and Radziwill (2010) used BAY11-7082 as an IKK inhibitor to inhibit both the canonical and the non-canonical pathways. Based on their study with TNFα and the inhibitor BAY11-7082, the authors proposed that CNK1 acts upstream of IKKα, but not IKKβ, to control IKKα-dependent substrate phosphorylation. In a subsequent study performed by Strickson *et al*. (2013), BAY11-7082 was described as an inhibitor of the enzymes that are involved in the ubiquitin degradation pathway and therefore of the proteasome. With this new information about the point of action of BAY11-7082, it merits the reinterpretation of the data reported by Fritz and Radziwill (2010). In addition, it highlights that the interacting partner of CNK1 in the NF-κB remains unknown.

4.1.3 Problem Statement

While published data indicated that CNK1 has a role in NF-κB signalling, the interacting partner of this protein remains unknown.

Fritz & Radziwell, suggest that the interacting partner of CNK1 is upstream of the IKK complex in the non-canonical NF-κB pathway. In this chapter, we explore NIK as the interacting partner of CNK1 using western analysis and confocal immunofluorescence microscopy.

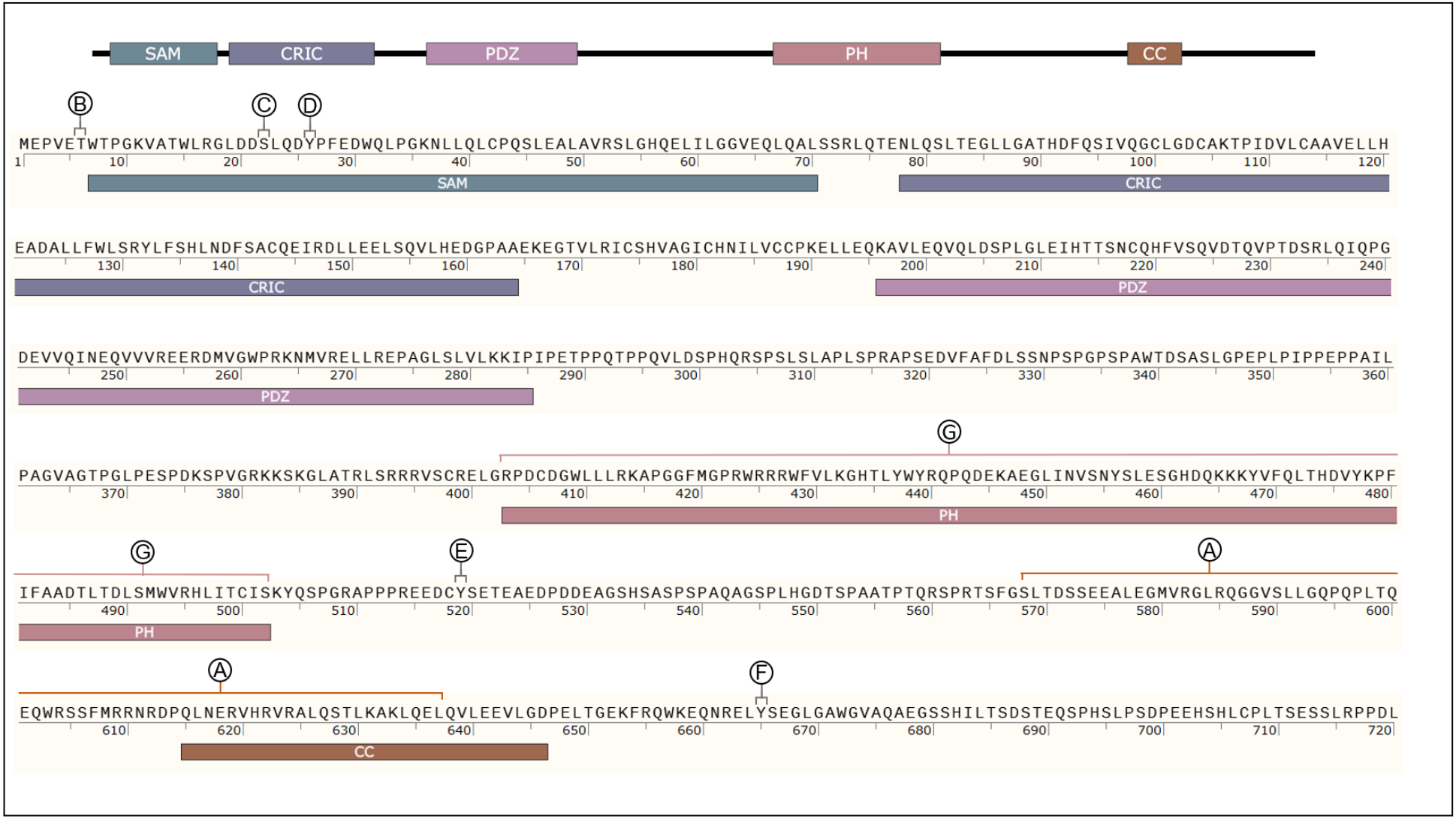

Figure 4.1: CNK1 protein sequence and interacting regions. A - Cytohesin interacting site; B – Ser22 site for AKT phosphorylation; C - Thr8 inhibition site for AKT; D – Tyr26 phosphorylation site for dimerization of CNK1; E – Tyr519 phosphorylation promotes nuclear localisation of CNK1; F – Tyr665 phosphorylation (with Tyr26 & Tyr519) promotes Src-CNK1-RAF-1 trimeric complex; G- Rho interaction domain

4.2 RESULTS AND DISCUSSION

4.2.1. The fluorescence levels of endogenous CNK1 in HeLa cells activated with TNFα

CNK1 has been reported to play a role in the NF-κB pathway; a pathway that is stimulated by treatment with TNFα. To visualise the effect of TNFα on CNK1, we treated HeLa cells with TNFα for 15 minutes and then fixed the HeLa cells for confocal immunofluorescence microscopy. These cells were probed with antibodies directed against endogenous CNK1 (Figure 4.2). When HeLa cells were treated with TNFα, we observed an increase in the levels of CNK1 (Figure 4.2B vs. 4.2A). The fluorescence level of CNK1 when activated with TNFα was approximately 2-fold higher than endogenous levels of CNK1 (Figure 4.2B vs.4.2A). This corroborates that there is a link between the NF-κB pathway and CNK1. Interestingly, the treatment of HeLa cells with TNFα results in the enhanced fluorescence of CNK1 in the nucleus of the cells, which suggests that CNK1 is translocating to the nucleus when induced. It is interesting to speculate about a possible role for CNK1 in the regulation of gene expression within the nucleus of the cell. If CNK1 functions as an inducer of gene expression, it then indicates that this multifunctional protein may also be a transcription factor.

Here, we focus on the interacting partners of CNK1 in the NF-κB pathway. It is therefore necessary to first optimise the immunoprecipitation reactions of CNK1 and its interacting partners and also to perform these experiments under conditions when the NF-κB pathway is induced with TNFα.

4.2.2. Analysis of Myc-CNK1-interacting partners in HeLa cells

In the previous chapter, we described and validated the Myc-tagged CNK1 expression construct (Myc-CNK1). Here, we performed experiments on untransfected HeLa cells (expressing endogenous and untagged CNK1) and Myc-CNK1 transfected HeLa cells (expressing both endogenous untagged CNK1 and Myc-tagged CNK1) that were untreated or treated with the inducer TNFα. Cell lysates containing these proteins were immunoprecipitated with anti-Myc antibodies linked to Protein A/G magnetic beads. These proteins were separated by SDS-PAGE and transferred to a PVDF membranes by western blotting. The membrane was probed with primary antibodies directed against CNK1, Myc, RAF-1 and NIK and then with HRP-linked secondary antibodies.

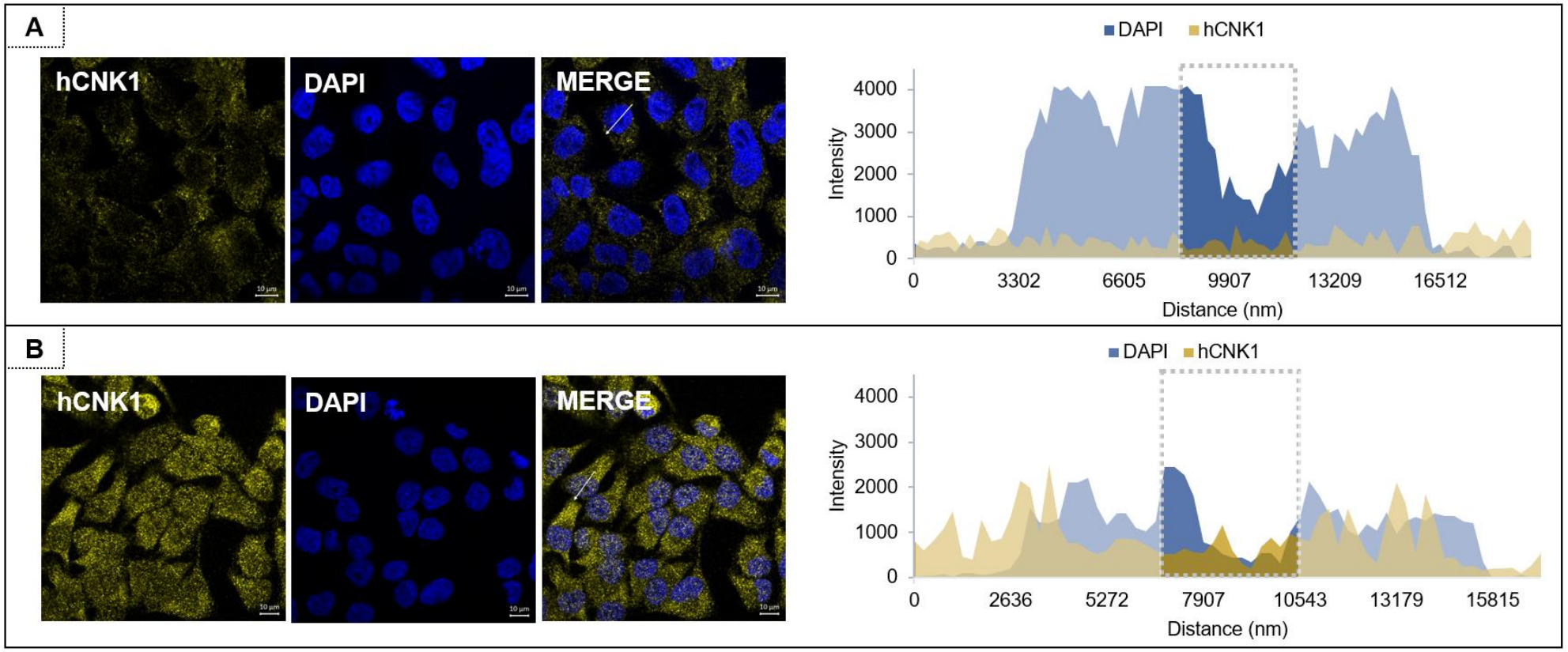

Figure 4.2: Endogenous CNK1 in TNFα-treated HeLa cells. A – Endogenous CNK1 probed with anti-CNK1 in untreated HeLa cells; B - Endogenous CNK1 probed with anti-CNK1 in TNFα-treated HeLa cells. Scale bars represent 10 μm.

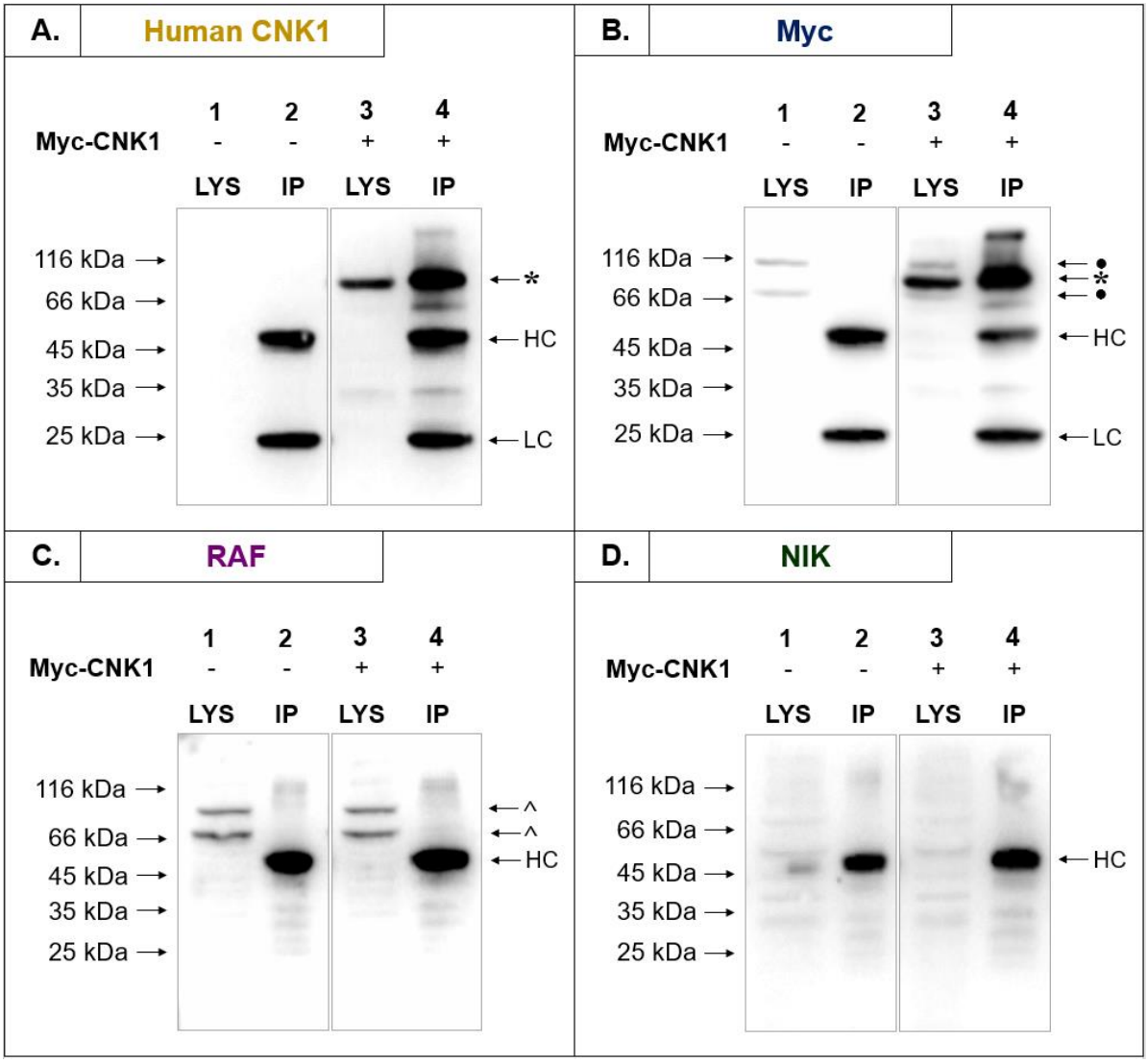

Figure 4.3: Western blot analysis of CNK1 from HeLa cells, immunoprecipitated with anti-Myc antibodies. Lane 1- Lysate (LYS) from untransfected (-) HeLa cells; Lane 2- immunoprecipitated (IP) Myc-CNK1 from untransfected (-) HeLa cells; Lane 3- lysate (LYS) from Myc-CNK1-transfected (+) HeLa cells; Lane 4- immunoprecipitated (IP) Myc-CNK1 from Myc-CNK1-transfected (+) HeLa cells. The proteins from one biological experiment were separated on SDS-PAGE gels and transferred to PVDF membranes which were probed with anti-CNK1 (mouse) (A), anti-Myc (mouse) (B), anti-RAF-1 (rabbit) (C) and anti-NIK (rabbit) (D). The HC and LC denote the bands for the heavy and light chains of the immunoprecipitating antibodies respectively. Myc-CNK1 is labelled with a (*). RAF-1 is labelled with (^). Unidentified interactions of the anti-Myc antibody are labelled with (•). These data represent one biological experiment but comparable data was obtained in replicate experiments.

There is no protein detected for endogenous CNK1 and for Myc-CNK1 in the lysate and the immunoprecipitation reactions from untransfected HeLa cells (Figure 4.3A and 4.3B, Lanes 1-2). This is because we used the anti-Myc antibody for the immunoprecipitation reactions and this would not immunoprecipitate or detect endogenous CNK1.

When HeLa cells were transfected with Myc-CNK, both the lysates and the immunoprecipitation reactions showed the presence of CNK1 and Myc-tagged CNK1 at ~90 kDa (Figure 4.3A and 4.3B, Lanes 3-4, CNK1 protein labelled with *). The detection of a protein of a similar size by the anti-CNK1 and the anti-Myc antibodies suggests that we are detecting Myc-CNK1 in transfected HeLa cells. The detection of higher levels of this protein in immunoprecipitated reactions when compared the lysates (Figure 4.3A and 4.3B, Lane 4 vs. Lane 3) indicates the efficiency of the immunoprecipitation of the Myc-CNK1.

The anti-Myc antibody detects two other proteins at ~116 kDa and ~64 kDa in the cell lysate (Figure 4.3B, Lanes 1 and 3, labelled with a •) however these are unidentified. It is possible that these proteins have a region with similarity to the Myc epitope that is recognised by the anti-Myc antibody. The anti-Myc antibody should detect the Myc protein (~ 49 kDa) in the cell lysates (Figure 4.3B, Lanes 1 and 3) however there is no detectable band that could represent this protein. It is likely that the level of the endogenous Myc protein is lower than the transfected Myc-CNK1 and so at this level of exposure, is undetected. The Myc protein should also be immunoprecipitated when using anti-Myc antibodies for the immunoprecipitation reactions however this band would be of the same size as the heavy chain of the immunoprecipitating antibody (~50 kDa), and so may be masked by this band (Figure 4.3B, Lanes 2 and 4).

Two protein bands are detected in the lysate of untransfected and Myc-CNK1 transfected HeLa cells at ~70 kDa and ~ 85 kDa (Figure 4.3C, Lanes 1 and 3, labelled with a ^). RAF-1 has been detected at between 73 - 75 kDa ((Roskoski, 2010); (Leicht, et al., 2007)) and the datasheet for the anti-RAF-1 antibody (Santa Cruz, C-20: sc-227) shows a positive protein band at ~90 kDa. These bands could represent RAF-1. There are no RAF-1 protein bands visible in the immunoprecipitated reactions (Figure 4.3C, Lanes 2 and 4) indicating that RAF-1 was not immunoprecipitated as an interacting partner of CNK1. The lack of RAF-1 could be attributed to the fact that the cells were not treated with an inducer of the MAPK or NF-κB pathways, which would enhance binding of RAF-1 and CNK1. Alternatively, it is possible that the conditions of the immunoprecipitation reactions were not optimal for the RAF-1 and CNK1 interaction and so the complex dissociated during the purification process.

No protein was detected in the lysates or in the immunoprecipitation reactions for NIK (Figure 4.3D, lanes 1-4). The lack of NIK, as was articulated for RAF-1, could be due to the lack of induction of the NF-κB pathway or a weak interaction. The lack of detection of the NIK protein

in all the samples could also indicate an antibody with poor sensitivity or very low levels of the NIK protein in the cells.

4.2.3. Investigating the effect of stabilizing the immunoprecipitation complexes on the identification of the binding partners of CNK1

In our previous data, we confirmed that our bait protein Myc-CNK1 was being immunoprecipitated by anti-Myc antibodies and being detected by anti-CNK1 and anti-Myc antibodies. We did not however detect RAF-1, a known interactor of CNK1, or NIK, our prey protein of interest. It is possible that we did not detect RAF-1 and NIK because the NF-κB pathway was not induced and so the prey proteins (RAF-1 and NIK) were not binding to CNK1. Alternatively, it was possible that the interactions between CNK1 and its interacting partners RAF-1 and NIK may be weak. If this was the case, then during immunoprecipitation under non-optimal conditions, we may not detect the proteins of interest.

We researched techniques to stabilise the protein complexes before immunoprecipitation and decided to modify a technique usually used during the preparation of cell culture samples for confocal microscopy. Cells being prepared for confocal microscopy are fixed in paraformaldehyde or methanol to stabilize protein-protein and protein-lipid interactions within the cells. We decided to use the fixative paraformaldehyde as it was preferential for the stabilization of protein-protein interactions prior to immunoprecipitation.

Here, we transfected HeLa cells with Myc-CNK1 and treated the cells with the inducer TNFα. We performed traditional immunoprecipitation reactions and in a parallel experiment, we treated the lysates with 4% paraformaldehyde to stabilize the protein-protein interactions prior to immunoprecipitation. These reactions were separated by SDS-PAGE and transferred to PVDF membranes by western blotting. Membranes were probed with primary antibodies directed against CNK1, Myc, RAF-1 and NIK and then with HRP-linked secondary antibodies.

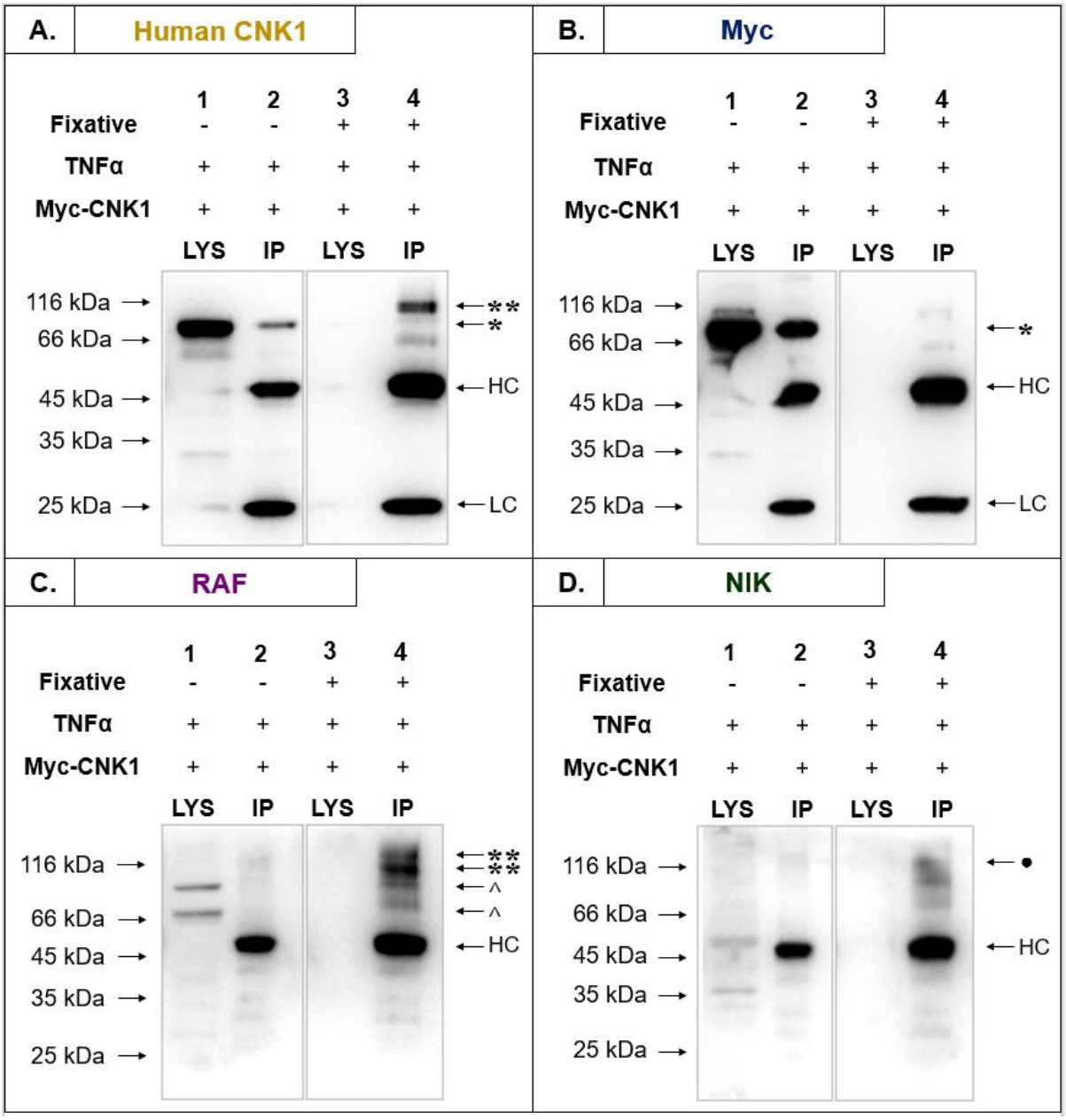

Figure 4.4: Western blot analysis of stabilized immunoprecipitation complexes of CNK1 and its interacting partners. Lane 1- Lysate (LYS) from Myc-CNK1 transfected (+) HeLa cells treated with 10 ng/µL TNFα (+); Lane 2- Immunoprecipitated (IP) proteins from Myc-CNK1 transfected (+) HeLa cells treated with 10 ng/µL TNFα (+); Lane 3- Lysate (LYS) from Myc-CNK1 transfected (+) HeLa cells treated with 10 ng/µL TNFα (+) and fixed with 4% paraformaldehyde (+); Lane 4- Immunoprecipitated (IP) proteins from Myc-CNK1 transfected (+) HeLa cells treated with 10 ng/µL TNFα (+) and fixed with 4% paraformaldehyde (+). The proteins from one biological experiment were separated on SDS-PAGE gels and transferred to PVDF membranes which were probed with anti-CNK1 (mouse) (A), anti-Myc (mouse) (B), anti-RAF-1 (rabbit) (C) and anti-NIK (rabbit) (D). The HC and LC denote the bands for the heavy and light chains of the immunoprecipitating antibodies respectively. Myc-CNK1 is

labelled with a (*). Bands detected by the same antibody and larger in size are marked by (**). RAF-1 is labelled with (^). A potential NIK band is labelled with (•). These data represent one biological experiment but comparable data was obtained in replicate experiments.

When lysate from TNFα-treated Myc-CNK1 expressing HeLa cells was probed with anti-CNK1 or anti-Myc antibodies, we see a band at ~79 kDa representing a protein of the expected size for CNK1 (Figure 4.4A and 4.4B, Lanes 1, CNK1 protein labelled with a *). Interestingly, when this protein is immunoprecipitated, we observe a reduction in the level of the CNK1 protein in the immunoprecipitated samples (Figure 4.4A and 4.4B, Lane 2, CNK1 protein labelled with a *). This suggests that the activation of the NF-κB pathway by the addition of TNFα results in the generation of a protein that is less efficiently recognised by the anti-CNK1 and anti-Myc antibodies. To understand this, we considered the binding sites for the anti-CNK1 and anti-Myc antibodies (Figure 4.5).

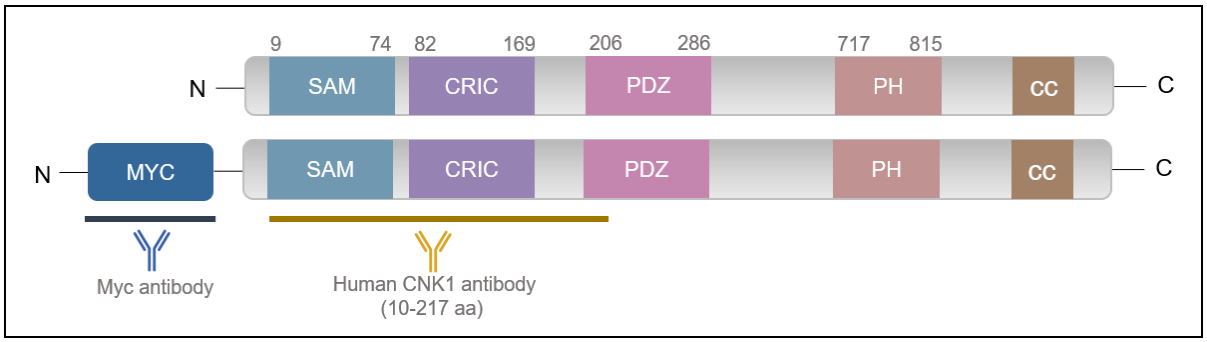

Figure 4.5: Analysis of the binding sites of the anti-CNK1 and anti-Myc epitope tag antibodies.

The anti-CNK1 antibody recognises the region between amino acids 10 and 217, which overlaps with the SAM and CRIC domains at the N-terminal of CNK1. This is the same region that is phosphorylated for the activation of the AKT (Fischer, et al., 2015), RAF-1 (Ziogas, et al., 2005) and Ras (Jaffe, et al., 2004) dependent signalling pathways. It is interesting to speculate that the activation of the NF-κB pathway by induction with TNFα results in the phosphorylation of the region at the N-terminal of CNK1 and that these phosphorylation events hinder the recognition by the anti-CNK1 antibodies. The anti-Myc antibody recognises the Myc epitope tag (EQKLISEEDL) at the N-terminal of the CNK1 protein, and close to the region that potentially affects the interaction between CNK1 and the anti-CNK1 antibody. The binding by the anti-Myc antibody could be affected by the same factors that affect the binding of the anti-CNK1 antibody. To determine whether this was the case, we attempted to generate

a Myc-CNK1 construct with the Myc epitope tag at the C-terminal of the protein. We were unsuccessful in our attempts to generate this construct.

Despite the induction of the NF-κB pathway with TNFα, we did not detect RAF-1 or NIK in the cell lysates or in the immunoprecipitation reactions of induced HeLa cells (Figure 4.4C and 4.4D, Lane 2 vs. Lane 1). This indicates that the limiting factor to the immunoprecipitation of CNK1 interacting partners was not the induction state of the NF-κB pathway.

We hypothesized previously that it is possible that the interactions between CNK1 and its interacting proteins (RAF-1 and potentially NIK) were weak or transitory and were unable to withstand the biochemical conditions of the immunoprecipitation reactions. For this reason, we treated the TNFα-induced cells with paraformaldehyde to stabilize the protein complexes. These complexes were immunoprecipitated with anti-Myc antibodies and Protein A/G magnetic beads, separated by SDS-PAGE and transferred to a PVDF membrane by western blotting. The proteins on these membranes were probed with antibodies directed against CNK1, Myc, RAF-1 and NIK and then with HRP-linked secondary antibodies (Figure 4.4).

All the lanes for TNFα-induced Myc-CNK1 transfected HeLa cell lysates that had been treated with paraformaldehyde showed no detectable protein (Figure 4.4A, 4.4B, 4.4C and 4.4D, lane 3). Before loading these samples on the SDS-PAGE gel, we centrifuged these samples at high speed to clarify them. It is possible that we may have inadvertently precipitated the protein complexes, especially if they were associated with cellular membranes.

The immunoprecipitation reactions for the same samples showed distinct protein bands detected by the antibodies used in this experiment.

The antibody for CNK1 detected one protein at ~116 kDa, a second protein at 60 kDa and a third faint band at ~79 kDa (Figure 4.4A, lane 4). The 79 kDa band (labelled *) is likely CNK1 that has not been cross-linked to partner proteins. The 60 kDa band is similar in size to the non-specific band present in the unstabilised TNFα-induced Myc-CNK1 transfected HeLa cells. The 116 kDa is particularly interesting as it suggests that this band represents the stabilized CNK1-interacting protein complex (Figure 4.4A, lane 4, labelled **). These same bands are present, albeit more faintly, in the anti-Myc antibody probed membrane (Figure 4.4B, lane 4). The detection by both the anti-CNK1 and the anti-Myc antibodies indicates that the approach being used has merit and the proteins are of interest. The fact that the protein bands detected by the anti-Myc antibody are fainter than those detected by the anti-CNK1 antibodies suggests that the Myc epitope tag is not optimally exposed in the stabilized protein complexes (Figure 4.4B lane 4 vs. Figure 4.4A lane 4). This may be a result of the folding of the Myc-epitope tag into the CNK1 protein or due to the masking of the interaction site for the anti-Myc antibody by CNK1-interacting proteins.

When stabilized CNK1-containing protein complexes were probed with antibodies for RAF-1, we detected bands for RAF-1 (Figure 4.4C, lane 4, labelled with ^) as well as two bands at ~120 and ~100 kDa (Figure 4.4C, lane 4, labelled with **). The bands that correspond in size to those for RAF-1 we hypothesize are associated with, perhaps trapped but not cross-linked, by the paraformaldehyde treatment into the CNK1-containing complexes and dissociate when the proteins are separated by denaturing PAGE. The larger bands at ~120 and ~100 kDa are RAF-1 proteins associated with proteins that have cross-linked and are now running at a higher molecular weight.

Probing stabilised protein complexes for the presence of NIK using anti-NIK specific primary antibodies results in the detection of faint protein bands at ~130, ~90 and ~70 kDa (Figure 4.4D, lane 4). The fact that these bands are not present in any of the other immunoprecipitations suggests that these are proteins that are associated with CNK1 and stabilised by the addition of paraformaldehyde. NIK protein is calculated to be ~125 kDa in size so it is possible that the band at ~130 kDa may be NIK (Figure 4.4D, lane 4, labelled with •). It is important to note that the protein band is the size that is expected for NIK, not NIK-CNK1, which suggests that the NIK protein is associated with CNK1 but has not been cross-linked by the addition of paraformaldehyde. These protein bands are not distinct which makes it difficult to draw definitive conclusions.

4.2.4 Relative densitometric analysis of immunoprecipitated proteins

In an attempt to gain clarity with respect to the immunoprecipitation reactions performed above, we performed densitometric analysis of the protein bands present on the western membranes using Image J software (Figure 4.6). The level of the proteins of interest in the immunoprecipitation reactions were quantified and normalized to the level of heavy chain protein as an equivalent concentration of anti-Myc antibody (10 µg/100 µL) was used in each immunoprecipitation reaction.

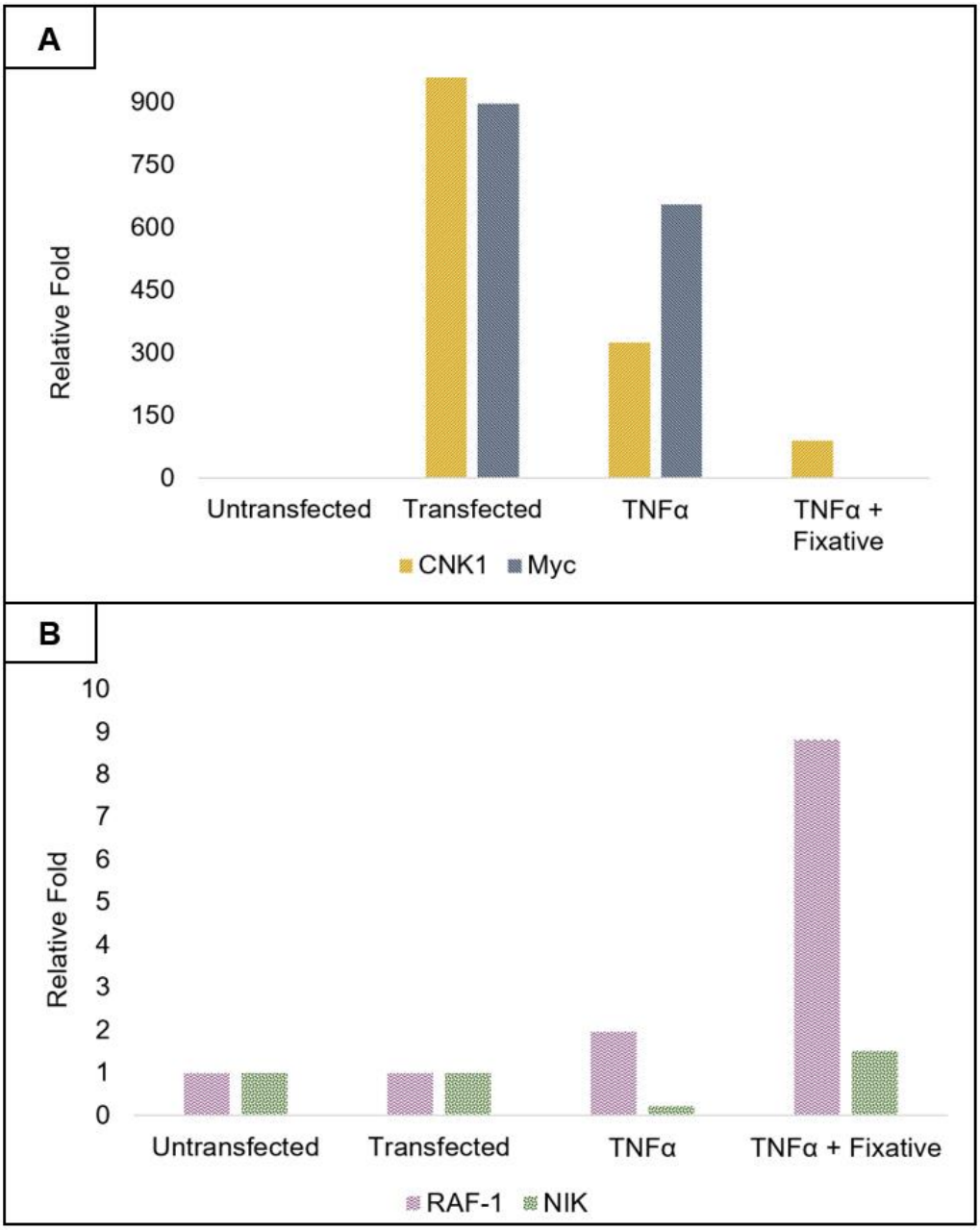

Figure 4.6: Relative densitometric analysis of proteins of interest in the immunoprecipitation reactions. Untransfected represents immunoprecipitation reactions performed on untransfected HeLa cells. Transfected represents immunoprecipitation reactions performed on Myc-CNK1 transfected HeLa cells. TNFα represents immunoprecipitation reactions performed on Myc-CNK1 transfected HeLa cells that were induced with 10 ng/µL TNFα. TNFα + Fixative represents immunoprecipitation reactions performed on Myc-CNK1 transfected HeLa cells that were induced with 10 ng/µL TNFα and treated with 4% paraformaldehyde prior to immunoprecipitation. A – Quantification of CNK1 and Myc; B – Quantification of RAF-1 and NIK. The levels of the proteins of interest were quantified with Image J and normalized to the level of the heavy chain of the antibody in the immunoprecipitation reactions.

The levels of CNK1 and Myc-CNK1 in untransfected HeLa cells is expectedly nil as there was no Myc-CNK1 to bind to the anti-Myc antibodies that were used in the immunoprecipitation reactions. In HeLa cells transfected with Myc-CNK1, there are high levels of CNK1 as detected by the anti-CNK1 and the anti-Myc antibodies. Quantification of the level of protein in TNFα-induced Myc-CNK1-transfected HeLa cells is lower than that present in uninduced and transfected HeLa cells. Upon fixation, we can detect CNK1 using the anti-CNK1 antibody but the detection by the anti-Myc antibody is poor (Figure 4.6A). When Myc-CNK1 transfected HeLa cells are induced with TNFα, we observe an increase in the level of RAF-1, which is enhanced significantly when the CNK1-containing complexes are stabilised by the addition of paraformaldehyde (Figure 4.6B). Most interestingly, only when the CNK1-containing complexes are stabilised with paraformaldehyde can we see a protein band that corresponds in size to that expected for NIK (Figure 4.6B). These quantifications permit us to evaluate the intensity of the bands detected in the western analyses and are interesting, however do not permit any conclusions to be drawn.

4.2.5. Co-localisation studies of CNK1 with p-NIK and NIK using confocal immunofluorescence microscopy

The detection of RAF-1 and perhaps NIK in the immunoprecipitation reactions led us to consider the localization of these proteins in the HeLa cells. If these proteins were interacting and involved in CNK1-associated complexes, we would expect to observe some co-localization of the protein-specific antibodies linked to their target proteins in the cell. To determine whether this was the case, we probed HeLa cells with antibodies for CNK1 and RAF-1 (Figure 4.7) and CNK1, p-NIK and NIK (Figure 4.8).

The fluorescent levels of endogenous CNK1 are observed to be low (Figure 4.7), however in certain regions of the cells there are slight increases in CNK1 (Figure 4.7B, indicated by *) that are matched by increased levels of RAF-1. These peaks in RAF-1 and CNK1 in the same region of the cell suggests that there may be interaction between these two proteins within the cell. In cells probed for p-NIK and NIK, we observed that p-NIK localises around the nuclear membrane within the cell whereas NIK is primarily cytoplasmic (Figure 4.8A). The levels of endogenous CNK1 and NIK are too low to observe any potential areas where their fluorescence overlaps (Figure 4.8C). Noting that activation of NF-κB pathway may be necessary in order to observe potential interaction between the CNK1 and NIK, we treated HeLa cells with TNFα and probed these cells for p-NIK, NIK and CNK (Figure 4.8B). We observed an increase in the immunofluorescence attributed to p-NIK, NIK and CNK1 when these cells were treated with TNFα (Figure 4.8B). When this fluorescence was quantified, there were certain regions

of the cell where there were slight increases in the levels of CNK1 (Figure 4.8D, indicated by *) that were matched by increases in the levels of NIK (Figure 4.8D). These peaks in NIK and CNK1 fluorescence in the same region of the cell suggests that these proteins may interact. While the confocal immunofluorescence microscopy data supports the potential for an interaction between NIK and CNK1, the low levels of immunofluorescence in the confocal immunofluorescence microscopy and the limitations of the co-immunoprecipitation reactions do not permit us to draw a conclusion.

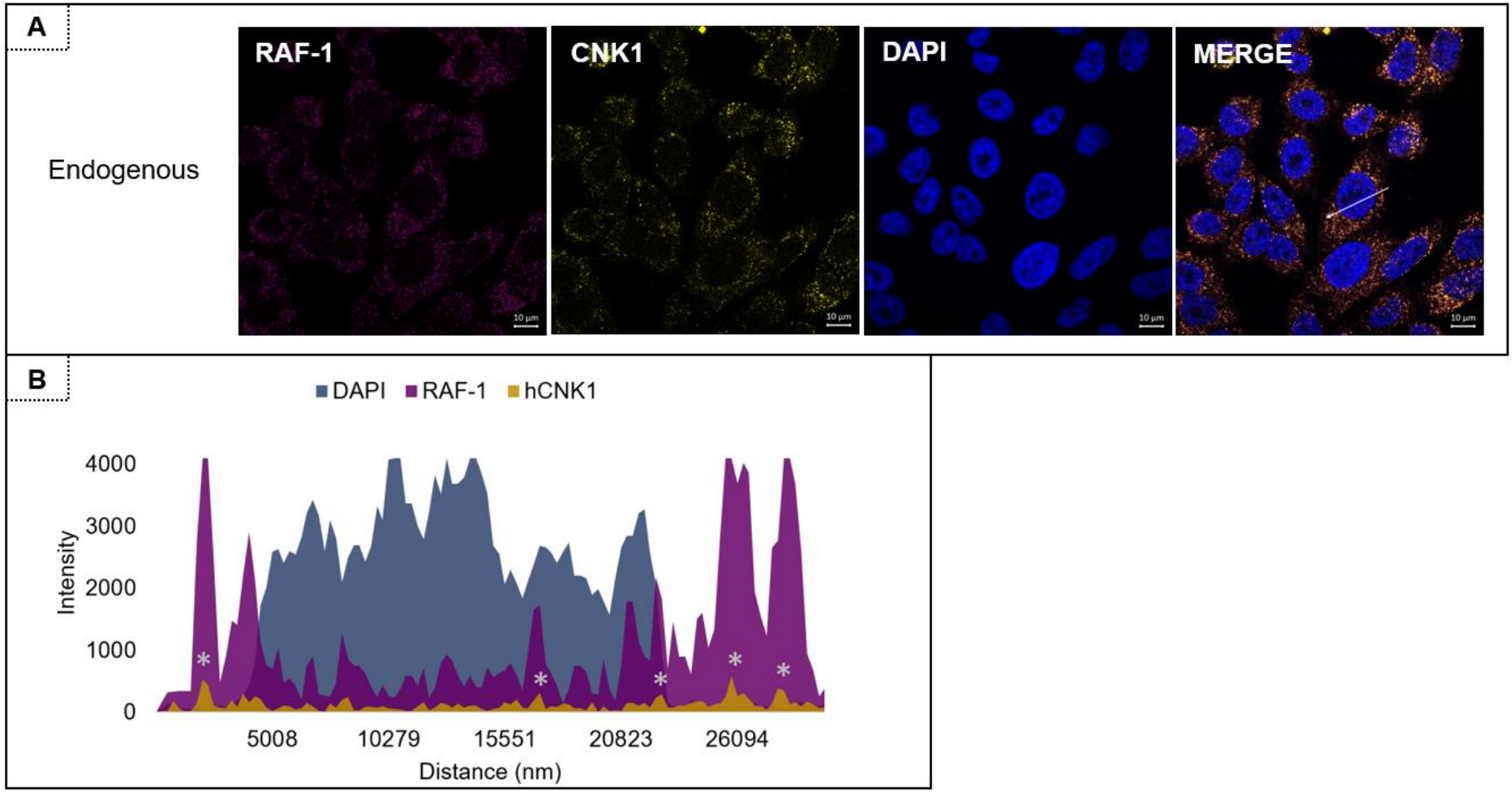

Figure 4.7: Co-localisation of CNK1 with RAF-1 in HeLa cells using confocal immunofluorescence microscopy. A: Interaction of CNK1 and RAF-1; B: Profile of fluorescence across cell. Permeabilised cells were probed with antibodies directed against the proteins of interested and anti-mouse AF546 and anti-rabbit AF633 secondary antibodies. Nuclei were stained with DAPI. Scale bars represent 10 µm.

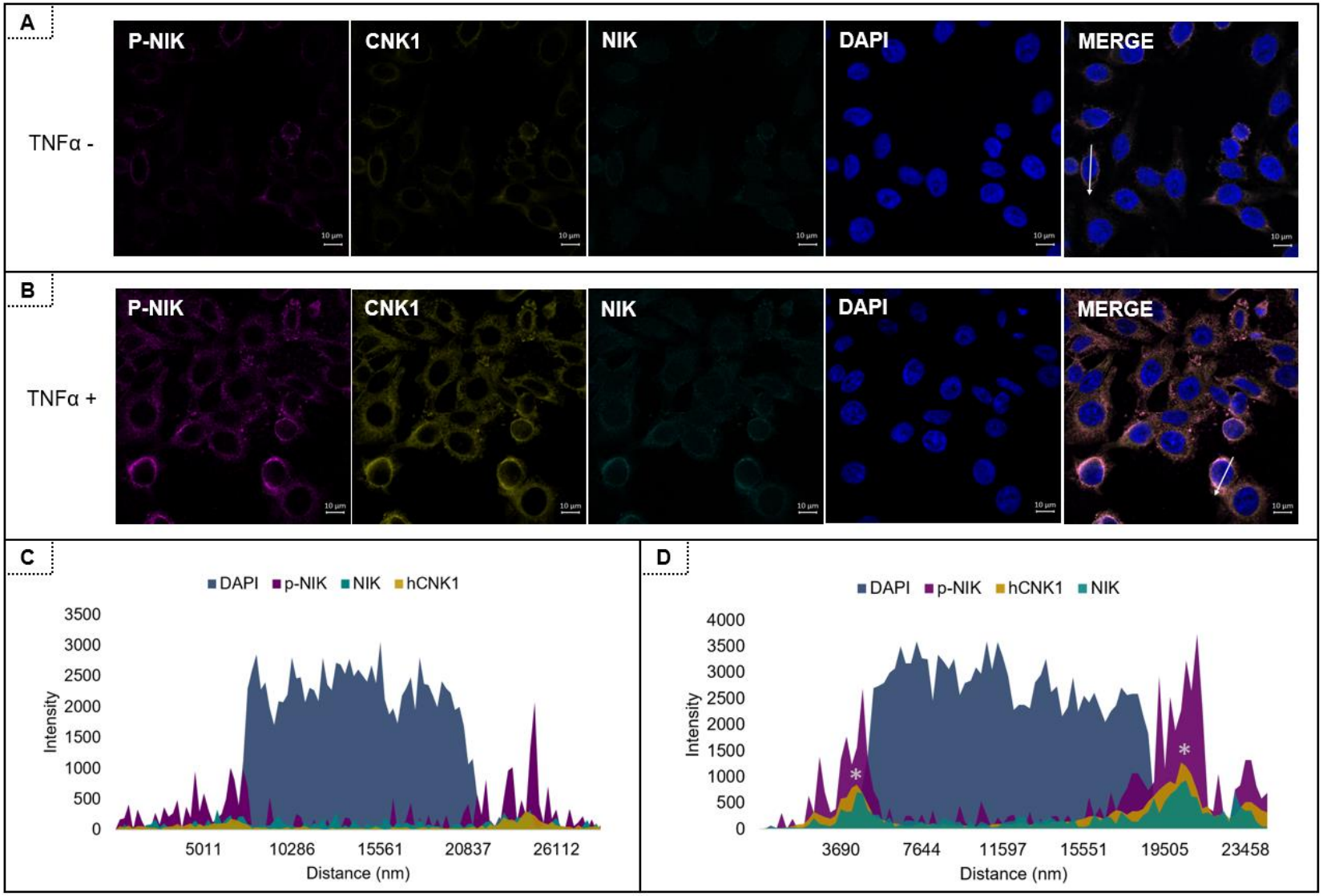

Figure 4.8: Co-localisation of CNK1 with NIK & p-NIK in HeLa cells using confocal immunofluorescence microscopy. Interaction of CNK1, NIK and p-NIK in uninduced (A) and TNFα-induced (B) cells. C and D - Profiles of fluorescence across cell. Permeabilised cells were probed with antibodies directed against the proteins of interested and anti-goat AF488, anti-mouse AF546 and anti-rabbit AF633 secondary antibodies. Nuclei were stained with DAPI. Scale bars represent 10 μm.

4.3 CONCLUSIONS

Co-immunoprecipitation reactions are the traditional technique with which we identify protein-protein interactions. This technique requires the use of antibodies that are specific to the proteins of interest and this highlights one of the weaknesses of this technique. If the antibody lacks sensitivity or specificity, it negatively affects the outcome of the co-immunoprecipitation experiments. We faced these challenges as the levels of some of the proteins of interest were low and some of the antibodies were not sufficiently specific. With the cost of each antibody, it is not possible for most researchers to try a range of antibodies in an effort to optimize the co-immunoprecipitation reactions. We are also assuming here that there is more than one antibody available for any specific target of interest.

Another challenge is the level of the protein of interest in the cell. In the first chapter, we discussed the level of CNK1 and demonstrated the need for an epitope-tagged CNK1 expression construct. In this chapter, we would need to consider co-expressing RAF-1 and NIK such that we could see a definitive interaction between CNK1 and its potential interacting partners. The co-transfection of more than one protein-expressing plasmid poses logistical problems and may result in proteins that are not appropriately regulated within the cell. This is particularly the case when dealing with critical cellular signalling pathways.

In this chapter, we establish that it is possible that NIK is an interacting partner of CNK1 within the NF-κB pathway; however, with the limitations highlighted, we have not proven this.

The data we have presented in this chapter have permitted us to discuss the many of the weaknesses of the traditional co-immunoprecipitation reactions. In addition, they have highlighted the need for an alternative system with which to identify interacting partners of CNK1. Our attempts to fix protein-protein interactions with paraformaldehyde also indicated another important consideration. The technique that is applied to identify protein interactors needs to be non-targeted, it needs to be able to detect interactors other than those that can be hypothesized using the information currently in the literature.

With these considerations in mind, we designed a modified co-immunoprecipitation technique with which we can study the interacting partners of CNK1. We will describe this system in the next chapter.

CHAPTER 5: DEVELOPMENT OF AN IN VIVO PROXIMITY LABELLING SYSTEM TO IDENTIFY THE INTERACTING PARTNERS OF CNK1 IN THE NF-κB PATHWAY

5.1 INTRODUCTION

5.1.1 Overview

Co-immunoprecipitations reactions are used to study the interaction of proteins *in vivo*. The method can be adapted and altered to achieve optimal conditions to immunoprecipitate interacting proteins and their macromolecular complexes from cells. The attachment of epitope tags to cellular proteins has provided a means of improving specificity and the availability of robust commercial antibodies against the epitope tags have improved the efficiency of the immunoprecipitation reactions. At the end of the previous chapter, we discussed some of the limitations of the traditional co-immunoprecipitation reactions. One of the main complications was that co-immunoprecipitation reactions are reliant on a strong interaction between the bait protein (in our case CNK1) and its interacting prey proteins, meaning proteins that interact transiently will be unsuitable candidates for this enrichment method (Viens, et al., 2008). We suspect that a lack of antibody efficiency (for p-NIK, NIK, RAF-1) combined with the low levels of interacting proteins result in the lack of conclusive data that we observe in the previous chapter. We researched alternative methods for labelling proteins proximal to proteins of interest and identified one proposed by (Roux, et al., 2012). Here, the authors used a biotin ligase (BirA) fused to their protein of interest to label proteins proximal to the proteins of interest with biotin, and subsequently use the addition of this biotin moiety to immunoprecipitate labelled proteins. In this chapter, we adapt this approach to identify the interacting partners of CNK1.

5.1.2 BirA: a promiscuous humanised biotin ligase

BirA is a 35 kDa DNA-binding biotin protein ligase expressed in *Escherichia coli*. The enzyme acts as a switch for the cellular demand of biotin by either regulating the biotinylation of acetyl-CoA carboxylase or by acting as a transcriptional repressor of the biotin operon (Roux, et al., 2012). *E. coli* have a different codon usage to human cells and to overcome the low translation efficiency, the expression of prokaryotic proteins in mammalian cells requires codon optimization. Mechold *et al*, developed a humanised version of the bacterial biotin ligase BirA by replacing the rare *E. coli* codons with those frequently used in humans (Mechold, et al., 2005).

In previous studies with BirA, a minimal recognition sequence referred to as a biotin acceptor tag (BAT) was fused to a protein of interest and co-expressed with BirA. The biotinylation of the target protein with BirA includes a two-step process. In the first step, biotin and ATP react to form biotinyl-5'AMP (bioAMP), this is a readily active form of biotin that is held within the BirA enzyme. The second step involves the recognition of a specific lysine residue within the BAT sequence by BirA, which then results in the release of BioAMP for attachment to the target region. The *in vivo* biotinylated proteins can be enriched by using streptavidin beads to precipitate proteins and their macromolecular complexes. The biotinylation event with BirA only has a strong selectivity for targets that are fused to the BAT tag so while BirA can label BAT tag-fused proteins with biotin, it does provide a means to label unknown proteins.

Roux *et al*, developed a mutant of BirA which prematurely releases the highly reactive bioAMP molecule from the BirA. This highly reactive and free bioAMP readily reacts with primary amines of proteins that are in proximity to the BirA (Roux, et al., 2012). This promiscuous BirA negates the need for the BAT sequence-fused protein to accept the biotin group and provides a means to label proteins proximal to the BirA-fused bait protein *in vivo* (Figure 5.1A).

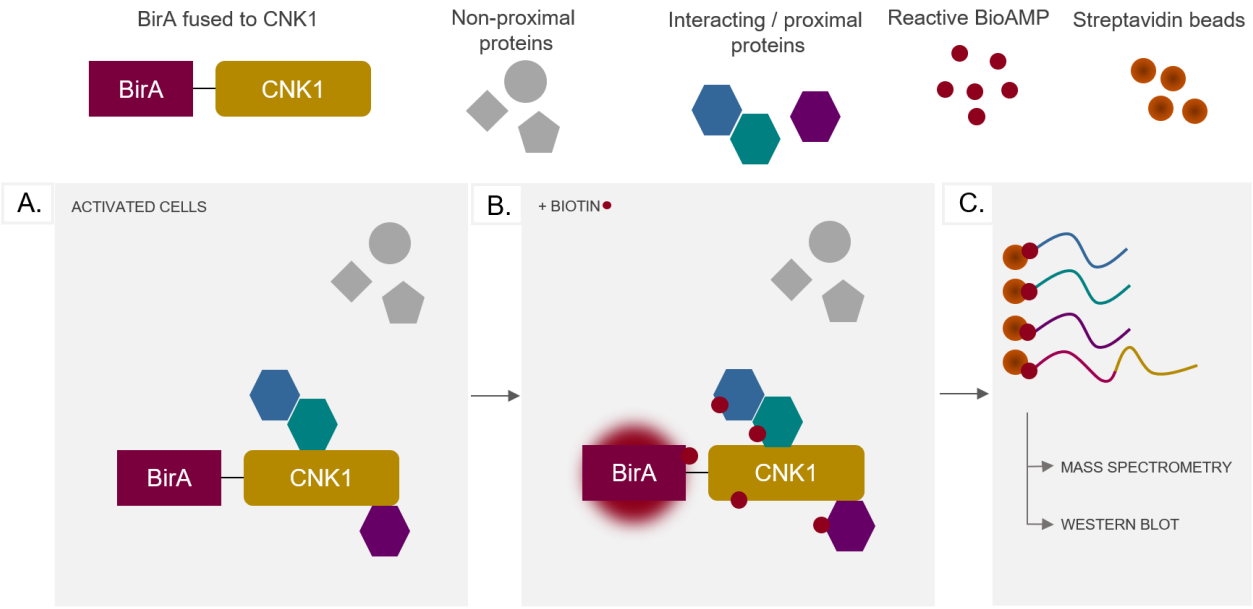

Figure 5.1: Schematic of the reaction that would occur between the promiscuous BirA-fused CNK1 and its proximal partners. A – In activated cells, transfected BirA-CNK1 interacts with binding partners; B- With the addition of biotin, readily reactive BioAMP is released by BirA and reacts with amine groups of proteins in proximity to BirA-CNK1; C – Pull down of biotinylated proteins with streptavidin beads permits subsequent identification of proteins using mass spectrometry and western blot analysis. (Adapted from Roux, et al., 2012).

The level of biotinylation in this system is regulated by the concentration of free and available biotin. As highlighted by (Roux, et al., 2012), there is some endogenous biotin which will be available for the biotinylation reactions *in vivo.* The labelling reaction can be enhanced by the addition of biotin (Figure 5.1B). These biotinylated protein complexes can be enriched and purified using streptavidin beads or anti-biotin antibodies and analysed using techniques like mass spectrometry and western blot analysis (Figure 5.1C).

5.1.3 Problem Statement

We were unable to conclusive identify the binding partners of CNK1 using traditional co-immunoprecipitation reactions. An alternative approach is required to identify proteins that bind to CNK1, albeit transiently or weakly.

We will adapt a method developed by (Roux, et al., 2012) to identify proteins that are proximal to CNK1, *in vivo*.

5.2 RESULTS & DISCUSSION

5.2.1 The development of a humanised BirA-CNK1 expression construct

We inserted the sequence for Myc-BirA-Gtx-EGFP into pcDNA3.1 (Figure 5.2A). This insertion includes the sequence for a Myc epitope tag-fused BirA which is detectable using anti-Myc antibodies. Following this, there is a sequence Gtx, which represents an internal ribosomal entry site (IRES) and the sequence for EGFP, a fluorescent reporter. The construct (referred to as BirA) is designed to generate one mRNA transcript encoding Myc-BirA and EGFP and two separate proteins, Myc-BirA and EGFP. Cells transfected with this plasmid should show EGFP fluorescence indicating successful transfection with the plasmid.

The sequence for CNK1 was excised from pRK5-Myc-CNK1 (Myc-CNK1, described in Chapter 3) and inserted into the BirA construct using the restriction enzymes *Bam* HI and *Eco* RI. The plasmid DNA (referred to as BirA-CNK1) was sequenced to confirm the presence of CNK1 and to ensure that the junction between BirA and CNK1 would result in a BirA-CNK1 fusion protein (Figure 5.2B). The BirA protein is expected to be ~40 kDa and BirA-CNK1 ~120 kDa in size.

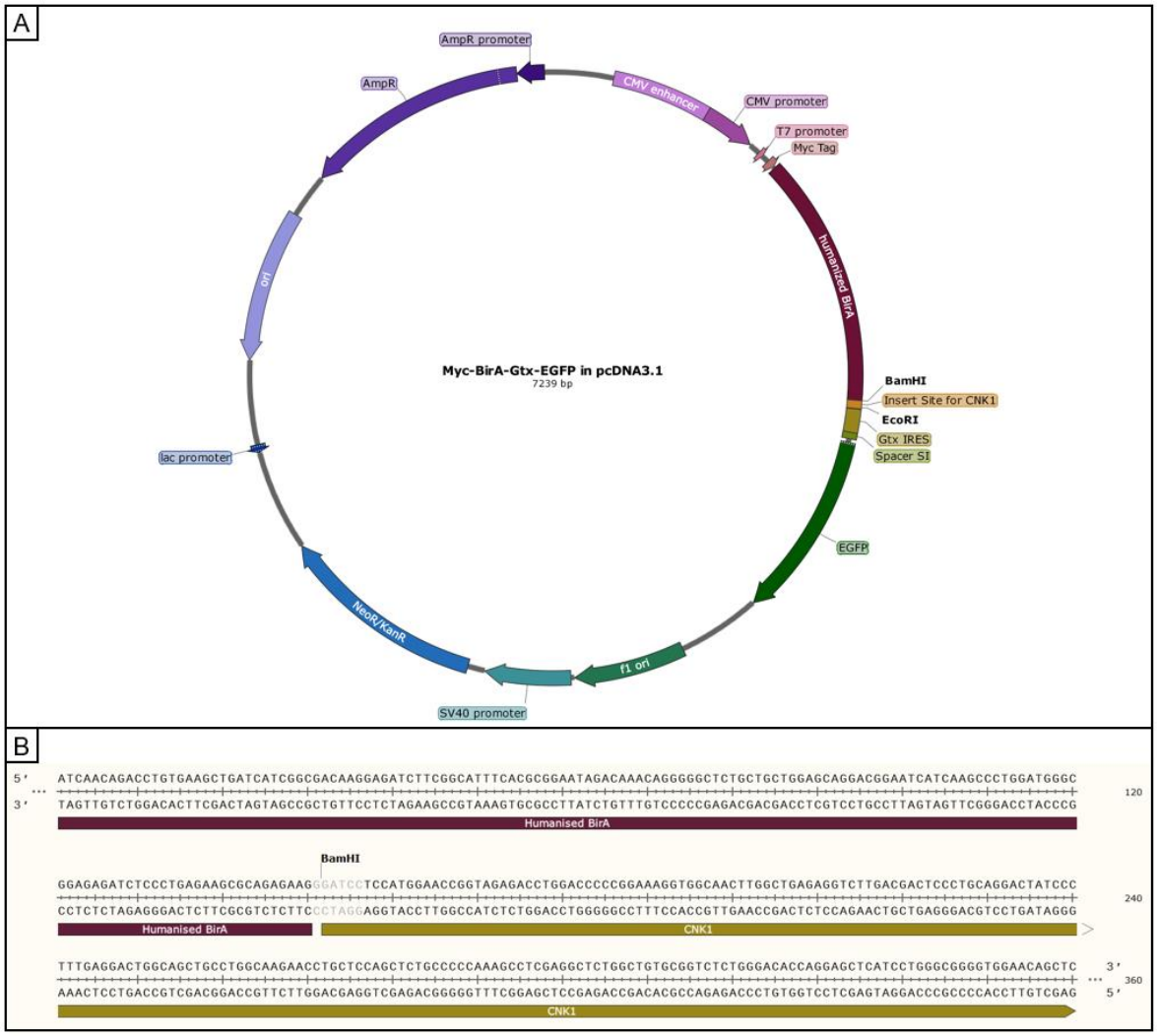

Figure 5.2: Plasmid map of the BirA-expressing plasmid Myc-BirA-Gtx-EGFP DNA and sequence analysis of BirA-CNK1. A - Plasmid map of Myc-BirA-Gtx-EGFP DNA (BirA) that will produce Myc-tagged BirA; B – DNA sequence analysis showing the junction between BirA and CNK1 in BirA-CNK1 which will produce a BirA-CNK1 fusion protein.

5.2.2 Analysis of HeLa cells transfected with the Myc-BirA expressing construct

1 x 10^5 HeLa cells in a 24-well plate were transfected with BirA DNA at a range of concentrations from 250 ng to 750 ng. The cells were fixed and probed with anti-Myc and anti-CNK1 antibodies and analysed using confocal immunofluorescence microscopy (Figure 5.3). Cells expressing BirA were detected using anti-Myc antibodies as well as EGFP fluorescence (Figure 5.3, 1A, 2A and 3A). The transfection efficiency was low, but the optimal concentration for transfection was determined to be 500-750 ng DNA. These cells were also probed with antibodies targeted to CNK1 and we observed low levels of fluorescence consistent with the levels expected for endogenous CNK1. None of the cells that showed EGFP fluorescence showed elevated levels of CNK1-specific fluorescence.

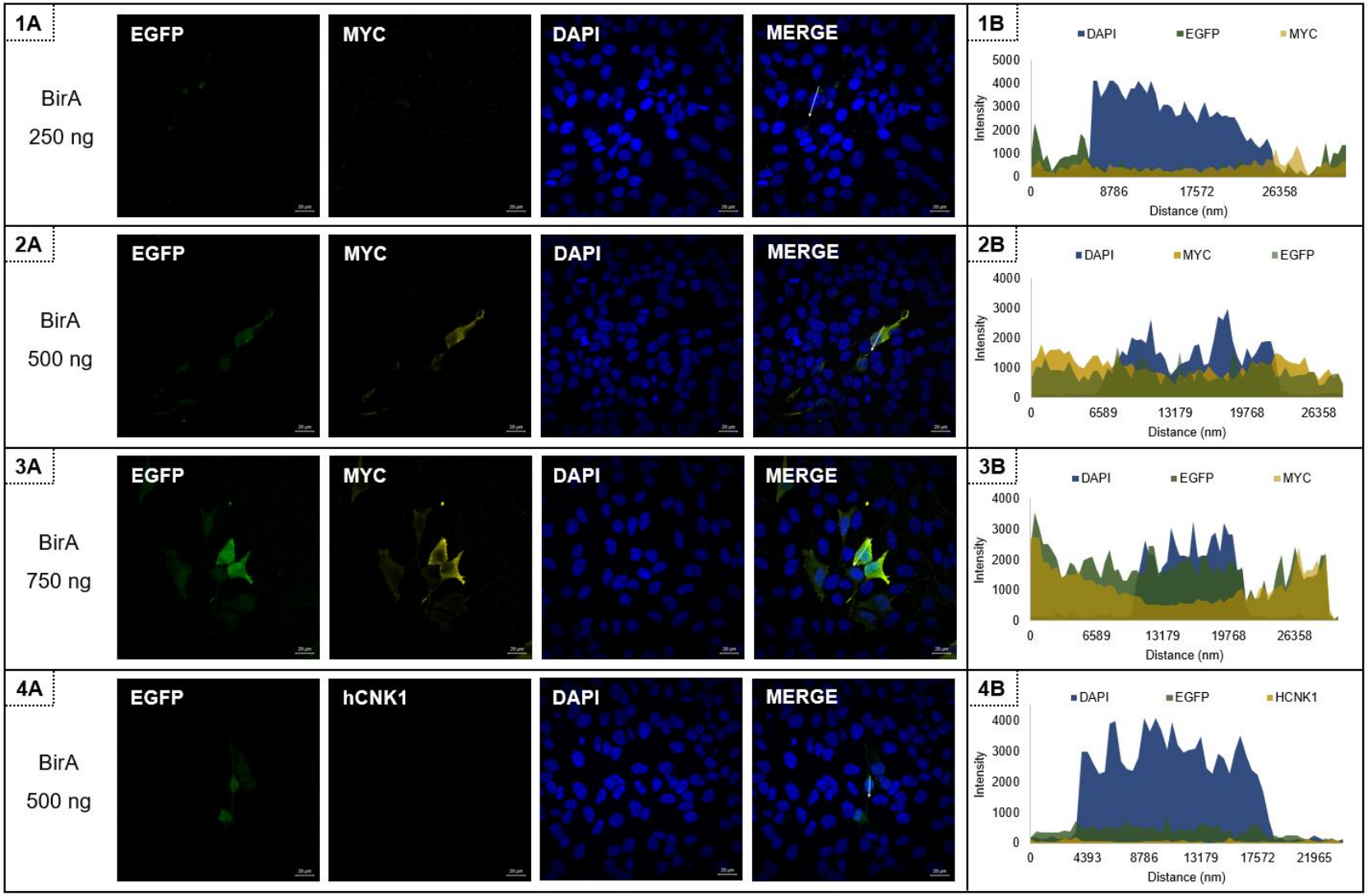

Figure 5.3: Detection of Myc-BirA expression using confocal immunofluorescence microscopy in HeLa cells transfected with the BirA-expressing construct. HeLa cells transfected with (1A) 250 ng, (2A) 500 ng or (3A) 750 ng BirA DNA. The profile of immunofluorescence levels for a single HeLa cell is shown in (1B) 250 ng, (2B) 500 ng or (3B) 750 ng. 4A- HeLa cells transfected with 500 ng BirA were probed with anti-CNK1 antibodies, 4B – profile of immunofluorescence levels of a single cell transfected with BirA using anti-CNK1. Scale bars represent 10 μm.

5.2.3 Western blot analysis BirA-transfected HeLa cells

HeLa cells in T75 flasks were transfected with BirA (at a range of 0 µg - 7.5 µg DNA). Proteins isolated from these cells was separated on a 12% SDS-PAGE then transferred onto a PVDF membrane via western blotting. The membranes were probed with primary antibodies for CNK1, Myc, and biotin and detected using secondary antibodies conjugated to HRP (Figure 5.4).

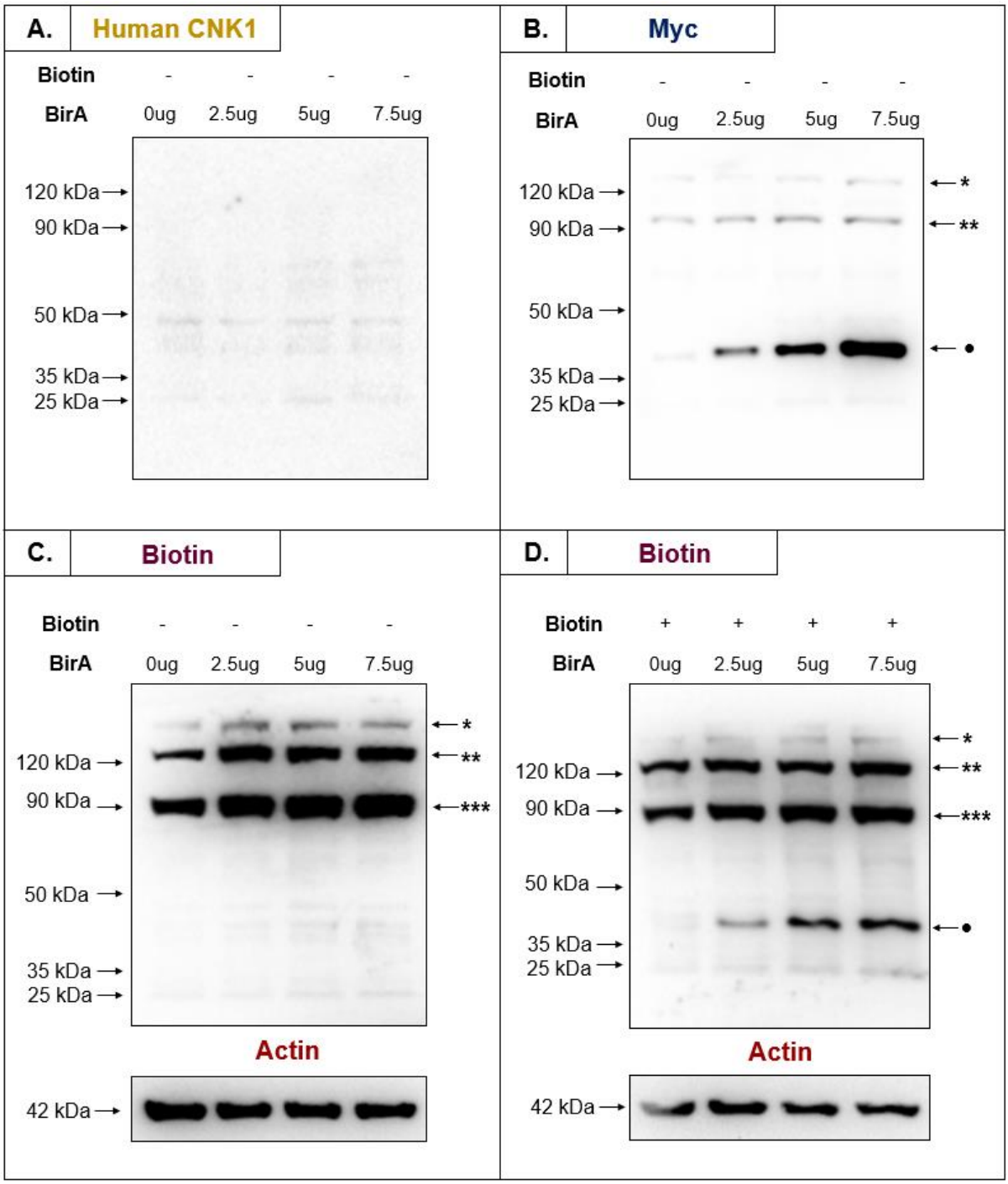

Figure 5.4: Western blot analysis of the expression of BirA in HeLa cells. Lane 1- untransfected HeLa cell lysate. Lysate prepared from HeLa cells transfected with 2.5 ug (Lane 2), 5 ug (Lane 3) or 7.5 ug (Lane 3) BirA DNA The proteins from one biological experiment

were separated on SDS-PAGE gels and transferred to PVDF membranes which were probed with anti-CNK (mouse) (A), anti-Myc (mouse) (B) and anti-Biotin (rabbit) (C, D). The anti-biotin PVDF membranes were re-probed with anti-actin (rabbit) (C,D). Myc-BirA was labelled with (•). 3 unidentified endogenous biotinylated protein were labelled (*), (**) and (***) respectively. These data represent one biological experiment but comparable data was obtained in replicate experiments.

HeLa cells transfected with BirA show no detectable levels of endogenous CNK1 at ~ 90 kDa (Figure 5.4A). This is consistent with our observations using immunofluorescence microscopy, the levels of endogenous CNK1 in the cells are low. When the membrane is exposed for an extended period of time, protein bands at the expected size for CNK1 are visible (data not shown). These cells do however show the presence of the Myc-tagged BirA protein at ~40 kDa when the membrane is probed with anti-Myc antibodies (Figure 5.4B, marked with •). As the concentration of DNA increases, we observe an increase in the intensity of the Myc-BirA band confirming that this ~40 kDa band is the Myc-BirA protein of interest.
In cells that are not treated with biotin (Figure 5.4C), we observe endogenous biotinylated proteins (Figure 5.4C, at ~160 kDa (*), ~130 kDa (**) and ~92 kDa (***)) however we do not detect Myc-BirA at ~40 kDa. This indicates that the Myc-BirA is not being endogenously biotinylated *in vivo.* When BirA-transfected HeLa cells treated with biotin are probed with anti-biotin antibodies (Figure 5.4D, •), we detect a clear band, of the same size as the Myc-BirA band at ~40 kDa (Figure 5.4B, •). This indicates that BirA, which is expected to biotinylate proteins in proximity to the enzyme, is functional in HeLa cells as it is biotinylating itself.

5.2.4 Analysis of BirA-CNK1 expression in HeLa cells

HeLa cells transfected with BirA-CNK1 were probed with anti-Myc and anti-CNK1 antibodies and analysed using confocal immunofluorescence microscopy (Figure 5.5). As we observed for the BirA construct, the transfection efficiency was low, however we did detect cells that exhibited low levels of EGFP fluorescence (Figure 5.5). These same cells showed elevated levels of fluorescence when probed with anti-Myc or with anti-CNK1 antibodies (Figure 5.5). We transfected the HeLa cells (1×10^5 cells in a 24 well plate) with between 250–1000 ng DNA and determined that the optimal transfection concentration was between 500-750 ng.
Having determined that the BirA-CNK construct was expressing a Myc-tagged protein and expressing higher levels of CNK1 than endogenous cells using confocal immunofluorescence microscopy, we performed western analyses on HeLa cells transfected with 40 µg of BirA-CNK1 in a T75 flask of HeLa cells.

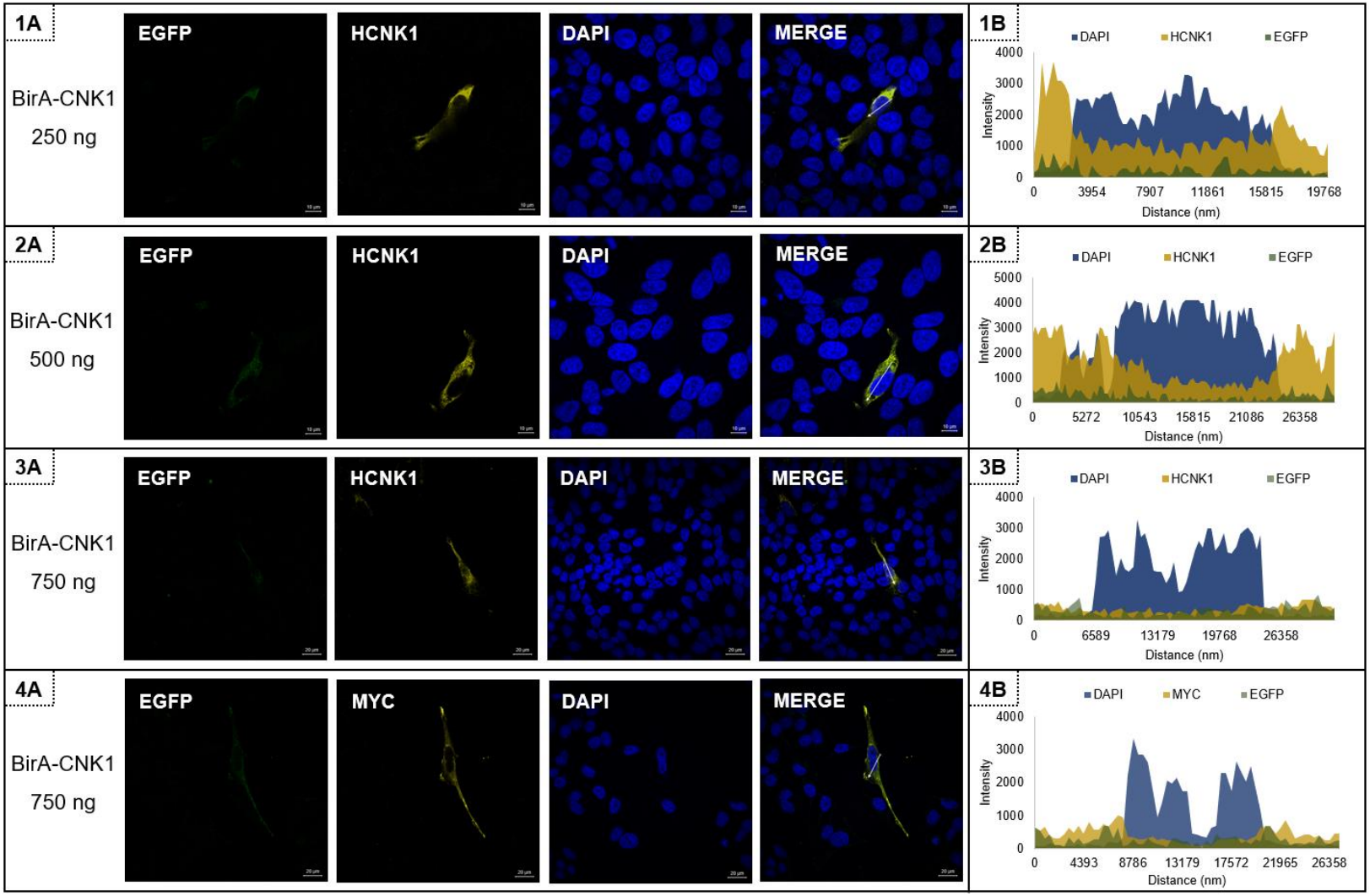

Figure 5.5: Evaluation of BirA-CNK1 expression in HeLa cells using confocal immunofluorescence microscopy. HeLa cells transfected with 250 ng (1A), 500 ng (2A) or 750 ng (3A) BirA-CNK1. The profile of immunofluorescence levels for a single HeLa cell is shown in (1B) 250 ng, (2B) 500 ng or (3B) 750 ng. 4A- HeLa cells transfected with 500 ng BirA-CNK1 were probed with anti-Myc antibodies, 4B – profile of immunofluorescence levels of a single cell transfected with BirA-CNK1 using anti-Myc. Scale bars represent 10 μm.

The proteins were expressed for 24 hours and if required, the cells were treated with 50 µM biotin for 24 hours. If required, the cells were induced with 100 ng/µl TNFα for 15 minutes. All treatment times were a total of 48 hours, so cells that were untransfected, untreated with biotin or uninduced were incubated alongside the treated cells for the duration of the experiment. Protein lysates were separated on 10% SDS-PAGE then transferred onto PVDF membranes using western blotting. The western blots were probed with primary antibodies for CNK1 and biotin and detected using secondary antibodies conjugated to HRP (Figure 5.6).

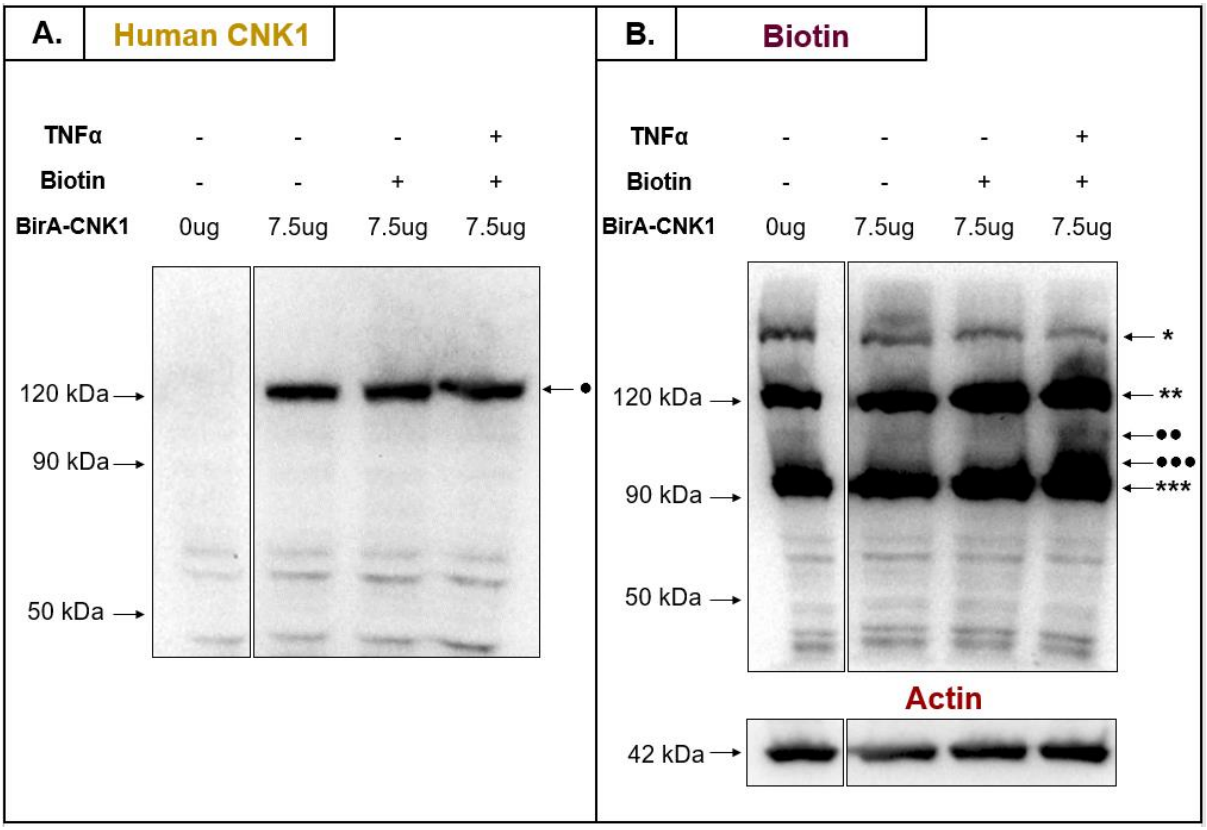

Figure 5.6: Western blot analysis of protein lysates from HeLa cells transfected with BirA-CNK1 and treated with TNFα and biotin. Lane 1- untransfected HeLa cells; Lane 2- HeLa cells transfected with 7.5 µg of BirA-CNK1. Lane 3- HeLa cells transfected with 7.5 µg of BirA-CNK1 and treated with 50 µM biotin. Lane 4- HeLa cells transfected with 7.5 µg of BirA-CNK1, treated with 50 µM biotin and induced with 100 ng/µl TNFα. The proteins from one biological experiment were separated on SDS-PAGE gels and transferred to PVDF membranes which were probed with anti-CNK (mouse) (A) and anti-Biotin (rabbit) (B). The anti-biotin PVDF membrane was re-probed with anti-actin (rabbit) (B). BirA-CNK1 was labelled with (•). 2 unidentified biotinylated proteins associated with BirA-CNK1 were labelled (••) and (•••) respectively. 3 unidentified endogenous biotinylated protein were labelled (*),

(**) and (***) respectively. These data represent one biological experiment but comparable data was obtained in replicate experiments.

BirA-CNK1 was detected using anti-CNK1 antibodies at ~120 kDa (Figure 5.6A, •). The absence of the ~120 kDa band in untransfected lysates supports this conclusion. When these samples were treated with biotin, we detect the same three endogenous bands observed previously (Figure 5.4C), however we can see additional bands at ~105 kDa (••) and ~96 kDa (•••). In addition, there is enhanced signal in the sample treated with both TNFα and biotin at ~120 kDa (Figure 5.6B). The enhanced signal at ~120 kDa is likely to be biotinylated BirA-CNK1.

While it is tempting to speculate about the identity of the proteins at ~105 kDa and ~96 kDa by analysing the potential partners in the NF-κB pathway, the number of protein bands and the lack of clear protein bands indicated the need for optimization. We deemed it prudent to enrich for the biotinylated proteins that interact with CNK1 from the lysate before western analysis. Our experiences with the anti-CNK1, anti-Myc and anti-biotin antibodies as well as the streptavidin beads led us to perform an experiment to determine which antibody would be best suited to perform the immunoprecipitation of BirA-CNK1 and its interacting proteins.

5.2.5 Immunoprecipitation of BirA-CNK1 and its interacting partners after induction with TNFα

In an effort to ensure that the BirA and BirA-CNK1 that we were expressing in the HeLa cells were the proteins we were interested in, we transfected a T75 flask of HeLa cells with 40 µg of BirA or BirA-CNK1 and treated the cells with TNFα and biotin. All the protein lysates from these cells were subjected to sequential immunoprecipitation reactions (Figure 5.7).

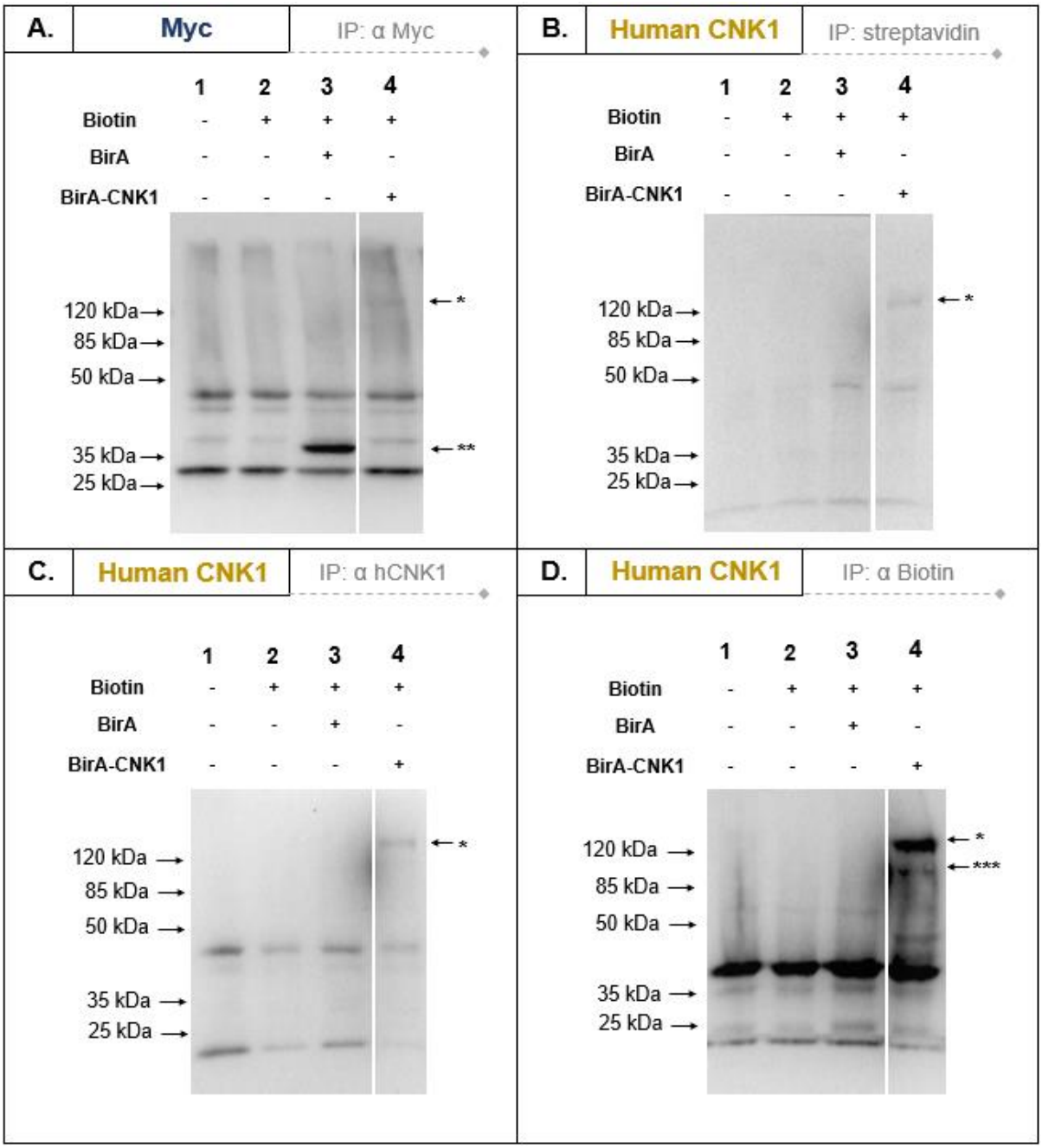

Figure 5.7: Efficiency of Bir-CNK1 immunoprecipitation. HeLa cells were transfected with BirA-CNK1 and treated with TNFα and biotin. Protein lysates were subjected to multiple immunoprecipitation reactions with anti-Myc (A), streptavidin beads (B), anti-CNK1 (C) and anti-biotin (D) antibodies. (Data generated by J. Swan). BirA-CNK1 was labelled (*). Myc-BirA was labelled (**). Endogenous CNK1 was labelled (***). These data represent one biological experiment but comparable data was obtained in replicate experiments.

The first immunoprecipitation was performed with anti-Myc antibody, which is expected to retain both BirA and BirA-CNK1. There are some bands that are present in all the

immunoprecipitation reactions. The heavy chain and light chain of anti-Myc antibody is at ~50 kDa and ~25 kDa respectively. Additional bands are observed that indicate interactions of the anti-Myc antibody with cellular Myc or non-specific binding with other cellular proteins. No BirA or BirA-CNK1 is detected in the reactions from untransfected cells (Figure 5.7A, Lanes 1 and 2). Where the cells were transfected with BirA, in the immunoprecipitation with the anti-Myc antibody, we see a band at ~40 kDa representing the Myc-tagged BirA protein (Figure 5.7A, **). In BirA-CNK1 transfected samples, we detect a faint band at ~120 kDa (Figure 5.7A, *) suggesting low levels of BirA-CNK1 expression.

The second immunoprecipitation was performed with streptavidin beads (Figure 5.7B). Previously we had struggled to pull down proteins with these streptavidin beads and observed an inability to bind even the endogenous biotinylated proteins (data not shown). In an effort to test the streptavidin beads, we performed an immunoprecipitation reaction with the streptavidin beads and probed the membrane for CNK1. We detected no band at the size expected for BirA (Figure 5.7B, Lane 3) and a very faint band at ~120 kDa (Figure 5.7B, Lane 4, *) which could represent BirA-CNK1.

When we performed an immunoprecipitation with anti-CNK1 antibodies and probed the membrane with anti-CNK1, we saw a similar sized band (Figure 5.7C, Lane 4, *) at ~120 kDa.

The final immunoprecipitation was performed with anti-biotin antibody and this should pull down all biotinylated proteins. To ensure we did not detect the endogenous biotinylated proteins, we probed the western membrane for CNK1 and detected a robust band at ~120 kDa (Figure 5.7D, Lane 4, *) as well as a second band at ~90 kDa (Figure 5.7D, Lane 4, ***). This indicates the immunoprecipitation of the biotinylated BirA-CNK1 protein and also biotinylated endogenous CNK1 protein. The levels of the endogenous protein are significantly lower than those of BirA-CNK1, however the presence of both bands indicates that BirA-CNK1 and CNK1 are in proximity in the cell, and may be interacting with each other.

These data highlight the susceptibility of antibody-based immunoprecipitation techniques to the sensitivity and specificity of the antibody. The same cell lysate was used in one immunoprecipitation after the other, so each immunoprecipitation reaction is pulling down protein that remains in the lysate after the previous immunoprecipitation reactions. The immunoprecipitation with the anti-biotin antibody yielded significantly more protein that the immunoprecipitations with the anti-Myc and anti-CNK1 antibodies or with the streptavidin beads. It is reassuring to note that with the use of sufficient protease inhibitor, the proteins remain stable for 5 days during the sequential immunoprecipitation reactions. It is also apparent that the anti-biotin antibody is a robust antibody for use in immunoprecipitation reactions. These data also make apparent the strength of this modification of the traditional

immunoprecipitation technique; with anti-biotin antibodies we are able to effectively immunoprecipitate and detect the bait protein BirA-CNK1.

5.2.6 Mass spectrometric analysis of proteins immunoprecipitated with BirA-CNK1

In an effort to identify the proteins that interact with CNK1, we transfected HeLa cells with BirA-CNK1 and treated the cells with biotin and TNFα. The protein lysates were subjected to immunoprecipitation reactions with anti-biotin antibodies such that we pulled down all the biotinylated proteins in the cell. We ran these proteins into a short SDS-PAGE gel, cut out the acrylamide and dehydrated it with acetonitrile. We sent these samples to Mare Vlok at the Central Analytical Facility (Stellenbosch University) who generously performed the tryptic digests and the mass spectrometry. We received the data as an MGF file and used SearchGUI (Compomics) to identify whether proteins of interest in the NF-κB pathway including NIK, IKKα and IKKβ were present in the immunoprecipitated biotinylated proteins.

Table 5.1: Mass Spectrometry analysis of potential interacting partners of CNK1 in the NF-κB signalling pathway.

Potential Interactors	% Coverage	# of peptides	# of spectra
CNK1	67.22%	678	891
IKKα	75.97%	1955	3206
IKKβ	90.48%	3024	5118
NIK	88.28%	1603	2505

We evaluated the coverage of the proteins of interest and noted good coverage of the bait protein CNK1. We also detected NIK, IKKα and IKKβ in the immunoprecipitated proteins. These were a significant number of peptides and spectra identifying these proteins lending weight to the argument that all these proteins were present in the immunoprecipitation reaction of the biotinylated proteins. This data expands on the hypothesis that we have been generating and indicates a role for NIK, IKKα and IKKβ as interactors of CNK1 in the NF-κB pathway. IKKα and IKKβ are proteins that are critical in the junction that decides the directionality of the NF-κB pathway (Figure 1.3). We decided to determine whether IKKα and IKKβ are interactors of CNK1 in the NF-κB pathway.

5.2.7 Do IKKα or IKKβ interact with CNK1 in the NF-κB pathway?

In an attempt to evaluate the levels of IKKα/β in the cell, we decided to visualise the proteins using confocal immunofluorescence microscopy (Figure 5.8).

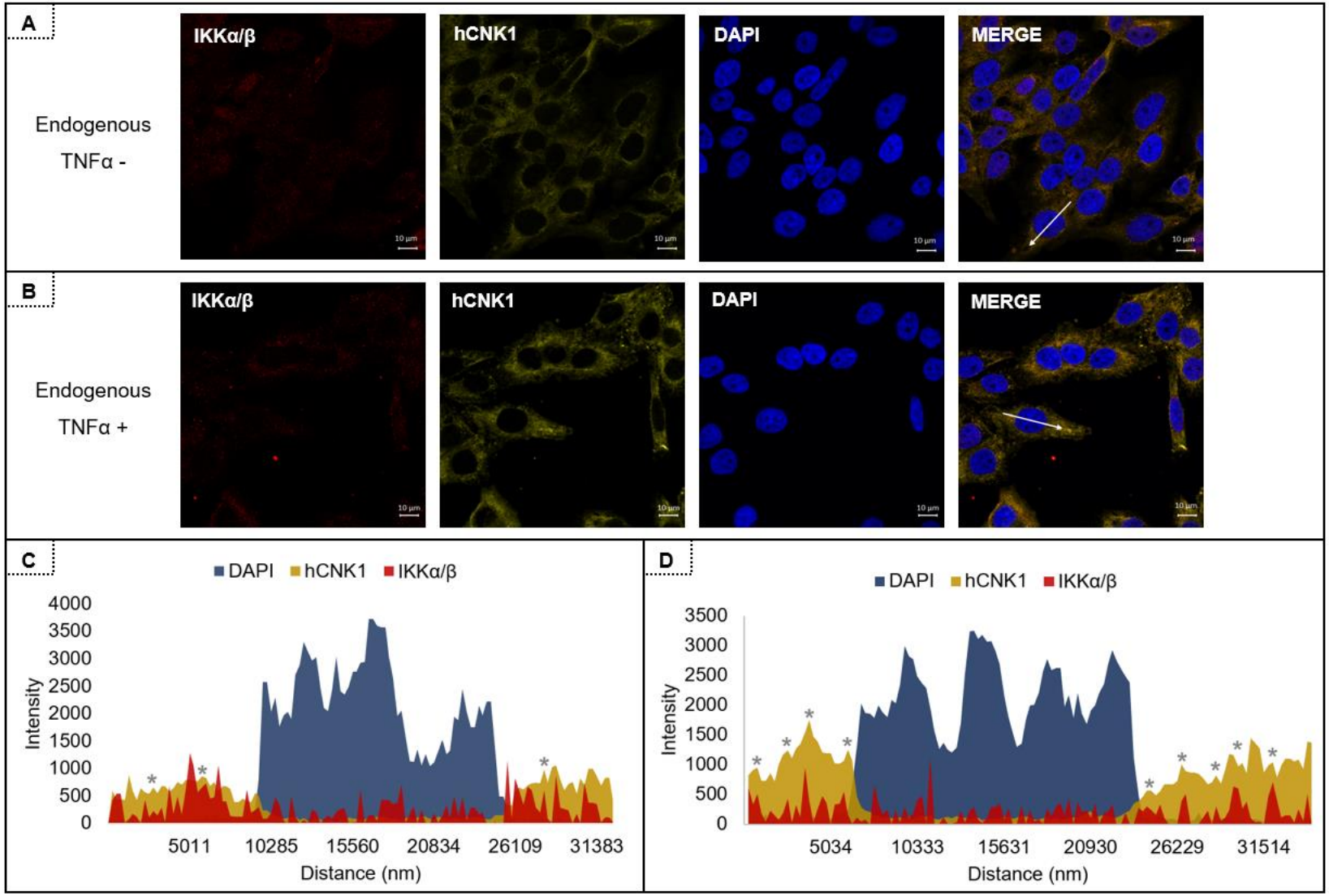

Figure 5.8: Co-localization studies of IKKα/β and CNK1 using confocal immunofluorescence microscopy. A - Endogenous levels of IKKα/β and CNK1 in HeLa cells; B – Induced levels of IKKα/β and CNK1 after treatment with TNFα; C – Profile of fluorescence levels of endogenous IKKα/β and CNK1 across a single HeLa cell; D - Profile of fluorescence of induced levels of IKKα/β and CNK1 in cells treated with TNFα across a single HeLa cell. Scale bars represent 10 μm. (Data generated by R. Jarvie).

First, we visualised the levels of IKKα and IKKβ (IKKα/β) in HeLa cells. The levels of fluorescence detected for endogenous IKKα/β and CNK1 were low in the cells (Figure 5.8A). Induction with TNFα resulted in a slight increase in the levels of IKKα/β and a clearer increase in the levels of CNK1 (Figure 5.8B). In an attempt to identify whether there was any co-localization between IKKα/β and CNK1, we studied the profile of immunofluorescence across a single cell (Figure 5.8C and 5.8D). There are areas in the cells where there are increased levels of both IKKα/β and CNK1 (Figure 5.8C and 5.8D, *), however these data are not convincing. The levels of the IKKα/β and CNK1 fluorescence are too low to draw any conclusions.

We decided to perform immunoprecipitation reactions from untransfected HeLa cells and HeLa cells that had been transfected with BirA-CNK1 and treated with 50 µM biotin and 100 ng/µl TNFα using anti-CNK1 or anti-IKKα/β antibodies. These immunoprecipitation reactions were separated by SDS-PAGE and the proteins transferred to a PVDF membrane by western blotting. The membranes were probed with anti-CNK1 or anti-IKKα/β antibodies (Figure 5.9).

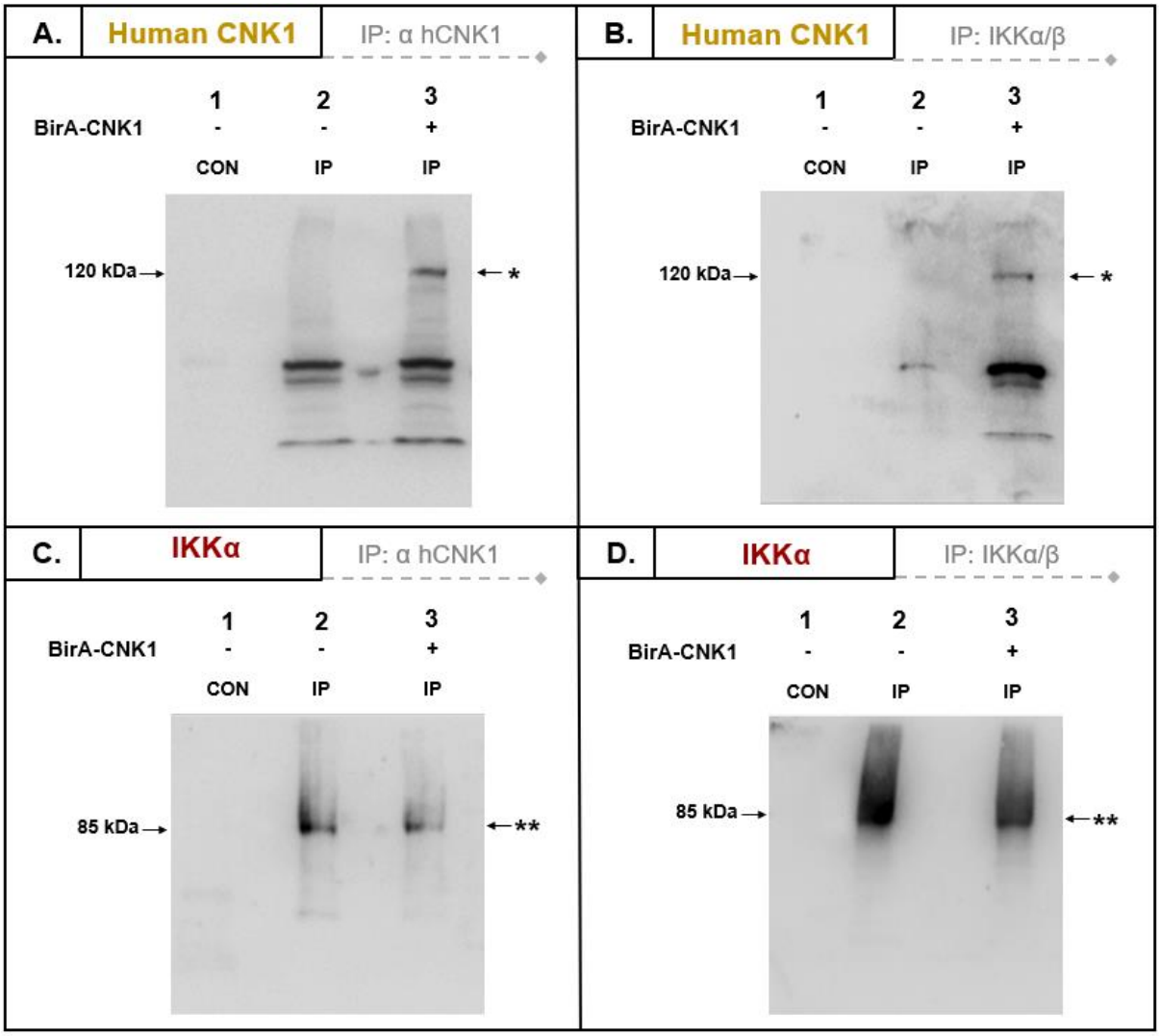

Figure 5.9: IKKα/β interacts with CNK1. A – Proteins immunoprecipitated using anti-CNK1, probed with anti-CNK1; B - Proteins immunoprecipitated using anti-IKKα/β, probed with anti-CNK1; C- Proteins immunoprecipitated using anti-CNK1, probed with anti-IKKα/β; D - Proteins immunoprecipitated using anti-IKKα/β, probed with anti-IKKα/β (Data generated by J. Swan). BirA-CNK1 was labelled with (*). IKKα/β was labelled with (**). These data represent one biological experiment but comparable data was obtained in replicate experiments.

Immunoprecipitation of CNK1 with anti-CNK1 antibodies from untransfected HeLa cells does not yield a clear ~90 kDa band for CNK1 (Figure 5.9A, Lane 2) however the cells transfected with BirA-CNK1 yield a clear band at ~120 kDa (Figure 5.9A, Lane 3, *). This highlights the low levels of endogenous CNK1 in HeLa cells. When the immunoprecipitation reaction

performed with anti-CNK1 was probed for IKKα/β, we detected a clear band at ~85 kDa in the immunoprecipitation reaction from the untransfected cells as well the immunoprecipitation reaction from BirA-CNK1 transfected cells (Figure 5.9C, Lanes 2 and 3, **). This suggests that despite the fact that we cannot detect CNK1 with the anti-CNK1 antibody (Figure 5.9A, Lane 2), there must be some CNK1 present in the immunoprecipitation as we are detecting the CNK1-binding partner IKKα/β. To ensure that we were detecting only specific interactions, we included one reaction where the lysate from BirA-CNK1 transfected cells was added to immunoprecipitation beads in the absence of antibody (Figure 5.9A-5.9D, Lane 1). If the protein was binding non-specifically to the bead, we would detect proteins in this lane. If we did not detect any proteins in this lane, it indicated that the proteins were binding the antibody in the immunoprecipitation reaction and that this detected interaction was specific.

When IKKα/β is immunoprecipitated with anti-IKKα/β, we detect a clear band for the IKKα/β proteins in untransfected and BirA-CNK transfected cells (Figure 5.9D, Lanes 2 and 3, **). When the immunoprecipitation reaction with IKKα/β is probed for CNK1, the immunoprecipitation from BirA-CNK1 transfected cells shows the presence of BirA-CNK1 (Figure 5.9B, Lane 3, *) but not the untransfected HeLa cells (Figure 5.9B, Lane 2) or the control (Figure 5.9B, Lane 1). This highlight again the low sensitivity of the anti-CNK1 antibody. More importantly, these immunoprecipitation reactions indicate strongly that there is an interaction between IKKα/β and CNK1 in the NF-κB signalling pathway.

5.3 CONCLUSIONS

In this chapter, we focussed on adapting the traditional immunoprecipitation reaction to identify the interacting partners of CNK1. We developed and tested BirA and BirA-CNK protein expression and biotin-tagging plasmids. We used these constructs to perform an immunoprecipitation reaction of biotinylated proteins that we analysed by mass spectrometry to identify potential binding partners of CNK1. We then used the traditional immunoprecipitation reactions with lysates from HeLa cells transfected with BirA-CNK1, to confirm that IKKα/β interact with CNK1.

One of the challenges with using the BirA and BirA-CNK1 constructs was the efficiency of transfection into HeLa cells. We used a large number of T75 flasks to generate sufficient protein for the immunoprecipitation reactions. This is not a sustainable option and while we were able to use the system to ask and answer some important questions, future studies will require a higher level of BirA and BirA-CNK1 expression. One option would be to make a stable cell line where we integrate the BirA-CNK1 expressing region onto the genome of the HeLa cell. With each cell producing the desired protein, it would be much easier to perform these experiments. The expression of BirA and BirA CNK1 in a stable cell line can be tightly regulated by the introduction of a tetracycline inducible expression system developed by Hermann Bujard and Manfred Gossen in 1992. The Tet-on/Tet-off inducible expression system will allow for control of BirA or BirA-CNK1 expression with the presence or absence of Tetracycline (Gossen & Bujard, 1992), enabling us to combat the oversaturation of the protein in cells and negating non-specific interaction during detection.

Our study here highlights the frustration of antibody-based protein studies. The antibody that we have used to detect CNK1 lacks sensitivity. In South Africa, access to antibodies is challenging. Orders when placed can take 2 – 3 months to arrive and then need to be tested to ensure that the cold chain was maintained. We are unable to import antibodies from some species, for example rabbits, at this time without securing import permits for each specific antibody. This places further strain on our research time and resources. Going forward, we would need to consider generating our own antibodies in South Africa, thus ensuring that we had a good supply of a robust antibody.

A final factor to consider is the disadvantages associated with the use of HeLa cells. HeLa cells were obtained from a cervical cancer patient named Henrietta Lacks over 60 years ago and is one of the most commonly used cervical cancer cell line in research laboratories (Mittelman & Wilson, 2013). However, above the aberrant behaviour of HeLa cells due to the genetic abnormalities commonly associated with cancer cells, whole genome sequencing studies have

shown variants of HeLa cells over the years (Landry, et al., 2013). The potential causative for the specific and mutated HeLa genomes isn't fully understood, but the change may be a potential consequence of over half a century of propagation in cell culture (Mittelman & Wilson, 2013). A way to improve the current study would be to observe the interacting partners of CNK1 in alternative cervical and breast cancer cell lines.

Despite these challenges, in this chapter we have ascertained that CNK1 interacts with other CNK1 molecules and that CNK1 interacts with IKKα/β in the NF-κB pathway.

CHAPTER 6: FINAL DISCUSSION AND CONCLUSIONS

One would think that if we have the identity of the signalling pathway and the bait protein, the identification of the binding partners of the bait protein should be straightforward. However, practically identifying the binding partners of CNK1 in the NF-κB pathway has proved challenging.

We used traditional immunoprecipitation assays and an adapted *in vivo* proximity labelling system to study the interacting partners of CNK1 in HeLa cells. Our mass spectrometry data indicate that CNK1 interacts with NIK, IKKα and IKKβ in the cell and this suggests that CNK1 has a role in the canonical as well as non-canonical NF-κB pathways. Our co-immunoprecipitation assay does not clarify this, as it confirms the interaction of CNK1 with IKKα and IKKβ, and these proteins are at the junction of the canonical and non-canonical NF-κB pathways.

Unfortunately, IKKα and IKKβ are similar in size (calculated at 85 and 87 kDa respectively) and reports have highlighted the difficulty separating the activities of IKKα and IKKβ. Antibodies putatively targeted against the one protein often cross-react with the other protein, limiting our ability to identify the specific interacting partner using antibody-based immunoprecipitation reactions.

There have been two studies whose data we can add to ours to build our understanding of the role of CNK1 in the NF-κB pathway. Analysis of the data presented by Fritz and Radziwill (2010) indicates that CNK1 plays a role in the non-canonical NF-κB pathway. In an effort to better understand the point of action, Pansare (2013) used sulphasalazine and quercetin to specifically inhibit proteins within the NF-κB pathway. Sulphasalazine is an inhibitor of IKKα and so of both the canonical and non-canonical NF-κB pathways. Treatment of HeLa cells with sulphasalazine resulted in the degradation of CNK1 as well as the loss of proteins in the canonical and non-canonical NF-κB pathways. In contrast, treatment of HeLa cells with quercetin, which is an inhibitor of the canonical NF-κB pathway, had no impact on the level of the CNK1 in the cell despite the fact that it inhibited the canonical NF-κB pathway. These data both lead to the conclusion that CNK1 functions in the non-canonical NF-κB pathway.

If we use the data presented by Fritz and Radziwill (2010) and Pansare (2013), we can identify the interacting partner of CNK1 in the NF-κB pathway, without refuting any of the past research.

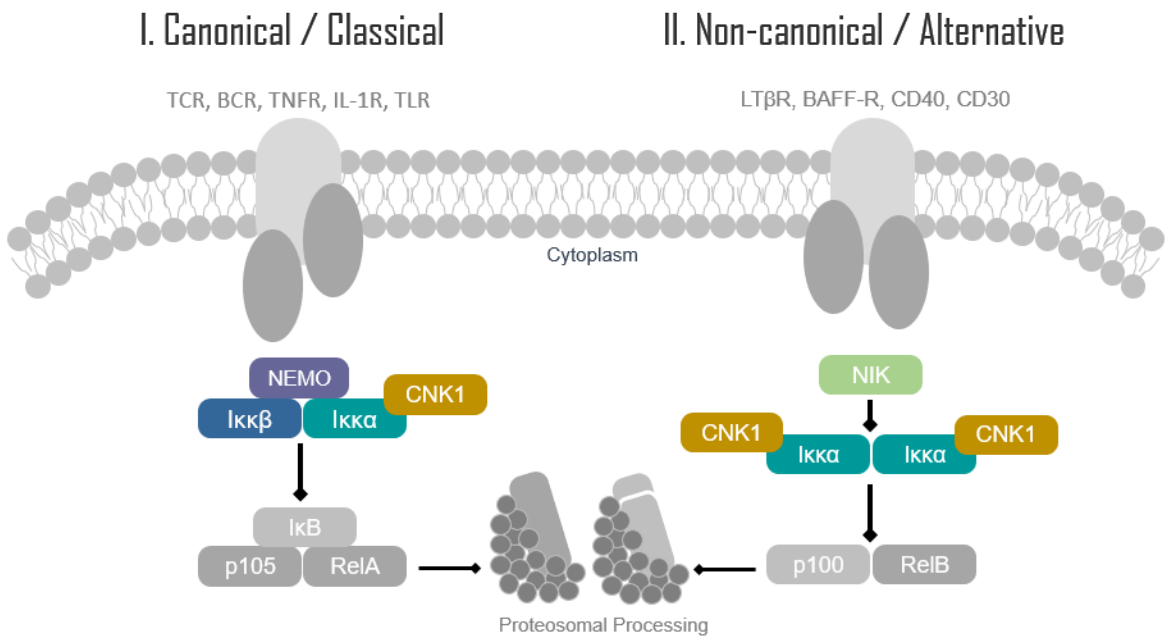

Figure 6.1: CNK1-interacting proteins in the NF-κB pathway.

When considering BirA-CNK1, and the transfer of biotin moieties to proximity partners of CNK1, our mass spectrometry data suggests that CNK1 interacts with proteins in the canonical and the non-canonical NF-κB pathways. To do this, CNK1 would need to interact with IKKα. In the non-canonical pathway, the interaction of CNK and IKKα would result in the proximity of CNK1-CNK1, CNK1-IKKα and CNK-IKKα-NIK resulting in the labelling of all of these proteins. In the canonical pathway, CNK1 would interact with IKKα, which in turn interacts with IKKβ. This would explain the labelling of IKKβ by BirA-CNK. Having identified the point at which CNK1 interacts with the NF-κB pathway, the question becomes- what role does CNK1 play in this pathway? And is CNK1 required to form the complex with IKKα to initiate signalling down the non-canonical NF-κB pathway?

The deregulation of the NF-κB pathways are critical in initiating oncogenic signalling that lead to cervical and breast cancer. In cervical cancer, the HPV oncoprotein E5 plays a role in the phosphorylation cascades evoking RAF-dependent MAPK-ERK activation in which CNK1 acts as a regulatory protein (Branca, et al., 2004). Upon persistent HPV infection, the NF-κB pathway is observed to be constitutively active. This is important to consider if CNK1 is mediating cross-talk of oncogenic signalling. This also highlights CNK1 as a potential target for drug therapy.

APPENDICES

A. The specificity of anti-FLAG, anti-MYC and anti-CNK1 antibodies

A1.1 Untransfected HeLa cells

HeLa cells were probed with anti-CNK1, anti-Myc and anti-FLAG antibodies to determine specificity and any possible cross reactivities. Confocal immunofluorescence microscopy show endogenous CNK1 levels detected using anti-CNK1 antibody. No fluorescence is detected with either anti-Myc or anti-FLAG antibodies, indicating no cross reactivity or non-specific interactions of the antibodies with endogenous CNK1.

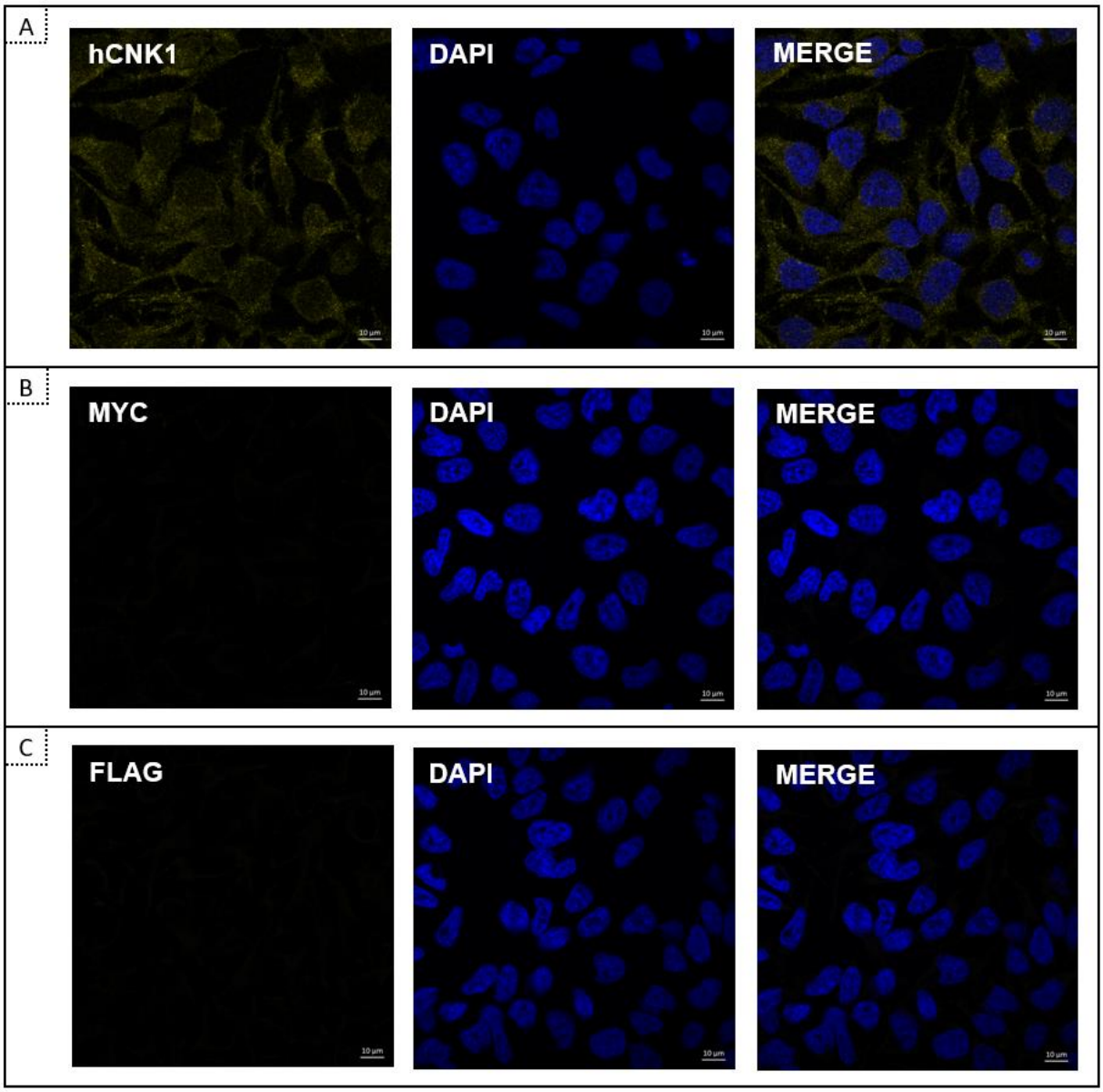

Figure A1: Antibody specificity in untransfected HeLa cells. A- probed with anti-CNK1; B- probed with anti-Myc; C- probed with anti-FLAG**.** Scale bars represent 10 µm.

A1.2 Myc-CNK1 transfected HeLa cells

HeLa cells were transfected with Myc-CNK1 encoding for CNK1 attached to a Myc tag at the N-terminal of the protein. The cells were probed with anti-CNK1, anti-Myc and anti-FLAG antibodies to determine specificity and any possible cross reactivities. Confocal immunofluorescence microscopy show CNK1 levels are detected using anti-CNK1 antibody and anti-Myc but no fluorescence is detected with anti-FLAG antibodies, indicating no cross reactivity or non-specific interactions of the anti-FLAG antibody with the Myc tag.

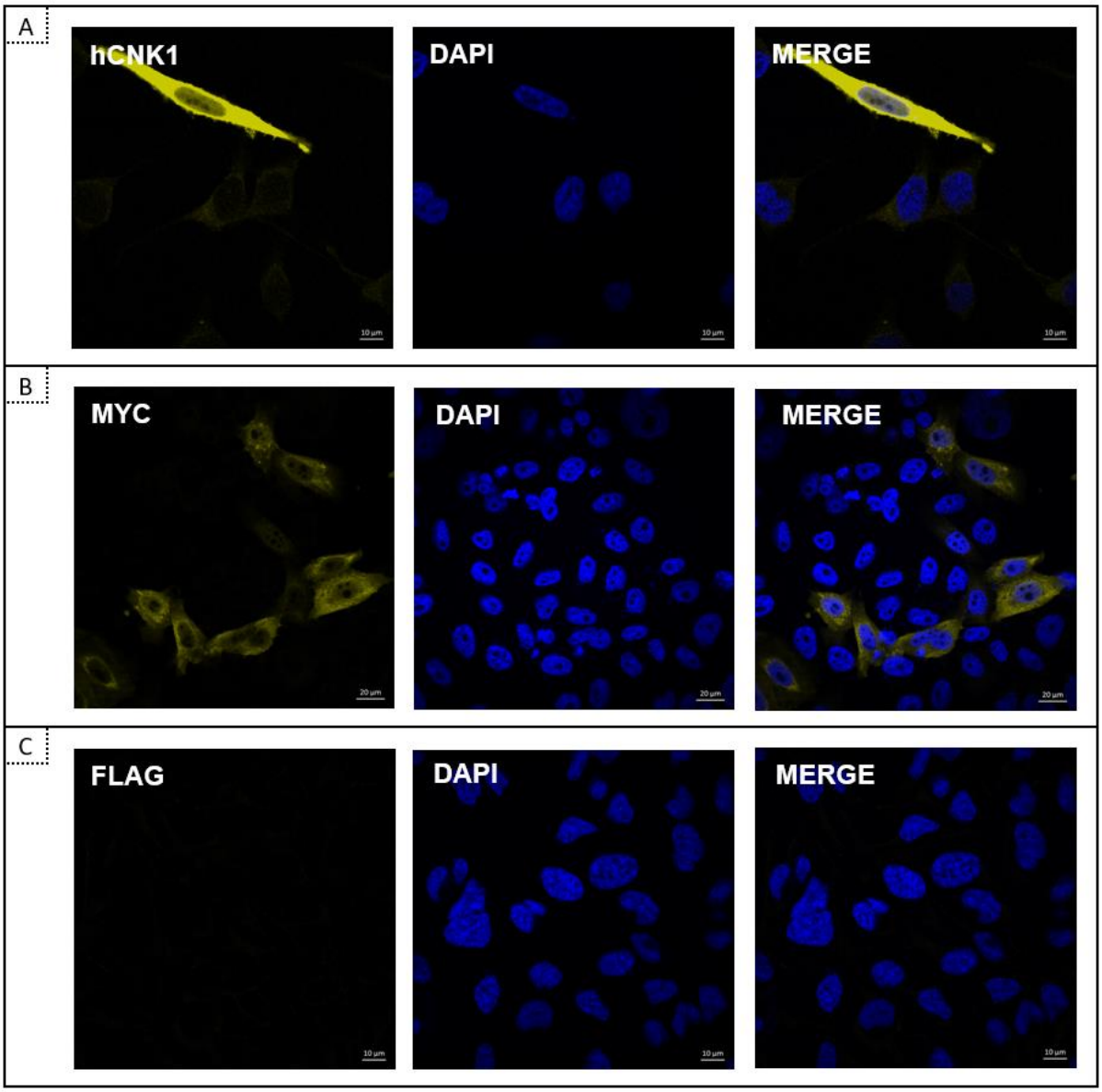

Figure A2: Antibody specificity of Myc-CNK1 transfected HeLa cells. A- probed with anti-CNK1; B- probed with anti-Myc; C- probed with anti-FLAG. Scale bars represent 10 μm.

A1.3 FLAG-CNK1 transfected HeLa cells

HeLa cells were transfected with FLAG-CNK1 encoding for CNK1 attached to a FLAG tag at the N-terminal of the protein. The cells were probed with anti-CNK1, anti-Myc and anti-FLAG antibodies to determine specificity and any possible cross reactivities. Confocal immunofluorescence microscopy shows CNK1 levels are detected using anti-CNK1 antibody and anti-FLAG antibody but no detection with anti-Myc antibody, indicating no cross reactivity or non-specific interactions of the anti-Myc antibody with the FLAG tag.

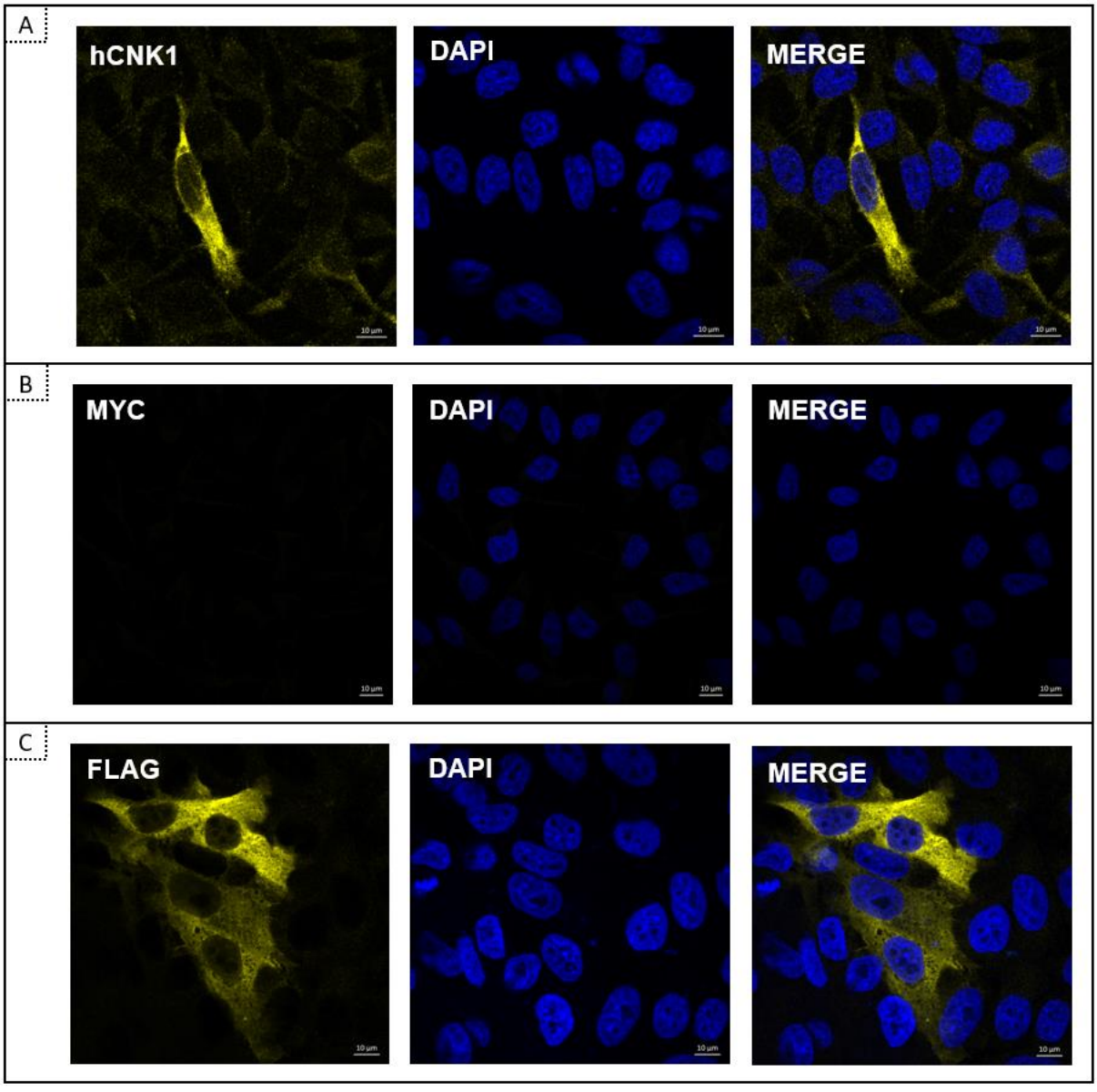

Figure A3: Antibody specificity of FLAG-CNK1 transfected HeLa cells. A- probed with anti-CNK1; B- probed with anti-Myc; C- probed with anti-FLAG. Scale bars represent 10 μm.

B. The quantification of the level of fluorescence of endogenous CNK1, Myc-CNK1 and FLAG-CNK1 in the nucleus and the nucleolus.

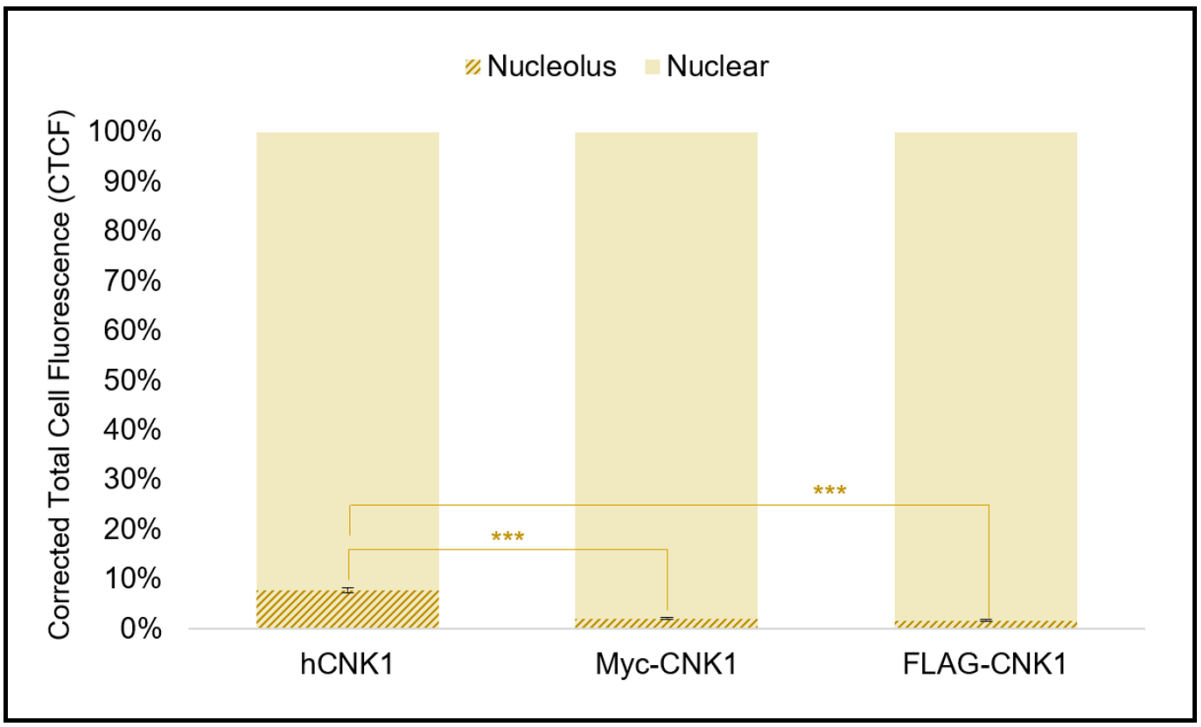

Figure B1: Quantification of nuclear and nucleolar CNK1 fluorescence in HeLa cells. Percentage of Endogenous CNK1, Myc-CNK1 & FLAG-CNK1 in the nuclear and nucleolar region of the HeLa cell nucleus. Statistical analysis: * = $p<0.05$, ** = $p<0.01$, *** = $p< 0.001$ where N = 10.

C. The quantification of the level of fluorescence of endogenous CNK1, Myc-CNK1 and FLAG-CNK1 in the nucleus and the nucleolus.

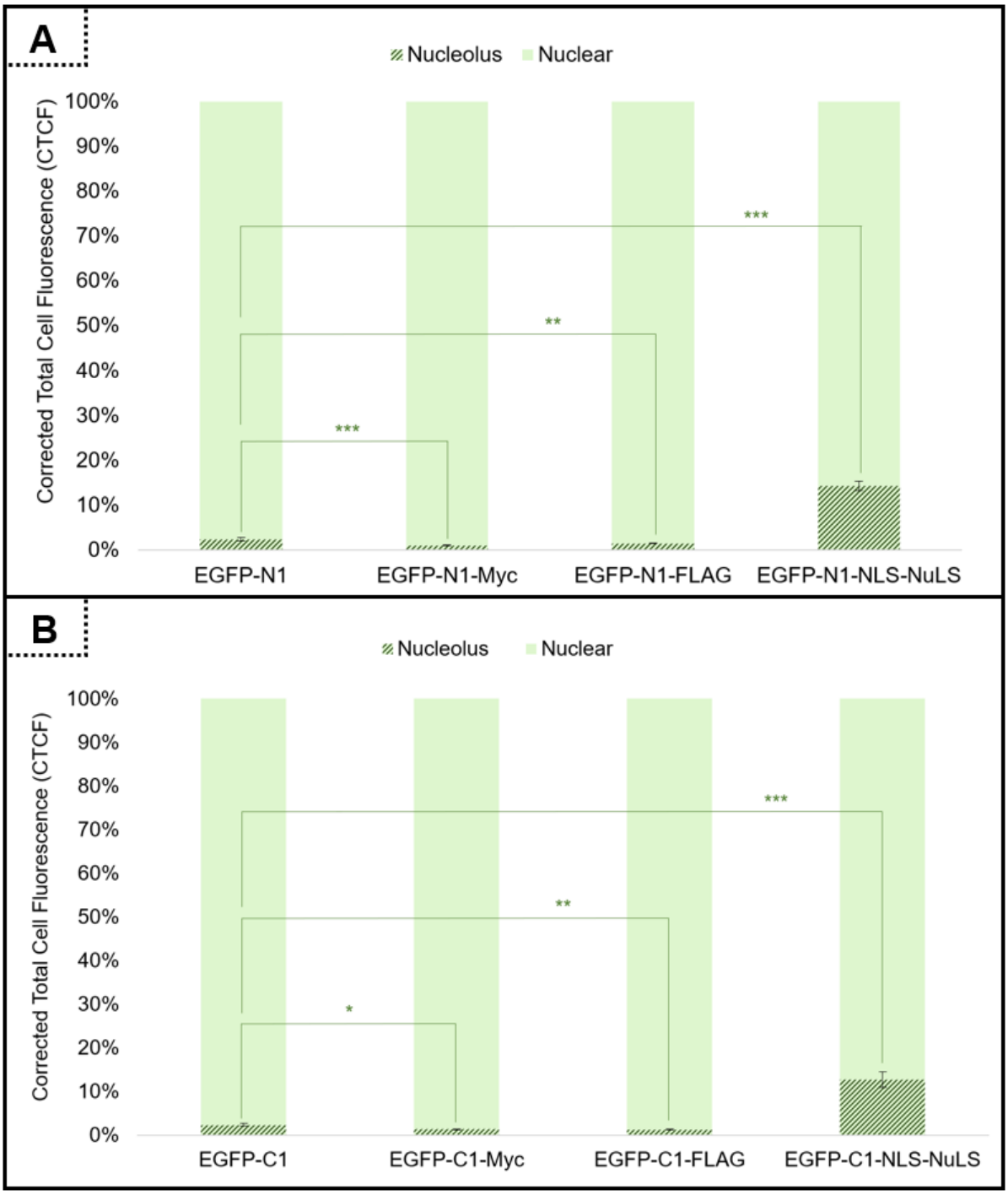

Figure C1: Quantification of nuclear and nucleolar Myc- and FLAG-tagged EGFP fluorescence in HeLa cells. A-Percentage of EGFP-N1, EGFP-N1-Myc and EGFP-N1-FLAG fluorescence in the nuclear and the nucleolar region of a HeLa cell; B- Percentage of EGFP-C1, EGFP-C1-Myc and EGFP-C1-FLAG fluorescence in the nuclear and nucleolar region of a HeLa cell. Statistical analysis: * = $p<0.05$, ** = $p<0.01$, *** = $p< 0.001$ where N = 10.

D. Sequence of the primers used in this study.

NAME	SEQUENCE	TARGET
CNK REVERSE	CTCTGTCAGGCTTTGCAGGTT CTCT	CNK SEQUENCING TO VALIDATE THE MYC AND FLAG TAG SEQUENCE
PRMJ682	AG CTT ATG GAG CAG AAG CTG ATC TCC GAG GAG GAC CTG ACG GTA C	MYC-N1 TOP
PRMJ683	CGT CAG GTC CTC CTC GGA GAT CAG CTT CTG CTC CAT A	MYC-N1 BOTTOM
PRMJ684	AG CTT ATG GAT TAC AAA GAT GAC GAT GAC AAG ACG GTA C	FLAG-N1 TOP
PRMJ685	CGT CTT GTC ATC GTC ATC TTT GTA ATC CAT A	FLAG-N1 BOTTOM
PRMJ690	CG ATT GGA TCC GAA TTC A	DELETING THE MYC/FLAG TAG FROM THE CNK EXPRESSION PLASMID-TOP
PRMJ691	GA TCT GAA TTC GGA TCC AAT	DELETING THE MYC/FLAG TAG FROM THE CNK EXPRESSION PLASMID-BOTTOM
PRMJ692	AG CTT CC GAG CAG AAG CTG ATC TCC GAG GAG GAC CTG GGT AC	MYC-C1 TOP
PRMJ693	C CAG GTC CTC CTC GGA GAT CAG CTT CTG CTC GG A	MYC-C1 BOTTOM

PRMJ694	AG CTT CC GAT TAC AAA GAT GAC GAT GAC AAG GGT AC	FLAG-C1 TOP
PRMJ695	C CTT GTC ATC GTC ATC TTT GTA ATC GG A	FLAG-C1 BOTTOM
PRMJ696_SEGFP-N	CGT CGC CGT CCA GCT CGA CCA G	SEQUENCING- EGFP-N
PRMJ697_SEGFP-C	CAT GGT CCT GCT GGA GTT CGT G	SEQUENCING- EGFP-C
PRMJ704-T	AG CTT ATG AAG AAG AAG CGC AAG CGC CGC CGC CGC CGC CGC CGC ACG GTA C	NLS-7R-N1-GFP-TOP
PRMJ705-B	CGT GCG GCG GCG GCG GCG GCG GCG CTT GCG CTT CTT CTT CAT A	NLS-7R-N1-GFP-BOTTOM
PRMJ706-T	AG CTT CC AAG AAG AAG CGC AAG CGC CGC CGC CGC CGC CGC CGC GGT AC	NLS-7R-C1-GFP-TOP
PRMJ707-B	C GCG GCG GCG GCG GCG GCG GCG CTT GCG CTT CTT CTT GG A	NLS-7R-C1-GFP-BOTTOM
PRMJ710- BIRA	TCTTCGGCATTTCACGCGG	SEQUENCING OUT OF BIRA

REFERENCES

Akbar, M. & Kim, H. Y., 2005. Green fluorescent protein tagging: novel tool in biomedical research. *Indian Journal of Biotechnology*, Volume 4, pp. 466-470.

Anselmo, A. N., Bumeister, R., Thomas, J. M. & White, M. A., 2002. Critical Contribution of Linker Proteins to Raf Kinase Activation. *Journal of Biological Chemistry*, Volume 277, pp. 5940-5943.

Baker, C. & Calef, C., 1996. Maps of Papillomavirus mRNA Transcripts, Maryland: Laboratory of Tumor Virus Biology - *National Institutes of Health*.

Banski, P., Kodiha, M. & Stochaj, U., 2010. Chaperones and multitasking proteins in the nucleolus: networking together for survival? *Cell Press - Trends in Biochemical Sciences*, 35(7), pp. 361-367.

Berridge, M. J., 2008. Cell Signalling Pathways. In: 1-114, ed. *Cell Signalling Biology*. Portland: Portland Press Limited.

Branca, M. et al., 2004. Activation of the ERK/MAP Kinase Pathway in Cervical Intraepithelial Neoplasia Is Related to Grade of the Lesion but Not to High-Risk Human Papillomavirus Virus Clearance, or Prognosis in Cervical Cancer. *Anatomic Pathology*, Volume 122, pp. 902-911.

Brizzard, B., 2008. Epitope Tagging. Biotechniques, Volume 44, pp. 693-695.

Burack, R. W. & Shaw, A. S., 2000. Signal transduction: hanging on a scaffold. *Current Opinion in Cell Biology*, Volume 12, pp. 211-216.

Chen, R. et al., 2014. Biomolecular scaffolds for enhanced signaling and catalytic efficiency. *Current opinion in Biotechnology*, Volume 28, pp. 59-68.

Cho, H. J. et al., 2014. EphrinB1 Interacts with CNK1 and Promotes Cell Migration through c-Jun N-terminal Kinase (JNK) Activation. *Journal of Biological Chemistry*, Volume 289, pp. 18556-18568.

Claperon, A. & Therrien, M., 2007. KSR and CNK: two scaffolds regulating RAS-mediated RAF activation. *Oncogene*, Volume 26, pp. 3143-3158.

Courtois, G. & Gilmore, T., 2006. Mutations in the NF-κB signaling pathway: implications for human disease. *Oncogene*, Volume 25, pp. 6831-6843.

Day, E. K., Sosale, N. G. & Lazzara, M. J., 2016. Cell Signaling Regulation by Protein Phosphorylation: A Multivariate, Heterogeneous, and Context-dependent Process. *Current Opinion Biotechnology*, Volume 40, pp. 185-192.

Doorbar, J., 2006. Molecular biology of human papillomavirus infection and cervical cancer. *Clinical Science*, 10(1042), pp. 525-541.

Einhauer, A. & Jungbauer, A., 2001. The FLAG peptide, a versatile fusion tag for the purification of recombinant proteins. *Journal of biochemical and biophysical methods*, Volume 49, pp. 455-465.

Fausti, F. et al., 2012. Hippo and rassf1a Pathways: A Growing Affair. *Molecular Biology International*, pp. 1-12.

Ferrell, J. E., 2000. What Do Scaffold Proteins Really Do? *Science Signaling*, Volume 52, pp. 1-3.

Fischer, A., Warschied, B., Weber, W. & Radziwell, G., 2016. Optogenetic clustering of CNK1 reveals mechanistic insights in RAF and AKT signalling controlling cell fate decisions. *Nature: Scientific Reports*, Issue 6:38155, pp. 1-15.

Fischer, A., Brummer, T., Warschied, B. & Radziwell, G., 2015. Differential tyrosine phosphorylation controls the function of CNK1 as a molecular switch in signal transduction. *Biochimica et Biophysica Acta*, pp. 2874-2855.

Fischer, A., Weber, W., Warscheid, B. & Radziwell, G., 2017. AKT-dependent phosphorylation of the SAM domains induces oligomerization and activation of the scaffold protein CNK1. *Biochimica et Biophysica Acta*, pp. 89-100.

Fritz, R. D. & Radziwell, G., 2010. CNK1 Promotes Invasion of Cancer Cells through NF-κB dependent signaling. *Molecular Cancer Research*, Volume 8, pp. 395-406.

Fritz, R. D. & Radziwell, G., 2011. CNK1 and other scaffolds for Akt/FoxO signaling. *Biochimica et Biophysica Acta*, Volume 1813, pp. 1971-1977.

Fritz, R. D., Varga, Z. & Radziwell, G., 2010. CNK1 is a novel Akt interaction partner that promotes cell proliferation through the Akt-FoxO signalling axis. *Oncogene*, Volume 29, pp. 3575-3582.

Ghim, S.-j., Basu, P. S. & Jenson, A., 2002. Cervical Cancer: Etiology, Pathogenesis, Treatment, and Future Vaccines. *Asian Pacific Journal of Cancer Prevention*, Volume 3, pp. 207-214.

Good, M. C., Zalatan, J. G. & Lim, W. A., 2011. Scaffold Proteins: Hubs for Controlling the Flow of Cellular Information. *SCIENCE*, Volume 332, pp. 681-686.

Gossen, M., & Bujard, H., 1992. Tight control of gene expression in mammalian cells by tetracycline-responsive promoters. *PNAS*, 5547-5551.

Hernandez-Verdun, D., 2004. The nucleolus: functional organisation and assembly. *Journal of Applied Biomedicine*, Volume 2, pp. 57-69.

Hoesel, B. & Schmid, J. A., 2013. The complexity of NF-κB signaling in inflammation and cancer. *Molecular Cancer*, 12(86), pp. 1-15.

Hoft, M., 2014. The effect of CNK1 scaffold protein on the NF-κB pathway, Grahamstown: *Rhodes University*.

Horiuchi, T. et al., 2010. Transmembrane TNF-a: structure, function and interaction with anti-TNF agents. *Rheumatology: Review*, Volume 49, pp. 1215-1228.

Jaffe, A. B., Apenstrom, P. & Hall, A., 2004. Human CNK1 Acts as a Scaffold Protein, Linking Rho and Ras Signal Transduction Pathways. *Molecular and Cellular Biology*, Volume 2004, pp. 1736-1746.

Jarvik, J. W. & Telmer, C. A., 1998. Epitope Tagging. *Annual Review of Genetics*, Volume 32, pp. 601-618.

Karin, M., Cao, Y., Greten, F. R. & Li, Z. W., 2002. NF-kappaB in cancer: from innocent bystander to major culprit. *Nature Review: Cancers*, Volume 4, pp. 301-310.

Kolch, W., 2000. Meaningful relationships: the regulation of the Ras/Raf/MEK/ERK pathway by protein interactions. *Biochemical Journal*, Volume 351, pp. 289-305.

Landry, J. J., Theodor, P., Rausch, T., Zichner, T., Tekkedil, M. M., Stutz, A. M., . . . Steinmetz, L. M., 2013. The Genomic and Transcriptomic Landscape od a HeLa Cell Line. *G3-Genes-Genomes-Genetics*, 1213-1224.

Lange, A., Mills, R. E., Lange, C. J., Stewart, M., Devine, S. E., Corbett, A. H., 2007. Classical nuclear localization signals: definition, function, and interaction with importin alpha. *Journal of biological chemistry*, 282(8), pp. 5101-5105.

Lawrence, T., 2009. The Nuclear Factor NF-κB Pathway in Inflammation. *Cold Spring Harbor Perspectives in Biology*, Volume 1, pp. 1-10.

Lee, M. J. & Yaffe, M. B., 2016. Protein Regulation in Signal Transduction. *Cold Spring Habour Perspectives in Biology*, Volume 7, pp. 1-19.

Leicht, D. T. et al., 2007. Raf kinases: Function, regulation and role in human cancer. *Biochimica et Biophysica Acta*, Volume 1773, pp. 1196-1212.

Lim , J., Zhou, M., Veenstra, T. D. & Morrison, D. K., 2010. The CNK1 scaffold binds cytohesins and promotes insulin pathway signaling. *Genes & Development*, Volume 24, pp. 1496-1506.

Lu, X., Gilbert, L., Rubin, J. & Nanes, M. S., 2006. Transcriptional regulation of the osterix (Osx, Sp7) promoter by tumor necrosis factor identifies disparate effects of mitogen-activated protein kinase and NF kappa B pathways. *Journal of Biological Chemistry*, Volume 10, pp. 6297-6306.

Ma, Y. Y, Wei, S. J., Lin, Y. C., Lung, J. C., Chang, T. C., Whang-Peng, J., Lui, J. M., Yang, D. M., Yang, W.K., Shen, C. Y., 2000. PIK3CA as an oncogene in cervical cancer. *Oncogene*, Volume 19, pp. 2739-2744.

Martin, R. M ., Ter-Avetisyan, G., Herce, H. D., Ludwig, A. K., Lattig-Tunnemann, G., Cardoso, M.C., 2015. Principles of protein targeting to the nucleolus. *Nucleus*, 6(4), pp. 314-325.

Mechold, U., Gilbert, C. & Ogryzko, V., 2005. Codon optimization of the BirA enzyme gene leads to higher expression and improved efficiency of biotinylation of target proteins in mammalian cells. *Journal of Biotechnology*, Volume 116, pp. 245-249.

Milella, M., Ciuffreda, L. & Bria, E., 2010. Signal Transduction Pathways as Therapeutic Targets in Cancer Therapy. In: L. H. Reddy & P. Couvreur, eds. *Macromolecular Anticancer Therapeutics*. Springer, pp. 37-83.

Mittelman, D., & Wilson, J. H., 2013. The fractured genome of HeLa cells. *Genome Biology*, 1-4.

Moynagh, P. N., 2005. The NF-κB pathway. *Journal of Cell Science,* 118(20), pp. 4589-4592.

Napetschnig, J. & Wu, H., 2013. Molecular Basis of NF-κB Signaling. *Annual Review of Biophysics,* Volume 42, pp. 19.1-19.26.

Nishikori, M., 2005. Classical and Alternative NF-κB Activation Pathways and Their Roles in Lymphoid Malignancies. *Journal of Clinical and Experimental Hematopathology*, 45(1), pp. 15-24.

O'Day, D. H. & Catalana, A., 2013. Proteins of the Nucleolus: An Introduction. In: Proteins of the Nucleolus: Regulation, Translocation, & Biomedical Functions. *USA: Springer Science*, pp. 3-15.

O'Dea, E. & Hoffmann, A., 2009. NF-κB signaling. In: WIREs Systems Biology and Medicine. *John Wiley & Sons*, Inc, pp. 107-115.

Pan, C. Q., Sudol, M., Sheetz, M. & Low, B. C., 2012. Modularity and functional plasticity of scaffold proteins as p(l)acemakers in cell signaling. *Cellular Signalling*, Volume 24, pp. 2143-2165.

Pansare, K. J., 2013. CNK1 scaffold protein and its role in the regulation of NF-κB signalling, Birmingham: *Aston Univeristy*.

Rabizadeh, S. et al., 2004. The Scaffold Protein CNK1 Interacts with the Tumor Suppressor RASSF1A and Augments RASSF1A-induced Cell Death. *Journal of Biological Chemistry*, Volume 279, pp. 29247-29254.

Raska, I., Shaw, P. J. & Cmarko, D., 2006. Structure and Function of the nucleolus in the spotlight. *Current Opinion in Cell Biology,* Volume 18, pp. 325-334.

Roskoski, R. J., 2010. RAF protein-serine/threonine kinases: Structure and regulation. *Biochemical and Biophysical Research Communications,* Volume 399, pp. 313-317.

Roux, K. J., Kim, D. L., Raida, M. & Burke, B., 2012. A promiscuous biotin ligase fusion protein identifies proximal and interacting proteins in mammalian cells. *The Journal of Cell Biology*, 196(6), pp. 801-810.

Sabapathy, K., 2012. Role of the JNK Pathway in Human Diseases. *Progress in Molecular Biology and Translational Science*, Volume 106, pp. 145-169.

Schmitz, L. M., dos Santos Silva, M. A. & Baeuerle, P. A., 1995. Transactivation Domain 2 (TA2) of p65 NF-κB. *Journal of biological Chemistry*, 270(26), pp. 15576-15584.

Schwarz, E., Freese, U. K., Gissmann, L., Mayer, W., Roggenbuck, B., Stremlau, A., & zur Hausen, H., 1985. Structure and transcription of human papillomavirus sequences in cervical carcinoma cells. *Nature*, 111-114.

Shaw, P., 2005. Nucleolus. In: Encyclopedia of Life Sciences. Norwich: *John Wiley & Sons*, pp. 1-9.

Strickson, S. et al., 2013. The anti-inflammatory drug BAY 11-7082 suppresses the MyD88-dependent signalling network by targeting the ubiquitin system. *The Biochemical Journal*, Volume 3, pp. 427-437.

Tanabe, S., 2017. Networking the Signaling Pathways in Stem Cells and Cancer. *Journal of Clinical Epigenetics*, 3(28), p. 1.

Therrien, M., Wong, A. M. & Rubin, G. M., 1998. CNK, a RAF-Binding Multidomain Protein Required for RAS Signaling. *Cell*, Volume 95, pp. 343-353.

Tilborghs, S., Corthouts, J., Verhoeven, Y., Arias, D., Rolfo, C., Trinh, X. B., Van Dam, P. A., 2017. The role of Nuclear Factor-kappa B signaling in human cervical cancer. *Critical Reviews in Oncology / Hematology*, Volume 120, pp. 141-150.

Venuti, A., Paolini, F., Nasir, L., Corteggio, A., Roperto, S., Campo, M. S., Borzacchiello, G., 2011. Papillomavirus E5: the smallest oncoprotein with many functions. *Molecular Cancer*, 10(140), pp. 1-18.

Verma, I. M., 2004. Nuclear factor (NF)-κB proteins: therapeutic targets. *Annals of the Rheumatic Diseases*, Volume 63, pp. ii57-ii61.

Viens, A., Harper, F., Pichard, E., Comisso, M., Pierron, G., Ogryzko, V., 2008. Use of Protein Biotinylation In Vivo for Immunoelectron Microscopy Localisation of a Specific Protein Isoform. *Journal of Histochemistry & Cytochemistry*, 56(10), pp. 911-919.

Viens, A., Mechold, U., Lehrmann, H., Harel-Bellan, A., Ogryzko, V., 2004. Use of protein biotinylation in vivo for chromatin immunoprecipitations. *Analytical Biochemistry*, Volume 325, pp. 68-76.

Vihinen, M., 2003. Signal transduction-related bioinformatics services. *Briefings in bioinformatics*, 4(4), pp. 325-331.

Wang, X., Meyers, C., Wang, H. K., Chow, L. T., Zheng, Z. M., 2011. Construction of a Full Transcription Map of Human Papillomavirus Type 18 during Productive Viral Infection. *Journal of Virology*, 85(16), pp. 8080-8092.

Xiao, G., Harhaj, E. W. & Sun, S.-C., 2001. NF-κB-Inducing Kinase Regulates the Processing of NF-κB2 p100. *Molecular Cell*, Volume 7, pp. 401-409.

Zhao, X., Li, G. & Liang, S., 2013. Several affinity tags commonly used in chromatographic purification. *Journal of Analytical Methods in Chemistry*, pp. 1-8.

Ziogas, A., Moelling, K. & Radziwell, G., 2005. CNK1 is a scaffold protein that regulates Src-mediated RAf-1 activation. *The Journal of Biological Chemistry*, 280(25), pp. 24205-24211.

zur Hausen, H., 2009. Papillomaviruses in the causation of human cancers — a brief historical account. *Virology*, 260-265.